5-6-2019

# Spectroscopic Characterization and Bioanalytical Applications of Benzophenoxazine Derivatives and the Use of Dyes and Dye-Encapsulated Silica Nanoparticles for Fingerprint Detection

Eman Alsolmy

# SPECTROSCOPIC CHARACTERIZATION AND BIOANALYTICAL APPLICATIONS OF BENZOPHENOXAZINE DERIVATIVES AND THE USE OF DYES AND DYE-ENCAPSULATED SILICA NANOPARTICLES FOR FINGERPRINT DETECTION

by

Eman Alsolmy

Under the Direction of Gabor Patonay, PhD

## ABSTRACT

The use of benzophenoxazine dyes such as Nile red and Nile blue in various applications has received increasing attention in recent years. Due to the limitations of using the two dyes in aqueous media because of their poor solubility, extensive efforts have been made to synthesize new benzophenoxazine analogues. Therefore, the first part of the work aims to characterize modified structures of benzophenoxazine derivatives as well as Nile red and Nile blue using spectroscopic techniques. The optical properties of the dyes involve the determination of molar absorptivity and quantum yield values as well as photostability studies. The absorbance and emission wavelengths are in the visible and near-infrared region of the electromagnetic spectrum

which is the most useful region for bioanalytical applications due to the reduced autofluorescence from biomolecules. The first part also includes the interactions between benzophenoxazine derivatives and human serum albumin. The affinity of the dye to the protein is hydrophobicity-dependent, but other parameters such as steric hindrance and electrostatic interaction play a role too as confirmed by binding constant values. Detection of fingerprints is considered one of the most valuable pieces of evidence in forensic investigations. The second part of the work aims to use benzophenoxazine derivatives for fingerprint detection on porous surfaces. The factors affecting the ability of Nile red and Nile blue derivatives to develop luminescent and visible fingerprints with good background contrast are discussed. The second part also contains the application of silica nanoparticles encapsulating some benzophenoxazine derivatives as well as fluorescein isothiocyanate as fingerprint reagents. The efficiency to develop fingerprints is governed by the nature of the encapsulated dye and organosilicate precursors.

INDEX WORDS: Benzophenoxazine derivatives, Nile red, Nile blue, Human serum albumin, Fingerprint detection, Silica nanoparticles

# SPECTROSCOPIC CHARACTERIZATION AND BIOANALYTICAL APPLICATIONS OF BENZOPHENOXAZINE DERIVATIVES AND THE USE OF DYES AND DYE-ENCAPSULATED SILICA NANOPARTICLES FOR FINGERPRINT DETECTION

by

Eman Alsolmy

A Dissertation Submitted in Partial Fulfillment of the Requirements for the Degree of

Doctor of Philosophy

in the College of Arts and Sciences

Georgia State University

2019

# SPECTROSCOPIC CHARACTERIZATION AND BIOANALYTICAL APPLICATIONS OF BENZOPHENOXAZINE DERIVATIVES AND THE USE OF DYES AND DYE-ENCAPSULATED SILICA NANOPARTICLES FOR FINGERPRINT DETECTION

by

Eman Alsolmy

Committee Chair: Gabor Patonay

Committee: Gangli Wang

Kathryn Grant

Electronic Version Approved:

Office of Graduate Studies

College of Arts and Sciences

Georgia State University

May 2019

## DEDICATION

I would like to dedicate this dissertation to my husband, Ahmed, and my amazing kids, Ruba and Yousef, who have helped me to achieve my dream and make it real. This dissertation also is dedicated to my parents who have encouraged me to accomplish my degree.

## ACKNOWLEDGEMENTS

I would like to acknowledge my primary investigator, Prof. Gabor Patonay, first for accepting me to join his research group. I have learned invaluable lessons from his classes and during conducting research. It has been truly an honor to be one of his students. I would like to thank also my committee members, Dr. Gangli Wang and Dr. Kathryn Grant for giving me the chance to share my work with them. Also, I would like to thank Dr. Maged Henary and Mr. Vincent Martinez for providing me with the benzophenoxazine derivatives for my project. In addition, I would like to thank all my labmates I have worked with during this educational journey. Special thank goes to the former Ph.D. student, Dr. Garfield Beckford, for his help and patience when I first joined Patonay's group. I would like to acknowledge Saudi Arabian Cultural Mission in USA, King Abdulaziz University, and University of Jeddah for the financial support. Last but not least, I thank all my family members who have helped and encouraged me during my journey.

# TABLE OF CONTENTS

# LIST OF TABLES

# LIST OF FIGURES

# 1 FLUORESCENCE APPLICATIONS RELATED TO DYES

## 1.1 Introduction

Fluorescence is a spectroscopic technique studying the interaction between electromagnetic radiation and species of interest based on photophysical properties. Fluorescence spectroscopy has become a powerful method in medical diagnosis, tumor detection, and optical imaging.[1-4] One of the most interesting features of fluorescence is the high sensitivity in which a single molecule can be detected by fluorescence intensity. In fact, the observed tracks of two molecules of rhodamine 6G in sol-gel film proved the random walk of diffusing molecules.[5] Fluorescence is one of many forms of luminescence which is the emission of light by a fluorophore not resulting from heat. It totally differs from incandescence which is the emission of light by a hot substance as a result of its temperature. There are several forms of luminescence according to the differences in method of light emission including chemiluminescence, electroluminescence, bioluminescence, cathodoluminescence, thermoluminescence, and photoluminescence. Chemiluminescence is based on the emission of light during a chemical reaction in which new excited species are formed. Electroluminescence is the emission of light resulting from the passage of an electric current through a substance. Bioluminescence is a form of luminescence generated by some biochemical reactions in a living organism such as a firefly. Cathodoluminescence is caused by an electron beam impacts on a luminescent substance resulting in the emission of light. Thermoluminescence is a luminescence process in which some crystal substances absorb electromagnetic radiation or ionizing radiation, and when they are heated re-emission of energy occurs. Photoluminescence is the emission of light from a higher excited state to the ground state due to the absorption of photons. It can be fluorescence or phosphorescence based on the type of excited state.[6]

## 1.2 Jablonski diagram

The best way to understand transitions between electronic states of a molecule is Jablonski diagram[7] as shown in Figure 1.1, where $S_0$ is the singlet ground state, $S_1$ and $S_2$ are the first and second singlet excited states, respectively, and $T_1$ is the first triplet excited state. Thick lines represent the electronic energy levels which are further divided into vibrational energy levels represented by thin lines. When a molecule absorbs a photon, the electron in the singlet ground state, $S_0$, is promoted to a higher singlet excited state $S_1$ or $S_2$. The energy difference between the ground and the excited states corresponds to the energy of the photon. Absorbance occurs as a result of an electronic transition from the highest occupied molecular orbital (HOMO) to lowest unoccupied molecular orbital (LUMO). It is a very rapid process and takes place in about $10^{-15}$-$10^{-14}$ second. Once the electron reaches the first excited state, many radiative and non-radiative processes can happen. One of the non-radiative processes is internal conversion which describes the transition between two excited states of the same multiplicity. It is most likely to occur when the energy gap between the two states is small, so there is an overlap in vibrational energy levels. Internal conversion is a fast process that occurs in $10^{-12}$ second or less. The photon energy is converted into heat. Another non-radiative process is vibrational relaxation which involves a decay from a higher vibrational level within the excited electronic state due to collisions between the excited species and the solvent molecules. The energy of the absorbed photon is converted into heat. The process is very fast and occurs in $10^{-12}$ second or less. One radiative process is fluorescence which occurs when the electron goes back from the lowest vibrational level in the first singlet excited state to the ground state by emitting a photon. Fluorescence occurs very rapidly in about $10^{-9}$-$10^{-6}$ second. Another non-radiative process is called intersystem crossing. In this case, the electron transfer between two electronic states of different multiplicity, for example, from

singlet excited state $S_1$ to triplet excited state $T_1$ with conversion in electron spin. It is most common in molecules containing oxygen or heavy atoms such as bromine and iodine. Intersystem crossing leads to a radiative process in which electron in triplet excited state $T_1$ returns to the singlet ground state $S_0$ by emitting a photon. Such an event is known as phosphorescence. This process is forbidden, so the lifetime is long of about $10^{-3}$ – 10 second.

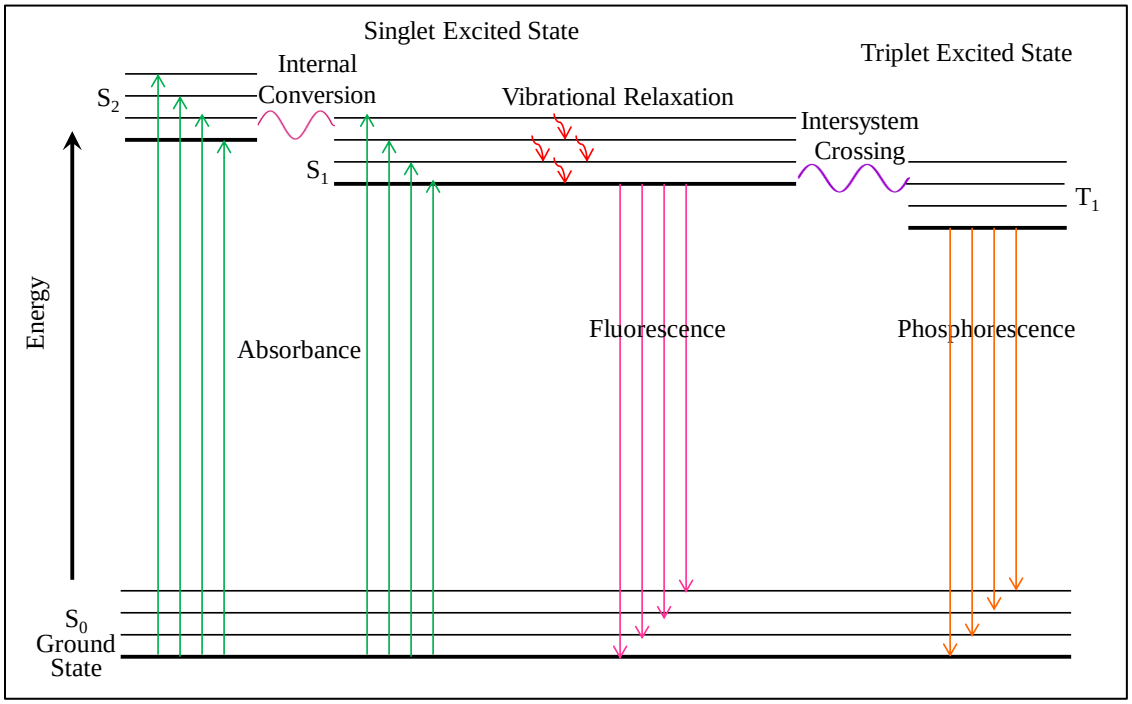


**Figure 1.1 Jablonski diagram**

## 1.3 General characteristics of fluorescence

Fluorescence properties of a molecule are usually presented as an emission spectrum, a plot of fluorescence intensity versus wavelength (nm). A molecule with a chemical group that causes the molecule to re-emit light upon excitation is called a fluorophore. There are general characteristics of fluorescence emission. For instance, the energy required for the emission to occur is less than that of the absorption. Consequently, the emission spectrum is observed at longer

wavelengths compared to the absorption spectrum. This characteristic is known as Stokes shift. Another characteristic of fluorescence is that the emission spectrum is located in the same wavelength irrespective of the excitation wavelength. As mentioned previously, fluorescence occurs as a result of the electronic transition from the lowest vibrational level of $S_1$. When the electron is excited to higher electronic and vibrational states, the excess energy is dissipated rapidly. This results in relaxation to the lowest vibrational level in the first singlet excited state. Therefore, the emission spectrum is independent of the excitation wavelength which is known as Kasha's rule. Another characteristic of fluorescence is that the emission spectrum is typically a mirror image of the absorption spectrum. This image is obtained because the distance among vibrational energy levels of the excited states is similar to that of the ground state. Moreover, fluorescence occurs by going back to a higher vibrational level of the ground state. However, there are many exceptions to the mirror image rule including pH-sensitive fluorophore, changes in $pK_a$, and excited-state reactions such as formation of complexes or dimer.[8]

One of the most important parameters of a fluorophore is quantum yield (Q). It is defined as the number of emitted photons relative to the number of absorbed photons. Moreover, quantum yield can be described in terms of rate constants by the equation:

$$Q = \frac{\Gamma}{\Gamma + k_{nr}} \qquad (1.1)$$

where ($\Gamma$) and ($k_{nr}$) are rate constants of radiative and non-radiative processes, respectively. Quantum yield value of some fluorescent compounds such as rhodamine 6G and fluorescein approaches unity because the non-radiative rate is much smaller than the radiative rate. Thus, these compounds exhibit the brightest emissions.[8]

The reliable measurement of quantum yield is challenging because the determination process is influenced by several factors including temperature, dye concentration, and solvent properties such as polarity, refractive index, and viscosity.[9] The most common method for quantum yield determination is the relative method[10] in which the quantum yield of the sample $\Phi_S$ is calculated relative to the quantum yield of standard $\Phi_{STD}$ according to the following equation:

$$\Phi_S = \Phi_{STD} \left[\frac{\text{Slope}_S}{\text{Slope}_{STD}}\right] \left[\frac{\eta^2_S}{\eta^2_{STD}}\right] \quad (1.2)$$

where Slope is the slope of plotting the area under the emission curve as a function of the absorbance value at the excitation wavelength and $\eta$ is the refractive index of solvent. Subscripts S and STD refer to the sample and the standard, respectively. In addition to the relative method, quantum yield can be determined by absolute methods such as optical spectroscopy using an integrating sphere setup and pulsed laser photoacoustic spectroscopy.[9]

### 1.4 Fluorescence quenching applications

Quenching is a non-radiative process that leads to a decrease in the fluorescence intensity of a molecule. It can occur by several molecular interactions such as energy transfer, molecular rearrangements, excited-state reactions, ground-state complex formation, and collisional quenching. The decrease in fluorescence intensity by quenching can be described by Stern-Volmer equation as:

$$\frac{F_0}{F} = 1 + K_{SV}[Q] \quad (1.3)$$

where $F_0$ and F are the fluorescence intensities in the absence and presence of quencher, respectively, $K_{SV}$ is Stern-Volmer quenching constant, and [Q] is the quencher concentration. The

quenching constant elucidates accessibility of the fluorophore to the quencher. A high value of K indicates that the fluorophore is exposed to the quencher because it is on the surface of a biomolecule. On the other hand, a low value of K depicts non-susceptibility of the quencher to the fluorophore due to its position inside the biomolecule.

Collisional or dynamic quenching is the most common type of quenching. It occurs when the quencher diffuses to the fluorophore during the lifetime of the excited state. Consequently, the fluorophore loses its energy due to the collision with quencher and returns to the ground state without emission of a photon. The constant of collisional quenching $K_D$ can be obtained by Stern-Volmer equation:

$$\frac{F_0}{F} = 1 + K_D [Q] = 1 + k_q \tau_0 [Q] \qquad (1.4)$$

where $k_q$ is the biomolecular quenching constant and $\tau_0$ is the lifetime of the fluorophore in the absence of the quencher. Numerous substances are considered as collisional quenchers, one of which is molecular oxygen which quenches almost all fluorophore molecules.[11] Another example of quenchers is halogenated molecules. The presence of heavy atoms such as iodide and bromide motivate intersystem crossing to the triplet state. Moreover, amines and electron-deficient molecules like acrylamide act as quenchers.[8, 12]

Besides collisional quenching, fluorescence quenching can occur in the ground state when a non-fluorescent complex is formed due to interaction between the fluorophore and the quencher. Such a process is called static quenching. The constant of static quenching $K_S$ or the association constant of the complex can also be obtained by Stern-Volmer equation:

$$\frac{F_0}{F} = 1 + K_S [Q] \qquad (1.5)$$

There are some different ways to distinguish between the two types of quenching. The most crucial method is measuring the lifetime of a fluorophore. The complex formed in static quenching does not fluoresce, and the fluorescence is only observed from the free fluorophore. Thus, the lifetime of the fluorophore is independent of quencher concentration since it does not appear in the equation (1.5). On the other hand, the fluorophore lifetime is influenced by the quencher concentration in the collisional quenching. Another way to distinguish between the two types of quenching is the effect of temperature. The constant of static quenching decreases as the temperature increases due to the complex dissociation. However, higher temperature increases diffusion rate resulting in a high constant of collisional quenching. Moreover, the absorbance spectrum of the fluorophore is affected in case of static quenching since it involves formation of the ground-state complex. However, the absorbance spectrum stays the same because collisional quenching occurs in the excited state.[8, 12]

One of the most significant applications of quenching is oxygen sensing. Bacon and coworker fabricated a sensor for oxygen determination consisting of a high fluorescent transition-metal complex, tris(4,7-diphenyl-1,10-phenanthroline) ruthenium (II) perchlorate, immobilized in a silicone rubber matrix. The oxygen concentration in solutions and gas phase was measured based on fluorophore lifetime or reduction of fluorescence intensity in the presence of the quencher.[13] Moreover, an optical oxygen sensor has been prepared by combining the oxygen-adduct forming cobalt porphyrin-polymer and a luminescent pyrene derivative quenched by oxygen. The sensor displayed a great response to the oxygen partial pressure of 10–21 kPa.[14] Recently, Li and coworkers have designed an optical sensor for the determination of dissolved oxygen levels based on fluorescence quenching measurements. The results indicated that the sensor performance was accurate, stable, and interference-free compared to other conventional methods such as iodometry

and electrochemical methods.[15] Besides the oxygen sensors, fluorescence quenching mechanism has been contributed to halide sensor productions. The sensor fabrication is based on the quenching of some fluorescent dyes such as quinolinium derivatives, iodolium salt, rhodamine B, and acridinium dyes immobilized in a hydrophilic copolymer. Stern-Volmer equation used to evaluate the concentration of halides in solutions indicated that sensors were stable and had a long shelf-life.[16-18] In addition to the sensor applications, fluorescence quenching methods help to detect several organic and inorganics analytes. For instance, dopamine, one of the most important neurotransmitters in the nervous system, was detected in biological samples by the quenching mechanism. Zhu and coworkers built a biosensor based on dopamine aptamer labeled carbon dots which was quenched by nano-graphite allowing sensitive and selective determination of dopamine.[19] Moreover, some inorganic ions such as $Fe^{2+}$ and $Fe^{3+}$ were detected in real samples of milk and water through fluorescence quenching.[20-21]

### 1.5 Benzophenoxazine dyes

Benzophenoxazine dyes belong to the oxazines family which is a class of heterocyclic systems containing one oxygen atom and one nitrogen atom in a six-membered ring with two double bonds.[22] Oxazines form several isomers depending on the relative positions of the two heteroatoms and the double bonds in the aromatic ring. Therefore, the most common isomers are 1,2-oxazine, 1,3-oxazine, and 1,4-oxazine[23] as shown in Figure 1.2. The 1,4-oxazine structure may be extended by adding two fused benzene rings to form a phenoxazine ring. Further extension of the phenoxazine skeleton with another fused benzene ring yields the benzophenoxazine structure. Nile red and Nile blue as the most prominent examples of benzophenoxazine dyes have been known for more than 100 years as fluorescent probes. Both compounds have been used in histology

for staining of some lipid compounds such as fatty acids and neutral fats.[24] They were first synthesized by the two Germen chemists, Möhlau and Uhlmann, in 1896.[25] The original synthesis of Nile red involves a condensation reaction of 5-(diethylamino)-2-nitrosophenol with 1-naphthol (Figure 1.3 a). Moreover, Nile red may be prepared by boiling Nile blue in 5% sulfuric acid under reflux for two hours[26] (Figure1.3 b). Similarly, Nile blue was first synthesized by a condensation reaction of 5-(diethylamino)-2-nitrosophenol with 1-aminonaphthalene in acetic acid, but the yield was very low of about 3%. However, the use of perchloric acid in ethanol increases the yield to 31%[27] (Figure 1.4).

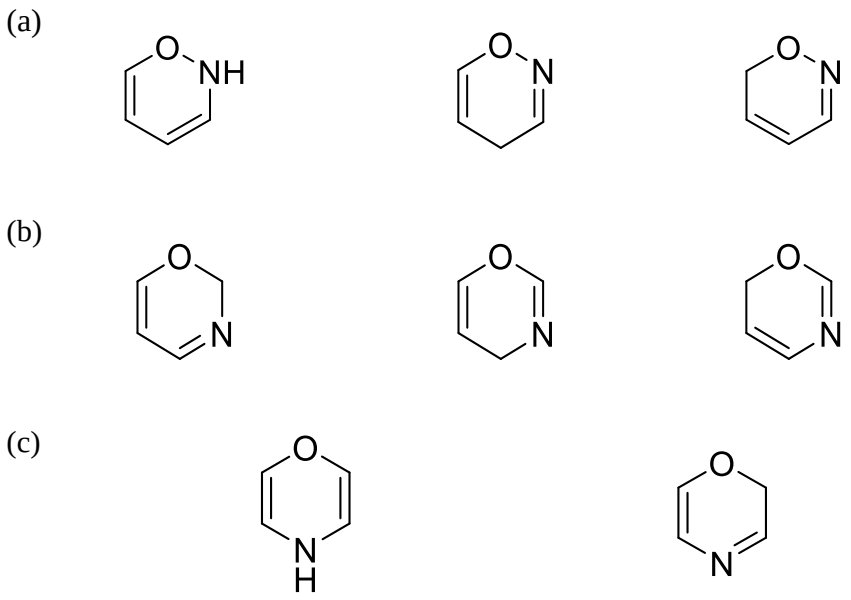


**Figure 1.2 Common oxazine isomers: (a) 1,2-oxazine, (b) 1,3-oxazine, and (c) 1,4-oxazin**

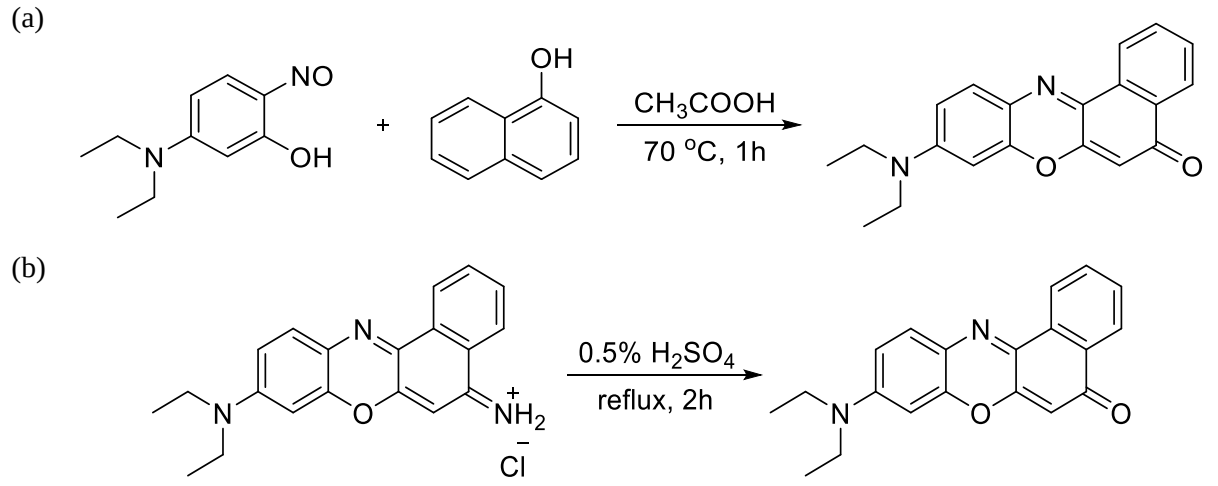


**Figure 1.3 (a) Original synthesis of Nile red and (b) synthesis from Nile blue**

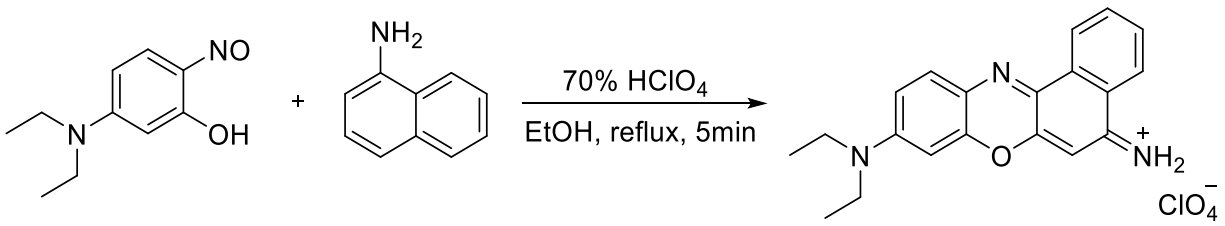


**Figure 1.4 Original synthesis of Nile blue**

Nile red is a neutral dye that has the benzophenoxazinone system while Nile blue is a cationic dye that has the benzophenoxazinium system. Both dyes have diethylamino group as an electron donor group but different acceptor groups, a carbonyl group in Nile red and an iminium group in Nile blue. The electron delocalization across the aromatic ring is shown in Figure 1.5. The uncharged heterocyclic structure of Nile red allows the compound to be a suitable hydrophobic probe.[28] The positively charged iminium group on Nile blue makes it a sensitive indicator for pH.[29] Due to the differences in the ionic charge between the two compounds, the water-solubility of Nile

blue is better compared to that of Nile red. As a result, Nile red does not fluoresce in aqueous solutions whereas Nile blue fluoresces in the same solution exhibiting a low quantum yield value.

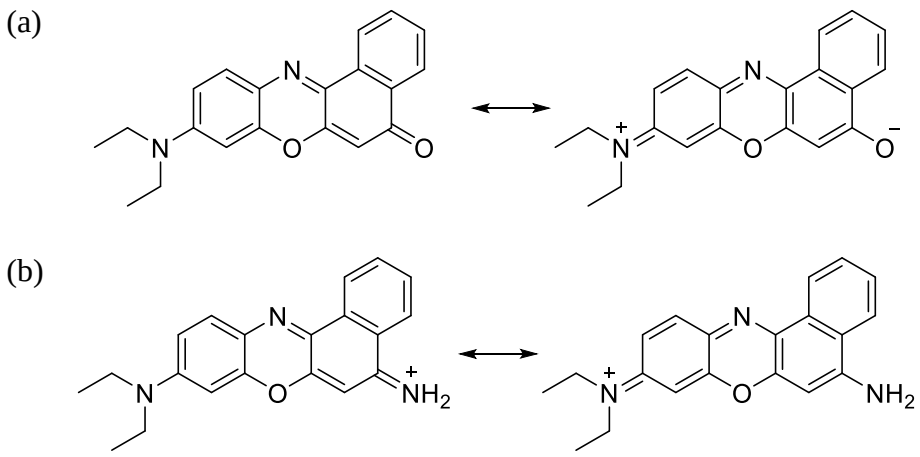


**Figure 1.5 Electron delocalization of (a) Nile red and (b) Nile blue**

The solvatochromic behavior of both compounds is a good indicator of solvent polarity. In non-polar solvents, they fluoresce in the visible to the near-infrared region of the spectrum with high quantum yield values. In polar solvents, however, the quantum yield values are reduced, and fluorescence spectra exhibit bathochromic shifts. The solvatochromic effect can be explained by the fact that Nile red undergoes large changes in the dipole moment in the excited state of the molecule. The diethylamino group can be twisted in polar solvents due to its flexibility making the donor orbital perpendicular to the acceptor orbital.[30] This corresponds to a twisted intramolecular charge transfer (TICT) state.[31] On the other hand, Nile blue forms H-aggregation due to plan-to-plan arrangement in aqueous solution.[32]

The compounds belong to this family have been recognized for their unique photophysical properties as they display strong absorbance and fluorescence in the visible to the near-infrared region. One obvious difference between the optical properties of Nile red and Nile blue is that the maximum absorption of Nile red is 550 nm in methanol whereas that for Nile blue is 630 nm. The difference in maxima wavelength of 80 nm between the two molecules can be attributed to the strength of the donor-acceptor system. Nile blue contains the positively charged iminium group that is stronger acceptor than the carbonyl group in Nile red. The Nile blue acceptor induces a strong net dipole across the ring making the character of orbital $sp^2$ more noticed compared to Nile red.[33]

## 1.6 Dye aggregation

One of the most distinctive features of dyes is their tendency to self-associate or aggregate in aqueous solutions. It is necessary to understand this behavior of dyes in non-covalent labeling because of the influence of non-covalent interaction on the binding between the dye and the protein as well as self-association of the dye. The aggregation band that is shifted to a longer wavelength (bathochromically shifted) is called J-aggregation in accord with its inventor E.E.Jelley.[34-35] In contrast, the aggregation band shifted to a shorter wavelength is called H-aggregation (H denotes hypsochromic shift) with respect to the monomer band. Dye molecules aggregate in different formations based on the angle of slippage (α). It was reported that a small slippage angle ($\alpha > \sim32°$) results in H-aggregation while J-aggregation is the result of a lager slippage angle ($\alpha < \sim32°$)[36]. Moreover, H-aggregation is similar to a card pack arrangement whereas J-aggregation can form different arrangements such as brickwork, ladder, or staircase[37-38] as indicated in Figure 1.6.

The aggregation behavior of dyes can be explained according to the exciton nature of electronic transitions as illustrated in Figure 1.7. According to exciton theory,[39] the dye molecule is considered a point dipole and the excitonic state of the dye aggregate splits into two levels: an upper and a lower level. A transition to the upper level with parallel transition moments results in a hypsochromic shift with respect to the monomer band. The blue-shifted H-aggregation is formed when dye molecules undergo a plane-to-plane arrangement. In this case, the dye becomes less fluorescent with low values of extinction coefficient and quantum yield and large Stokes shift because the transition to the upper state is not allowed. On the other hand, a transition to the lower level with perpendicular transition moments leads to a bathochromic shift with respect to the monomer band. The red-shifted J-aggregation is observed when dye molecules aggerate in a head-to-tail arrangement. The aggregation is characterized by a high quantum yield value and small Stokes shift since the transition to the lower state is allowed.[40-41] Such a classification into H-aggregation and J- aggregation is just for clarification. However, in some cases the two types of aggregation can be observed simultaneously. Belfield and coworkers mentioned that the absorption spectrum of pseudoisocyanine dyes in aqueous solutions includes the long wavelength J-band as well as H-band.[42]

It has been known that formation of aggregation occurs at high concentration of the dye. Nonetheless, the degree of aggregation is influenced by some parameters such as the dye structure, ionic strength of the media, temperature, pH level, and polarity of solvent.[43] Dye aggregation, for instance, is more pronounced in water than in organic solvents. The aggregation phenomenon of dyes is of great importance in several applications. J-aggregation has been used in silver halide film photography, organic solar cells, and photonic devices whereas H-aggregation is mainly applied in biological imaging and binding studies.[36, 41]

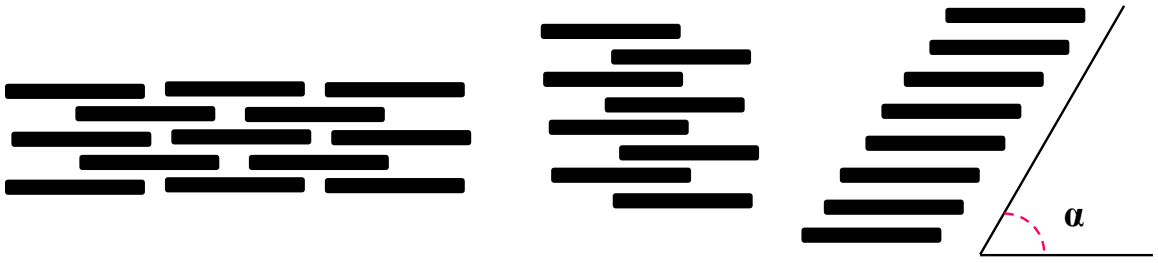


**Figure 1.6 Schematic representation of different arrangements of dye aggregates: (a) brickwork, (b) ladder, and (c) staircase**

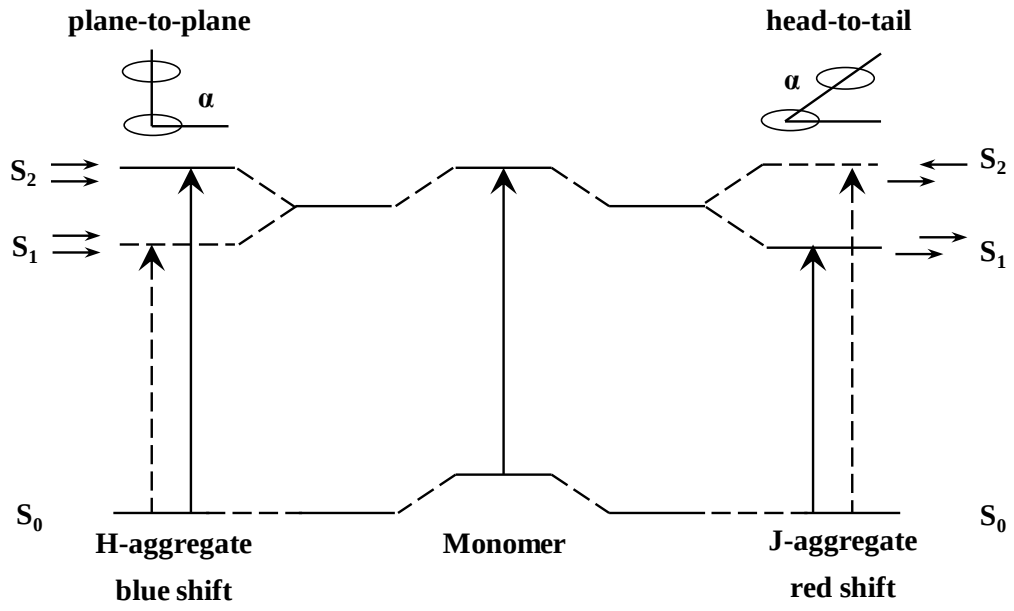


**Figure 1.7 Schematic representation of the energy variations on electronic transitions and their relationship to dye aggregation based on the molecular exciton theory**

## 1.7 Protein labeling

Studying protein labeling requires consideration of the type of labeling, the binding sites, and interaction with a ligand. Many labeling methods such as SDS-PAGE, mass spectrometry (MALDI-TOF MS), colorimetric sensors, fluorescent probes, liquid chromatography, and electrochemical biosensors have been used for this purpose.[44-47] Among these methods, labeling with fluorescent probes has many advantages including the high sensitivity and non-destructive character of fluorescence technique as well as small volume and low concentration of the fluorophore.[48]

The fluorophore can either bind to the protein by the formation of covalent bonds or non-covalently through different interactions such as hydrogen bonding, hydrophobic effect, and electrostatic interaction. The covalent labeling is achieved when the fluorescent probe contains reactive moieties that bind specifically to a functional group in the protein. Such reactive moieties of the fluorophore are isothiocyanate, isocyanate, acyl azide, N-hydroxysuccinimide (NHS) ester, sulfonyl chloride[49] as shown in Figure 1.8. They are conjugated predominantly with proteins via the α-amino group of the lysine side chains or N-terminal amino groups. Functional groups of proteins such as amines, thiols, phenols, and carboxylic acids are targeted by fluorophore for covalent binding. Due to the formation of bonds between the protein and the fluorophore in covalent labeling, the resulting complex is more stable than that of non-covalent. However, covalent labeling is laborious and time-consuming due to the need for purification steps. For example, purification of the labeled protein by ultrafiltration is considered a necessary step to remove unreacted reagents and fragment products.[50] Another disadvantage of the covalent method is labeling conditions are strict and must be selected carefully. Moreover, reduced separation efficiency and detection sensitivity because of the multiple labeling of the protein is one of the

drawbacks of covalent labeling. Jing and coworkers observed that multiple labeling of bovine serum albumin by cyanine dye (Cy5) due to the heterogeneity of final products led to a band broadening.[51]

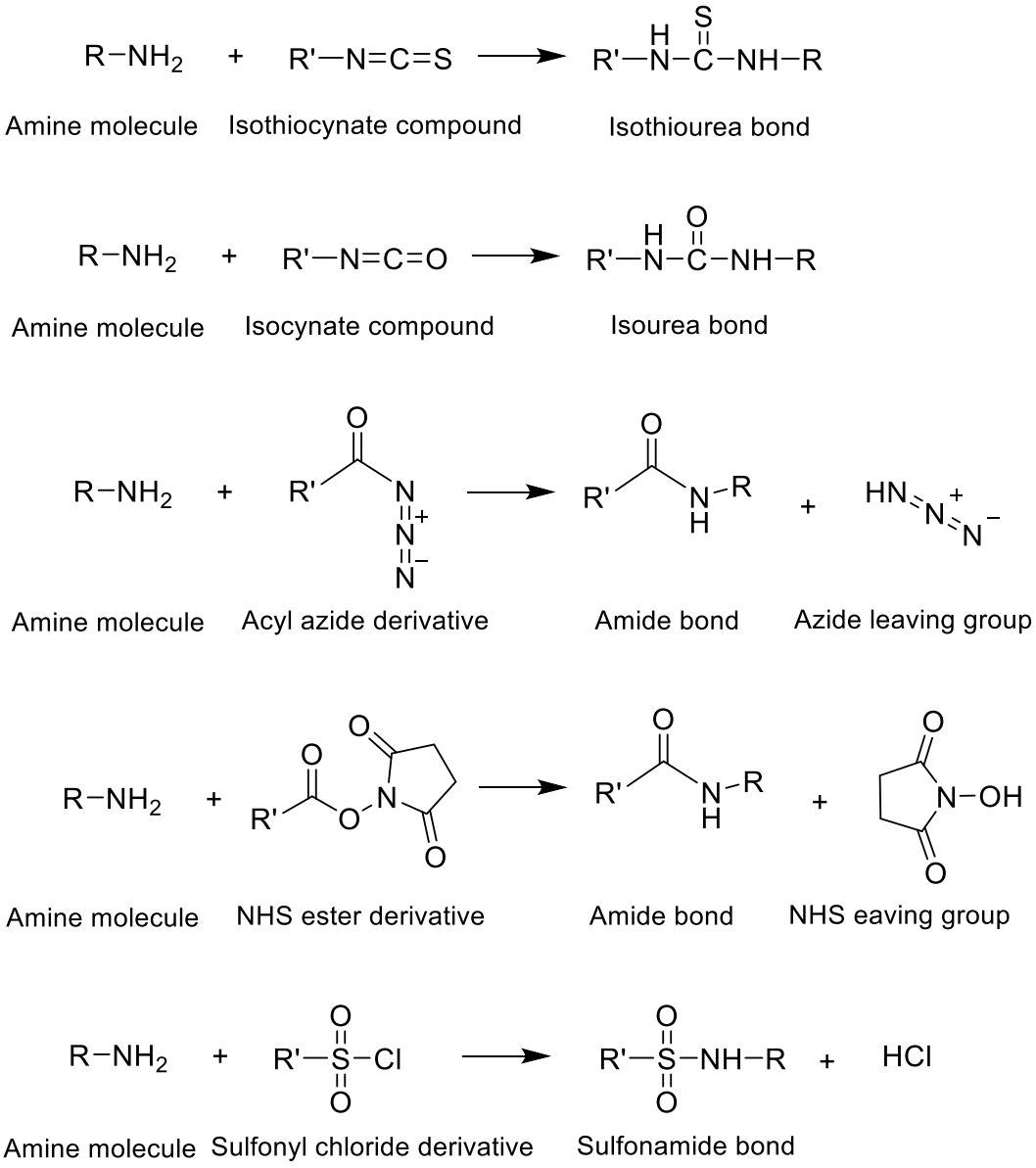


**Figure 1.8 Covalent labeling of proteins with fluorescent molecules containing functional groups**

In contrast, non-covalent labeling is fast and occurs at a physiological pH range. Unlike covalent labeling, non-covalent labeling is simple and can easily be attained by mixing the fluorescent probe with the protein of interest. In addition, the influence of non-covalent methods on the functional activity of the labeled proteins is less than covalent methods.[52] However, determination the mechanism of the non-covalent labeling such as hydrogen bonding, hydrophobic effect, and electrostatic interaction is quite challenging.

## 1.8 Human serum albumin

The interactions between a ligand and human serum albumin (HSA), a drug carrier in the circulatory system, is an important factor to understand the pharmacokinetics of drugs as well as for designing and developing new drugs.[53] HSA is one of the most abundant proteins in human blood plasma with a concentration of 30-50 g/L. This protein is secreted by liver cells with a molecular mass of 66.5 kDa and a long half-life of approximately 20 days. HSA is comprised of 585 amino acids with 17 disulfide bonds that help to stabilize its structure. The amino acid sequence contains a large percentage of cysteine residues (6%), a large number of charged amino acids (31%), and only one tryptophan residue.[54]

The three-dimensional structure of HSA was determined first by He and Carter to a resolution of 2.8 Å.[55] The tertiary structure of the protein consists of three homologous domains: domain I, domain II, and domain III that form a heart-shaped molecule and each domain is further divided into subdomains: A and B. The main ligand binding sites are located in hydrophobic pockets in subdomains IIA and IIIA, known as Sudlow site I and II, respectively.[56] Ligands bind to HSA in site I mainly through hydrophobic interaction whereas binding in site II is a combination of electrostatic and hydrophobic nature.[57] Ligands targeting site I are often dicarboxylic acids with

bulky heterocyclic systems and a negative charge in the middle of the molecule. Alternatively, ligands binding to site II are typically aromatic carboxylic acids with a negative charge at one end of the molecule.[53] Despite the tremendous number of ligands interacting with HSA, it is particularly difficult to predict the binding site for a given ligand.

HSA has several important functions such as sustaining pH of blood, maintaining osmotic pressure, and transportation of fatty acids and hormones. Moreover, it possesses various catalytic activities for many reactions such as hydrolytic reactions, double bond formation, isomerization reactions, and oxidative-reductive transformations. In addition to its significant role in many physiological activities, HSA has a unique binding capability to ligands making the protein an excellent candidate for drug delivery.[54] Owing to its physiological importance and extraordinary ligand-binding capability, HSA has been extensively studied by several methods such as absorbance[58-59], fluorescence[58-60], 3D fluorescence[58, 61], high performance liquid chromatography (HPLC)[52], nuclear mass resonance (NMR)[58], capillary electrophoresis[62-63], capillary electrophoresis-laser induced fluorescence detection (CE-LIF)[60], circular dichroism[61], induced circular dichroism[64], and molecular modeling.[58]

**Spectroscopic determination of binding constant**

In non-covalent labeling, the binding constant of the protein-probe complex can be evaluated using spectroscopic measurements such as the absorbance and fluorescence. In the case of fluorescent probes, the optical properties of the probe are affected by interaction with the protein. Some spectral changes can be observed due to variations in surrounding environment of the fluorophore such as shifting the maximum wavelength bathchromically or hypsochromically and shifting the intensity hyperchromically or hypochromically.

The reaction between two species such as a dye (D) and a metal ion (M)[65-66], assuming 1:1 reaction stoichiometry, can be represented as:

$$D^- + M^+ \rightleftharpoons DM \quad (1.6)$$

where DM is the dye-metal complex, $D^-$ is the uncomplexed dye, and $M^+$ is the free metal ions in the solution. The equilibrium constant K can be expressed as:

$$K = \frac{[DM]}{[D^-][M^+]} \quad (1.7)$$

The total concentration of the dye $D_T$ is the sum of the DM complexed and uncomplexed forms:

$$[D_T] = [D^-] + [DM] \quad (1.8)$$

The equilibrium constant can be rewritten as:

$$K = \frac{[DM]}{([D_T] - [DM])\, a_{M^+}} \quad (1.9)$$

The equation (1.9) can be rearranged for solving DM as followed:

$$[DM] = \frac{K\,[D_T]\, a_{M^+}}{(1 + K\, a_{M^+})} \quad (1.10)$$

The intensity of fluorescence $I_f$ can be described by the following equation:

$$I_f = \varepsilon\, b\, c\, I_I Q \quad (1.11)$$

where ε is the molar absorptivity, b is the path length, c is the concentration, $I_I$ is the laser intensity, and Q is the quantum yield. In the dye-metal complex analysis, the only variable is concentration while other parameters are constant. Then, the intensity of fluorescence is written as:

$$I_f = k\,[DM] \quad (1.12)$$

where k is fluorescence proportionality constant and can be given by the following equation:

$$k = \varepsilon\, b\, I_I Q \qquad (1.13)$$

Substituting equation (1.10) into equation (1.12) to give the following relationship:

$$I_f = \frac{k\, K\, [D_T]\, a_{M^+}}{(1 + K\, a_{M^+})} \qquad (1.14)$$

Equation (1.15) is written in double reciprocal expression as followed:

$$\frac{1}{I_f} = \frac{1}{k\, [D_T]} + \left(\frac{1}{k\, [D_T]\, K}\right) \frac{1}{a_{M^+}} \qquad (1.15)$$

The equilibrium constant, K can be calculated by constructing a plot of $\frac{1}{I_f}$ versus $\frac{1}{a_{M^+}}$ which produces a straight-line relationship. As illustrated by the equation, dividing the intercept by the slope gives the equilibrium constant.

In case of non-covalent labeling of a protein such as HSA with a dye, the equilibrium or binding constant can be described according to the following equation:[67]

$$\frac{1}{\Delta F} = \frac{1}{k[\text{Dye}]} + \left(\frac{1}{k[\text{Dye}]K}\right) \frac{1}{[\text{HSA}]} \qquad (1.16)$$

## 1.9 Summary

Fluorescence spectroscopy is considered one of the most widely used techniques in many areas such as analytical chemistry, biology, and medicine due to its great sensitivity. Joblanski diagram that illustrates fluorescence and other radiative and non-radiative processes is depicted. Some common characteristics of fluorescence spectrometry are mentioned. A brief description of the two types of fluorescence quenching (collisional and static quenching), differences between the two types, and their applications are included. Some physical and chemical properties of

benzophenoxazine dyes as well as the original synthesis of Nile red and Nile blue are described. Aggregation or self-association is one of the most common behaviors of dyes in aqueous solutions. Dye molecules aggregate in different arrangements such as H-aggregation (plane-to-plane stacking) and J-aggregation (head-to-tail fashion). A comparison between the two types of protein labeling (covalent and non-covalent labeling) with fluorescent probes in term of experimental conditions, labeling rate, detection sensitivity, and purification steps is demonstrated. The chemical structure, ligand binding sites, and biological functions of human serum albumin are stated. Spectroscopic techniques allow for determination of the binding constant of a protein such as HSA and a dye.

**References**


1. Raymond, S. B.; Skoch, J.; Hills, I. D.; Nesterov, E. E.; Swager, T. M.; Bacskai, B. J., Smart optical probes for near-infrared fluorescence imaging of Alzheimer's disease pathology. *Eur J Nucl Med Mol Imaging* **2008,** *35 Suppl 1*, S93-8.
2. Moon, W. K.; Lin, Y. H.; O'Loughlin, T.; Tang, Y.; Kim, D. E.; Weissleder, R.; Tung, C. H., Enhanced tumor detection using a folate receptor-targeted near-infrared fluorochrome conjugate. *Bioconjugate Chemistry* **2003,** *14* (3), 539-545.
3. Alford, R.; Ogawa, M.; Choyke, P. L.; Kobayashi, H., Molecular probes for the in vivo imaging of cancer. *Mol. Biosyst.* **2009,** *5* (11), 1279-1291.
4. Pham, W.; Medarova, Z.; Moore, A., Synthesis and application of a water-soluble near-infrared dye for cancer detection using optical imaging. *Bioconjugate Chem.* **2005,** *16* (3), 735-740.
5. McCain, K. S.; Hanley, D. C.; Harris, J. M., Single-Molecule Fluorescence Trajectories for Investigating Molecular Transport in Thin Silica Sol-Gel Films. *Anal. Chem.* **2003,** *75* (17), 4351-4359.
6. Virk, H. S., *Luminescence : Basic Concepts, Applications and Instrumentation*. Switzerland: Trans Tech Publications: 2014.
7. Skoog, D. A.; Holler, F. J.; Crouch, S. R., Molecular Luminescence Spectrometry. In *Principles of instrumental analysis*, Thomson Brooks/Cole, 6th ed: Belmont, CA, 2007.
8. Lakowicz, J. R., *Principles of Fluorescence Spectroscopy*. New York: Springer, 3rd ed: 2006.
9. Würth, C.; González, M. G.; Niessner, R.; Panne, U.; Haisch, C.; Genger, U. R., Determination of the absolute fluorescence quantum yield of rhodamine 6G with optical

and photoacoustic methods – Providing the basis for fluorescence quantum yield standards. *Talanta* **2012,** *90*, 30-37.

10. Williams, A. T. R.; Winfield, S. A.; Miller, J. N., Relative fluorescence quantum yields using a computer-controlled luminescence spectrometer. *Analyst* **1983,** *108* (1290), 1067.
11. Kautsky, H., Quenching of luminescence by oxygen. *Transactions of the Faraday Society* **1939,** *35*, 216.
12. Zu, F.; Yan, F.; Bai, Z.; Xu, J.; Wang, Y.; Huang, Y.; Zhou, X., The quenching of the fluorescence of carbon dots: A review on mechanisms and applications. *Microchimica Acta* **2017,** *184* (7), 1899-1914.
13. Bacon, J. R.; Demas, J. N., Determination of oxygen concentrations by luminescence quenching of a polymer-immobilized transition-metal complex. *Anal. Chem.* **1987,** *59* (23), 2780-5.
14. Hyakutake, T.; Okura, I.; Asai, K.; Nishide, H., Dual-mode oxygen-sensing based on oxygen-adduct formation at cobaltporphyrin-polymer and luminescence quenching of pyrene: an optical oxygen sensor for a practical atmospheric pressure. *Journal of Materials Chemistry* **2008,** *18* (8), 917-922.
15. Li, F. M.; Wei, Y. G.; Chen, Y. Y.; Li, D. L.; Zhang, X., An Intelligent Optical Dissolved Oxygen Measurement Method Based on a Fluorescent Quenching Mechanism. *Sensors* **2015,** *15* (12), 30913-30926.
16. Jayaraman, S.; Verkman, A. S., Quenching mechanism of quinolinium-type chloride-sensitive fluorescent indicators. *Biophysical Chemistry* **2000,** *85* (1), 49-57.

17. Geddes, C. D., A halide sensor based on the quenching of fluorescence of an immobilised indolium salt. *Journal of Photochemistry and Photobiology A: Chemistry* **2000,** *137* (2), 145-153.

18. Geddes, C. D., Optical thin film polymeric sensors for the determination of aqueous chloride, bromide and iodide ions at high pH, based on the quenching of fluorescence of two acridinium dyes. *Dyes and Pigments* **2000,** *45* (3), 243-251.

19. Zhu, L.; Xu, G. H.; Song, Q.; Tang, T.; Wang, X.; Wei, F. D.; Hu, Q., Highly sensitive determination of dopamine by a turn-on fluorescent biosensor based on aptamer labeled carbon dots and nano-graphite. *Sensors and Actuators B-Chemical* **2016,** *231*, 506-512.

20. Wang, F.; Hao, Q.; Zhang, Y.; Xu, Y.; Lei, W., Fluorescence quenchometric method for determination of ferric ion using boron-doped carbon dots. *Microchimica Acta* **2016,** *183* (1), 273.

21. Iqbal, A.; Tian, Y.; Wang, X.; Gong, D.; Guo, Y.; Iqbal, K.; Wang, Z.; Liu, W.; Qin, W., Carbon dots prepared by solid state method via citric acid and 1,10-phenanthroline for selective and sensing detection of Fe2+ and Fe3+. *Sensors & Actuators: B. Chemical* **2016,** *237*, 408-415.

22. Gilchrist, T. L., *Heterocyclic Chemistry*. Longman: 1997.

23. Eicher, T.; Hauptmann, S.; Speicher, A., *The Chemistry of Heterocycles: Structures, Reactions, Synthesis, and Applications*. Wiley: 2013.

24. Smith, J. L., On the simultaneous staining of neutral fat and fatty acid by oxazine dyes. *Journal of Pathology & Bacteriology* **1908,** *12* (1), 1.

25. Möhlau, R.; Uhlmann, K., Zur Kenntniss der Chinazin- und Oxazinfarbstoffe. *Justus Liebigs Annalen der Chemie* **1896,** *289* (1), 90-130.

26. Greenspan, P.; Fowler, S. D., Spectrofluorometric studies of the lipid probe, nile red. *Journal Of Lipid Research* **1985,** *26* (7), 781-789.

27. Kanitz, A.; Hartmann, H., Preparation and characterization of bridged naphthoxazinium salts. *Eur. J. Org. Chem.* **1999,** (4), 923-930.

28. Brown, M. B.; Miller, J. N.; Seare, N. J., An investigation of the use of Nile Red as a long-wavelength fluorescent probe for the study of α1-acid glycoprotein-drug interactions. *Journal of Pharmaceutical and Biomedical Analysis* **1995,** *13*, 1011-1017.

29. Wu, L.; Ru, S.; Jian-Feng, G.; Yu-Jie, X.; Ying, X.; Jian-Mei, L.; Itoh, I.; Ihara, M., Reversible Near-Infrared pH Probes Based on Benzo[a]phenoxazine. *Analytical Chemistry* **2013,** *85* (15), 7419-7425.

30. Kawski, A.; Kuklinski, B.; Bojarski, P., Photophysical properties and thermochromic shifts of electronic spectra of Nile Red in selected solvents. Excited states dipole moments. *Chemical Physics* **2009,** *359* (1-3), 58-64.

31. Dutta, A. K.; Kamada, K.; Ohta, K., Spectroscopic studies of nile red in organic solvents and polymers. *J. Photochem. Photobiol. A-Chem.* **1996,** *93* (1), 57-64.

32. Ho, N. H.; Weissleder, R.; Tung, C. S., Development of water-soluble far-red fluorogenic dyes for enzyme sensing. *Tetrahedron* **2006,** *62* (4), 578-585.

33. Martinez, V.; Henary, M., Nile Red and Nile Blue: Applications and Syntheses of Structural Analogues. *Chem.-Eur. J.* **2016,** *22* (39), 13764-13782.

34. Jelley, E. E., Spectral Absorption and Fluorescence of Dyes in the Molecular State. *Nature* **1936,** *138*, 1009.

35. Scheibe, G., Variability of the absorption spectra of some sensitizing dyes and its cause. *Angew. Chem.* **1936,** *49*, 563.

36. Patonay, G.; Kim, J. S.; Kodagahally, R.; Strekowski, L., Spectroscopic study of a novel bis(heptamethine cyanine) dye and its interaction with human serum albumin. *Appl. Spectrosc.* **2005,** *59* (5), 682-690.

37. Czikkely, V.; Foersterling, H. D.; Kuhn, H., Extended dipole model for aggregates of dye molecules. *Chem. Phys. Lett.* **1970,** *6* (3), 207-10.

38. Harrison, W. J.; Mateer, D. L.; Tiddy, G. J. T., Liquid-Crystalline J-Aggregates Formed by Aqueous Ionic Cyanine Dyes. *J. Phys. Chem.* **1996,** *100* (6), 2310-21.

39. Philpott, M. R.; Lee, J. W., Exciton theory of the excited electronic states of coupled molecular aggregates. *J. Chem. Phys.* **1972,** *57* (5), 2026-33.

40. Mishra, A.; Behera, R. K.; Behera, P. K.; Mishra, B. K.; Behera, G. B., Cyanines during the 1990s: A Review. *Chemical Reviews* **2000,** *100* (6), 1973-2012.

41. Bricks, J. L.; Slominskii, Y. L.; Panas, I. D.; Demchenko, A. P., Fluorescent J-aggregates of cyanine dyes: basic research and applications review. *Methods and Applications in Fluorescence* **2018,** *6* (1), 31.

42. Belfield, K. D.; Bondar, M. V.; Hernandez, F. E.; Przhonska, O. V.; Yao, S., Two-photon absorption of a supramolecular pseudoisocyanine J-aggregate assembly. *Chem. Phys.* **2006,** *320* (2-3), 118-124.

43. Valdes-Aguilera, O.; Neckers, D. C., Aggregation phenomena in xanthene dyes. *Acc. Chem. Res.* **1989,** *22* (5), 171-7.

44. Elpidina, E. N.; Semashko, T. A.; Smirnova, Y. A.; Dvoryakova, E. A.; Dunaevsky, Y. E.; Belozersky, M. A.; Serebryakova, M. V.; Klyachko, E. V.; Abd El-latif, A. O.; Oppert, B.; Filippova, I. Y., Direct detection of cysteine peptidases for MALDI-TOF MS analysis using fluorogenic substrates. *Analytical Biochemistry* **2019,** *567*, 45-50.

45. Jung, Y. K.; Park, H. G., Colorimetric polydiacetylene (PDA) liposome-based assay for rapid and simple detection of GST-fusion protein. *Sensors and Actuators B: Chemical* **2019,** *278*, 190-195.

46. Bravo-Veyrat, S.; Hopfgartner, G., High-throughput liquid chromatography differential mobility spectrometry mass spectrometry for bioanalysis: determination of reduced and oxidized form of glutathione in human blood. *Anal. Bioanal. Chem.* **2018,** *410* (27), 7153-7161.

47. Bing, X. H.; Wang, G. R., Label Free C-reactive Protein Detection Based on An Electrochemical Sensor for Clinical Application. *International Journal of Electrochemical Science* **2017,** *12* (7), 6304-6314.

48. Sahoo, H., Fluorescent labeling techniques in biomolecules: a flashback. *Rsc Advances* **2012,** *2* (18), 7017-7029.

49. Hermanson, G. T., *Bioconjugate Techniques.* London : Academic Press, 3rd ed: 2013.

50. Miki, S.; Kaneta, T.; Imasaka, T., Immunoassay for human serum albumin using capillary electrophoresis-semiconductor laser-induced fluorometry. *J. Chromatogr. B: Biomed. Sci. Appl.* **2001,** *759* (2), 337-342.

51. Jing, P.; Kaneta, T.; Imasaka, T., Band broadening caused by the multiple labeling of proteins in micellar electrokinetic chromatography with diode laser-induced fluorescence detection. *Journal of Chromatography A* **2002,** *959* (1), 281-287.

52. Williams, R. J.; Lipowska, M.; Patonay, G.; Strekowski, L., Comparison of covalent and noncovalent labeling with near-infrared dyes for the high-performance liquid chromatographic determination of human serum albumin. *Anal. Chem.* **1993,** *65* (5), 601-5.

53. Kragh-Hansen, U.; Chuang, V. T. G.; Otagiri, M., Practical aspects of the ligand-binding and enzymatic properties of human serum albumin. *Biol. Pharm. Bull.* **2002,** *25* (6), 695-704.

54. Alekseev, R. J.; Rebane, A. L., *Serum Albumin: Structure, Functions and Health Impact*. New York: Nova Science Publishers: 2012.

55. He, X. M.; Carter, D. C., Atomic structure and chemistry of human serum albumin. *Nature* **1992,** *358*, 209.

56. Sudlow, G.; Birkett, D. J.; Wade, D. N., Characterization of two specific drug binding sites on human serum albumin. *Mol. Pharmacol.* **1975,** *11* (6), 824-32.

57. Artali, R.; Bombieri, G.; Calabi, L.; Del Pra, A., A molecular dynamics study of human serum albumin binding sites. *Il Farmaco* **2005,** *60*, 485-495.

58. Zhou, X.; Li, X.; Chen, X., Binding mechanism of Orange G to human serum albumin: Saturation transfer difference-NMR, spectroscopic and computational techniques. *Dyes and Pigments* **2013,** *98*, 212-220.

59. Tatikolov, A. S.; Panova, I. G., Spectral and fluorescent study of the noncovalent interaction of a meso-substituted cyanine dye with serum albumins. *High Energy Chemistry* **2014,** *48* (2), 87-92.

60. Yan, W. Y.; Colyer, C. L., Fluorimetric studies and noncovalent labeling of protein with the near-infrared dye HIM for analysis by CE-LIF. *Journal of Separation Science* **2005,** *28* (12), 1409-1415.

61. Byadagi, K.; Meti, M.; Nandibewoor, S.; Chimatadar, S., Investigation of binding behaviour of procainamide hydrochloride with human serum albumin using synchronous,

3D fluorescence and circular dichroism. *Journal of Pharmaceutical Analysis* **2017,** *7* (2), 103-109.

62. McCorquodale, E. M.; Colyer, C. L., Indocyanine green as a noncovalent, pseudofluorogenic label for protein determination by capillary electrophoresis. *Electrophoresis* **2001,** *22* (12), 2403-2408.

63. Kim, H. S.; Austin, J.; Hage, D. S., Identification of drug-binding sites on human serum albumin using affinity capillary electrophoresis and chemically modified proteins as buffer additives. *Electrophoresis* **2002,** *23* (6), 956-963.

64. Tramarin, A.; Tedesco, D.; Naldi, M.; Baldassarre, M.; Bertucci, C.; Bartolini, M., New insights into the altered binding capacity of pharmaceutical-grade human serum albumin: site-specific binding studies by induced circular dichroism spectroscopy. *Journal of Pharmaceutical and Biomedical Analysis* **2019,** *162*, 171-178.

65. Casay, G. A.; Shealy, D. B.; Patonay, G., Near-Infrared Fluorescence Probes. In *Topics in Fluorescence Spectroscopy, Volume 4: Probe Design and Chemical Sensing*, Lakowicz, J. R., Ed. Boston, MA: Springer US: 2000.

66. Tarazi, L.; Narayanan, N.; Sowell, J.; Patonay, G.; Strekowski, L., Investigation of the spectral properties of a squarylium near-infrared dye and its complexation with Fe(III) and Co(II) ions. *Spectrochim. Acta, Part A* **2002,** *58A* (2), 257-264.

67. Welder, F.; Paul, B.; Nakazumi, H.; Yagi, S.; Colyer, C. L., Symmetric and asymmetric squarylium dyes as noncovalent protein labels: a study by fluorimetry and capillary electrophoresis. *Journal of Chromatography B* **2003,** *793* (1), 93-105.

# 2 SPECTROSCOPIC CHARACTERIZATION OF BENZOPHENOXAZINE DYES IN SOME SOLVENTS

## 2.1 Introduction

Benzophenoxazine dyes such as Nile red and Nile blue have received significant attention in numerous applications due to their unique properties. Nile red has been used for histochemical staining of lipids because of its high hydrophobicity. Greenspan and coworkers applied Nile red for the detection of neutral lipids such as triacylglycerols and cholesteryl esters in some animal cells. The dye showed specificity and selectivity for lipid droplets as indicated by fluorescence microscopy and flow cytofluorometry.[1] Moreover, Nile red exhibited superior performance as a hydrophobic probe compared to the traditional lipid stains such as Oil Red O in which intense fluorescence and more lipid deposits were obtained.[2] Recently, Nile red has been proposed as a determination method of neutral lipids in some biological samples such as microalgal cell.[3-4] Over the last decade, microalgae have received considerable attention for their potential use for biofuel production. Moreover, microalgae containing 50% of neutral lipids by dry weight are considered a promising source of renewable fuel. Chen and coworkers described a rapid and effective method with high output to analyze the lipid content in nine algal species by the use of the fluorescent dye, Nile red.[5] More recently, Nile red has been investigated to study the interaction with some saturated and unsaturated phospholipid membranes as well as lipid-cholesterol membranes.[6-7] On the other hand, one of the most significant applications of Nile blue is a DNA marker. Nile blue binds to DNA through static quenching in two different binding models based on the concentration. At low concentrations of DNA, Nile blue is electrostatically bound to DNA. At high concentrations of DNA, the binding model changes to intercalative interaction. The use of Nile blue in such

application is more favorable than other DNA intercalators such as ethidium bromide (EB) in terms of low toxicity and cost.[8-10] Due to the high affinity of the dye to DNA, a group of researchers has extended the binding interaction to include some benzo[a]phenoxazinium derivatives. Raju and coworkers developed four novel derivatives of Nile blue with different alkyl groups attached to the amine at the 9-position for DNA binding. The results indicated that all dyes interact with DNA, and the derivatives with diethyl and octyl substituents specifically showed intercalative behavior.[11] Nile red and Nile blue have been employed in the study of microheterogeneous systems such as SDS (sodium dodecyl sulfate) and CTAP (cetyltrimethylammonium bromide) micelles and reverse micelles.[10, 12-14] Furthermore, it has been reported that both dyes form complexes with cyclo-dextrines of different stoichiometries such as 1:1 and 2:1.[6, 9, 15]

Nile red and Nile blue has been known for a long time as fluorescent dyes. An excellent fluorophore would be a molecule that has particular characteristics including high molar absorptivity and quantum yield values, large Stokes shifts, good photostability, functional groups capable of interacting with biomolecules, excitation wavelength accessible to the fluorometer detection limit, and a sharp emission spectrum in the near-infrared (NIR) region of the electromagnetic spectrum. This region is the most useful for bioanalytical application because the interference of autofluorescence background is limited, and biomolecules are exposed to the least damages from excitation process.[16] Despite the vast applications of Nile red and Nile blue, there are some restrictions of using the dyes in aqueous media due to the poor solubility and the reduction of fluorescence intensity. Therefore, extensive efforts have been paid to synthesizing several derivatives of Nile red and Nile blue for improved optical properties. The synthesis process involves incorporating several functional groups capable of binding to biomolecules with high quantum yield values in the region of 600 nm or higher which is the most useful region for

biological application. The groups can be mono or disubstituted at the 2-position and the amino side chain at the 9-position for Nile red derivatives. In addition to the two positions, there is an extra position for Nile blue derivatives at the 5-amino position. For instance, water solubility can be enhanced by incorporating polar substituents into the benzophenoxazine backbone such as hydroxyl group, carboxylic acid, sulfonic acid, triethylene glycol, and side-chain chlorinated.[16-19] Moreover, several Nile blue derivatives have been designed with different alkyl groups at the side chain for binding enhancement with DNA.[11] Several derivatives of Nile Red and Nile blue have been successfully synthesized by Henary's group. These compounds have been designed with specific structures to be good fluorophores. Thus, it is of great interest to characterize both types of these derivatives as well as Nile Red and Nile blue using UV-visible and fluorescence spectroscopy and evaluate their optical properties.

## 2.2 Experimental

### *2.2.1 Instrumentation*

Absorbance spectra were acquired using a Cary 3G UV-visible spectrophotometer (Varian Inc., Palo Alto, CA) interfaced to a PC. Fluorescence spectra were achieved using a K2 Spectrofluorometer (ISS Inc., Champaign, IL) interfaced to a PC. Excitation was achieved using a Xenon Arc lamp, model PS 300-1, (ILC Technology Inc., Sunnyvale, CA). All measurements were performed in 1.0 cm disposable plastic cuvettes. Photostability studies were acquired using a UV-Vis lamp with an input power of 120V-60Hz, Output PWR of 78W, lamp type of T5-G1439W, and model SE-42336 (SolarMax HO). Nanopure water was obtained using an ELGA Purelab.

### *2.2.2 Chemicals and reagents*

Nile red (NR) and Nile blue (NB) were obtained from Sigma-Aldrich (St. Louis, MO). Rhodamine 6G and rhodamine B were obtained from Aldrich Chemical Company (Milwaukee, WI). Dimethyl sulfoxide (DMSO), methanol, and ethanol (200 proof ethanol) were obtained from Acros Organics (99.9%) (Belgium), Sigma-Aldrich (≥ 99.9%) (St. Louis, MO), and Koptec (King of Prussia, PA), respectively. Sodium phosphate monobasic and sodium phosphate dibasic obtained from Aldrich Chemical Company (Milwaukee, WI). Benzophenoxazine derivatives were provided by the research group of Dr. Maged Henary; synthesized by Vincent Martinez. Dye formation involves several chemical reactions starting with an alkylation reaction followed by a nitrosation reaction and finally a condensation reaction. The dyes have been designed with particular structures and different substituent groups on the amine side chain to be good fluorophores. These derivatives can be classified into two types according to the type of amine attached to benzophenoxazine backbone at the 9-position which are dialkylated and monoalkylated derivatives containing tertiary and secondary amine, respectively. The chemical structures of Nile red derivatives and Nile blue derivatives are shown in Figures 2.1 and 2.2.

**(a)**

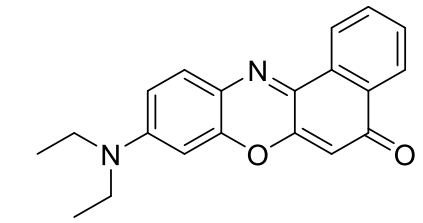

**NR**

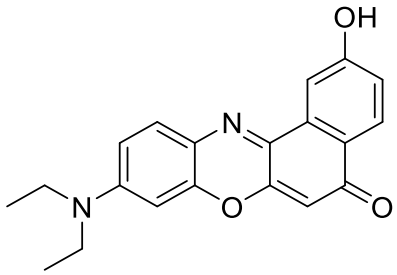

**VM3**

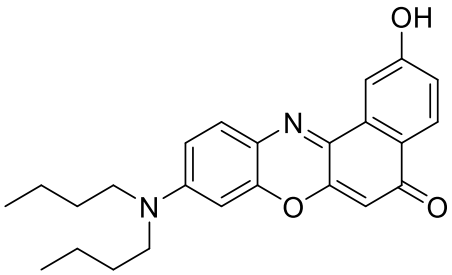

**VM6**

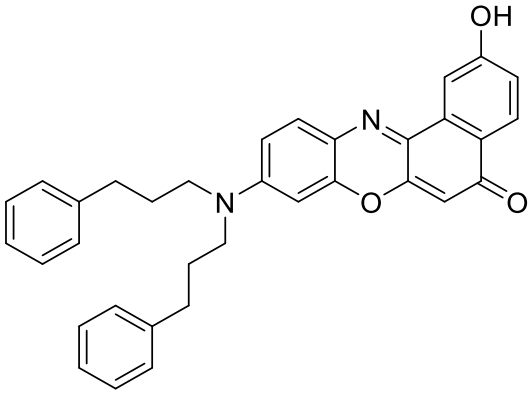

**VM8**

**(b)**

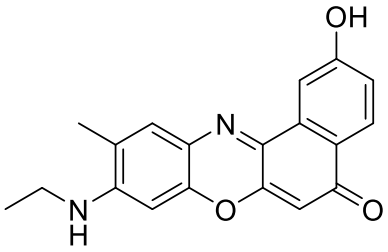

**VM20**

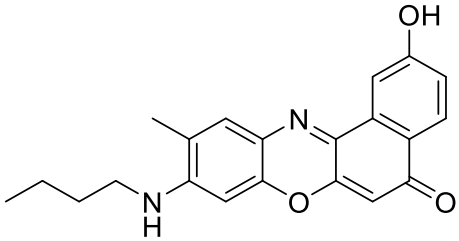

**VM25**

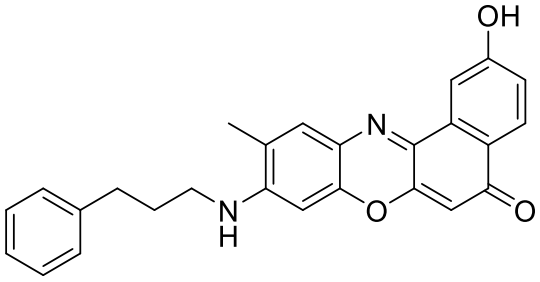

**VM23**

**Figure 2.1 Chemical structures of (a) dialkylated derivatives and (b) monoalkylated derivatives of Nile red**

**(a)**

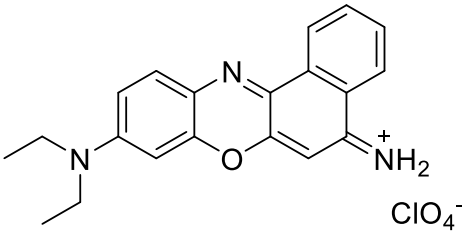

**NB (VM47)**

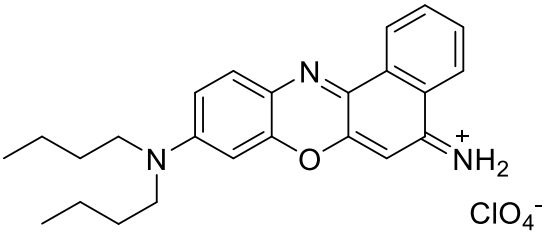

**VM38**

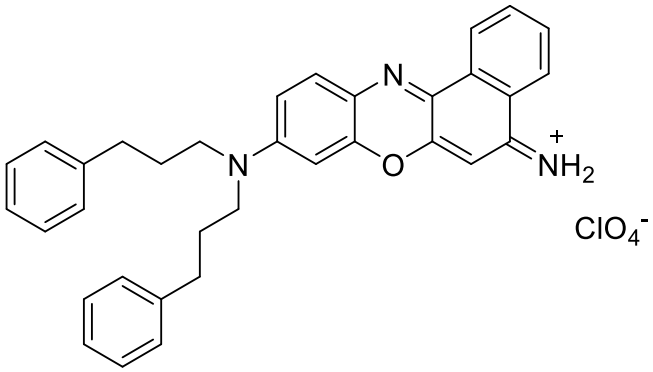

**VM46**

**(b)**

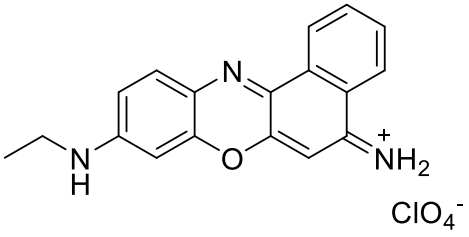

**VM41**

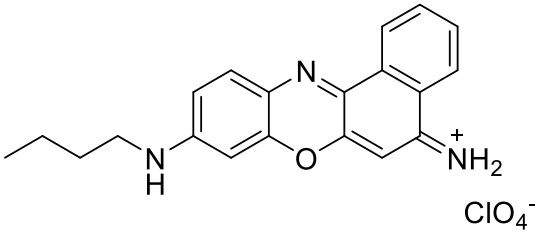

**VM44**

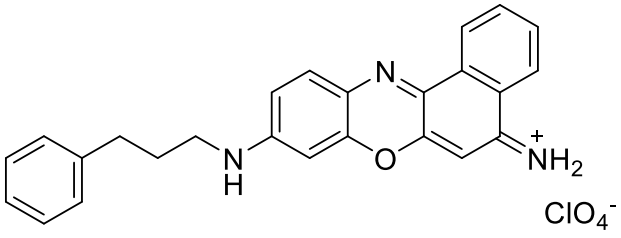

**VM45**

**Figure 2.2 Chemical structures of (a) dialkylated derivatives and (b) monoalkylated derivatives of Nile blue**

### *2.2.3 Stock solutions preparation*

Stock solutions of Nile red and Nile blue derivatives were prepared by dissolving an appropriate amount of each dye in DMSO and then sonicated for 60 minutes in cold bath to ensure complete dissolution of the dye to a final concentration of 1.0 mM. All stock solutions were stored in dark vials at 4 °C when not in use. Phosphate buffer solution was prepared from sodium phosphate monobasic and sodium phosphate dibasic to a final concentration of 20 mM, pH 7.2. Dilutions of stock solutions were made as needed.

### *2.2.4 Determination of molar absorptivity*

Serial dilutions of each dye were prepared in DMSO and methanol with concentrations ranging from $0.5\times10^{-5}$ – $3.0\times10^{-5}$ and $0.2\times10^{-5}$ – $1.60\times10^{-5}$ M for Nile red derivatives and Nile blue derivatives, respectively. It was possible to determine the molar absorptivity values in 20 mM phosphate buffer (pH 7.2) for some monoalkylated Nile blue derivatives namely **VM41** and **VM44** in the same concentration range. All working solutions in methanol and phosphate buffer contained less or about 3.0% (v/v) DMSO to facilitate the dye dissolution. The maximum wavelength of absorption ($\lambda_{Abs}$) of each dye was determined, and the molar absorptivity values of each dye were calculated using Beer's law:

$$A = \varepsilon bc \qquad (2.1)$$

where A is the sample absorbance recorded by the spectrometer, $\varepsilon$ is the molar absorptivity (or extinction coefficient) in $M^{-1}$ $cm^{-1}$, b is the path length of light in centimeter, c is the sample concentration in molarity. Plotting absorbance values at $\lambda_{Abs}$ as a function of the dye concentration yields a straight line in which the slope is the molar absorptivity ($\varepsilon$). Duplicate absorbance measurements were obtained, and the average molar attenuation values were reported.

### *2.2.5 Determination of quantum yield*

Serial dilutions of each dye were prepared in DMSO and methanol at concentrations diluted tenfold more than the absorbance measurements in which the absorbance values were below 0.1 units to avoid inner filter effects or self-quenching. It was possible to determine the quantum yield values of monoalkylated derivatives of Nile blue particularly **VM41** and **VM44** in 20 mM phosphate buffer (pH 7.2) in the same concentration range. All working solutions in methanol and phosphate buffer contained less or about 3.0% (v/v) DMSO to facilitate the dye dissolution. The relative method was used to determine quantum yield values for all dyes using rhodamine 6G and Nile blue as standards and applying the equation:

$$\Phi_S = \Phi_{STD}\left[\frac{\text{Slope}_S}{\text{Slope}_{STD}}\right]\left[\frac{\eta^2_S}{\eta^2_{STD}}\right] \qquad (2.2)$$

where $\Phi_S$ and $\Phi_{STD}$ are the quantum yield of the sample and the standard, $\text{Slope}_S$ and $\text{Slope}_{STD}$ are the slopes of plotting the area under the emission curve as a function of the absorbance value at excited wavelength of the sample and the standard. $\eta_S$ and $\eta_{STD}$ are the refractive index of the solvent of the sample and the standard. Duplicate measurements were obtained, and the average quantum yield values were reported. Nile red derivatives were excited at 500 nm in both solvents, DMSO and methanol. Nile blue derivatives in DMSO were excited at 580 nm and for those in methanol and phosphate buffer were excited at 560 nm. The excitation wavelengths have been changed to ensure a full integration of emission peaks especially for the monoalkylated derivatives since they are blue-shifted compared to dialkylated derivatives.

To obtain quantitative information about benzophenoxazine derivatives, some parameters should be taking into account other than molar absorptivity and quantum yield. Such parameter is the molecular brightness (MB) of the dye which is the product of the extinction coefficient (ε) and

the quantum yield (Φ).[20] Another parameter should be considering is the full width at half maximum (FWHM)[19] which defines as the difference in wavelength between two points on both sides of a peak in which the intensity is 50% of the maximum value. FWHM is a useful way of describing the sharpness of a spectrum since a sharp emission spectrum is a feature of the good fluorophore as mentioned previously.

### *2.2.6 Photostability studies*

In this study, two sets of experiments were performed to investigate the photostability of the dye. The first set was a fixed concentration in micromolar range of benzophenoxazine derivatives in DMSO; $1.5\times10^{-5}$ M and $1.0\times10^{-5}$ M for Nile red and Nile blue derivatives, respectively. This set was kept in sealed tubes and exposed to the UV-Vis lamp (about 20-25 cm away from the source) 24 hours for fifteen consecutive days. The entire set with the lamp was kept in a closed box to control the amount of light exposed to the sample and to avoid any chance of stray light. The second set was the same concentration of the dyes in DMSO in sealed tubes and kept in the dark (as a control) for the same period of time. The dye concentration was chosen to maintain reasonable absorbance response during the fifteen days. Absorbance values at maximum wavelengths of absorbance for both sets were acquired every three days. Duplicate measurements were obtained, and the average values were reported.

## 2.3 Results and discussion

### *2.3.1 Spectroscopic characterization of Nile red derivatives*

Spectroscopic studies were conducted to characterize Nile red derivatives and evaluate their optical properties in some solvents such as DMSO and methanol. Photophysical analyses

using UV-vis spectroscopy and fluorescence spectroscopy consider the first stage to examine some bioanalytical applications of benzophenoxazine derivatives. Dialkylated derivatives (NR, **VM3**, **VM6**, and **VM8**) and monoalkylated derivatives (**VM20**, **VM25**, and **VM23**) displayed similar optical properties in both solvents. For instance, the maximum wavelengths of absorbance ($\lambda_{Abs}$) in DMSO and methanol for dialkylated and monoalkylated derivatives were in the same wavelength range. Moreover, similar maximum wavelengths of emission ($\lambda_{em}$) for dialkylated and monoalkylated derivatives were recorded in both solvents. The absorption and emission spectra of monoalkylated derivatives displayed a blue shift compared to those of dialkylated derivatives of about 4-10 and 8-14 nm in DMSO and methanol respectively. This can be explained by the fact that dialkylated derivatives have an extra alkyl group, and thus more vibrational and rotational energy levels are added to the dye molecules. Furthermore, all Nile red derivatives had good molar absorptivities as confirmed by the linear increase in the absorbance value as the concentration of the dye increased. Stokes shift is determined by the differenc between the maximum wavelengths of absorption and emission spectra. As mentioned previously large Stokes shift is one characteristic of a good fluorophore, so differentiation between absorption and emission spectra becomes easy. Such fluorophores have been used extensively for probe design and bioimaging applications.[21-22] Large and similar Stokes shifts were obtained for Nile red derivatives in the two solvents. The quantum yield values of all derivatives were determined using the relative method to rhodamine 6G and rhodamine B. Quantum yield values of all dyes were good and comparable using the two standards. It was noticeable that quantum yield values in DMSO were greater than those in methanol due to the difference in hydrogen bond strength between the two solvents. Cser and coworkers pointed out that quantum yield value decreases as the hydrogen bonding of solvent increases because hydrogen bonding increases the internal conversion, the non-radiative decay.[23]

Moreover, monoalkylated derivatives showed higher quantum yield values in comparison to dialkylated derivatives in methanol only. The increase in quantum yield can be attributed to suppression of twisted intramolecular charge transfer due to hydrogen bonding formed between the dye and methanol since secondary amine at the 9-position in monoalkylated derivatives acts as hydrogen donor forming hydrogen bonds with the protic solvent. The use of rhodamine B as a standard for quantum yield determination resulted in higher values in DMSO compared to those obtained by rhodamine 6. However, lower quantum yield values were determined in the other solvent, methanol. This could be because rhodamine B is a temperature-dependent compound. Its quantum yield value is the range of 0.41 to 0.97, and the most common used value is 0.70.[24] The full width at half maximum (FWHM) of Nile red derivatives were similar in DMSO. However, in methanol small values were obtained for monoalkylated derivatives compared to those for dialkylated derivatives. The smaller the value is, the sharper the emission peak is and less aggregation the dye undergoes. Similar molecular brightness values for all Nile red derivatives in both solvents were obtained.

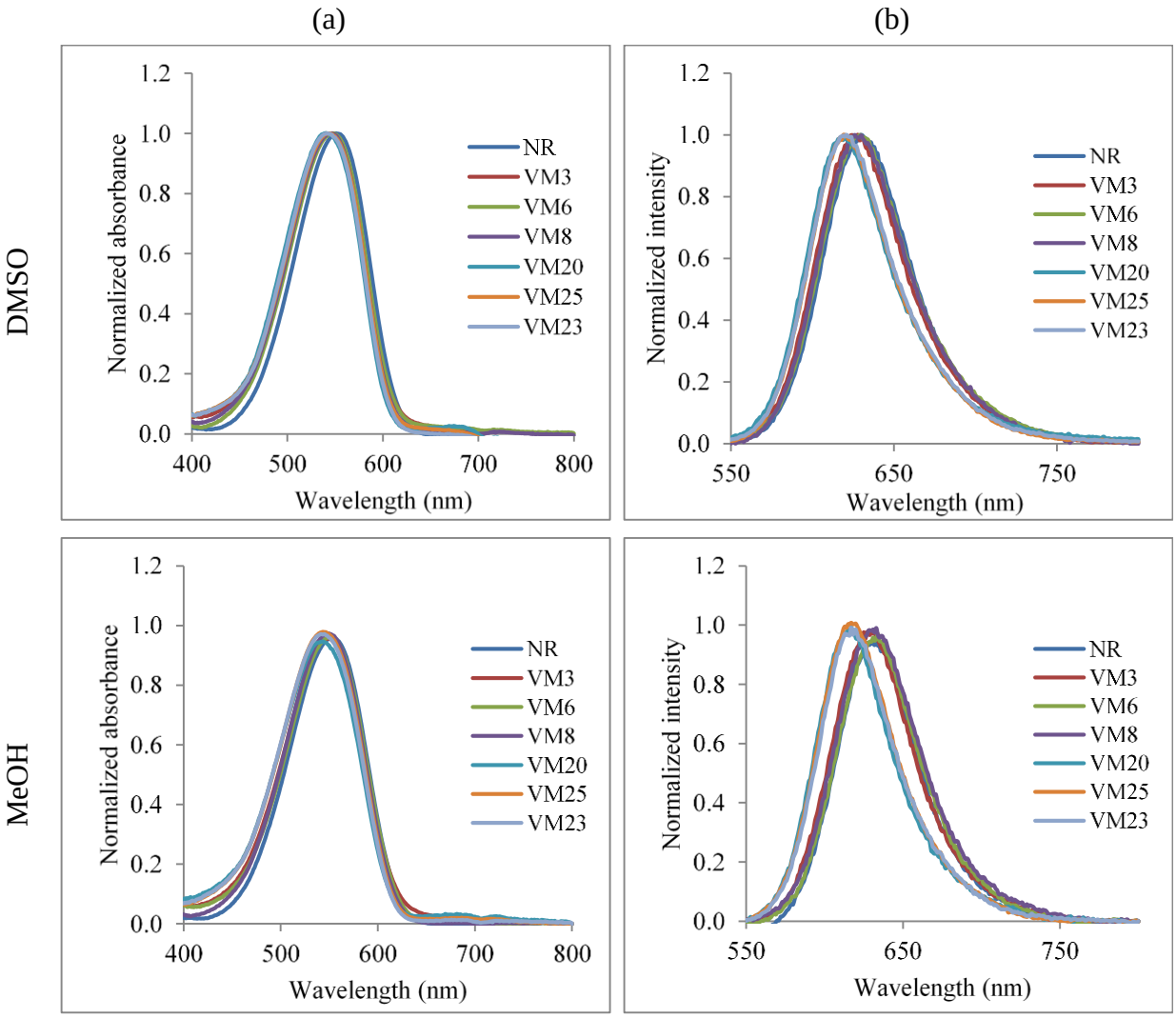


**Figure 2.3 (a) Absorbance and (b) emission spectra of Nile red derivatives in in some solvents**

**Table 2.1 Optical properties of Nile red derivatives in some solvents**

| Dye | $\lambda_{Abs}$ / $\lambda_{em}$ (nm) | ε ($M^{-1}cm^{-1}$) | Stokes shift (nm) | $\Phi_f$-R6G* | $\Phi_f$-RB* | FWHM (nm) | MB ($M^{-1}cm^{-1}$) | Solvent |
|---|---|---|---|---|---|---|---|---|
| NR | 552 / 633 | $4.03\times10^4$ | 81 | 0.42 | 0.45 | 62 | 16.91 | DMSO |
| | 554 / 631 | $3.91\times10^4$ | 77 | 0.28 | 0.23 | 61 | 10.96 | MeOH |
| **VM3** | 546 / 627 | $3.25\times10^4$ | 81 | 0.43 | 0.47 | 62 | 13.96 | DMSO |
| | 548 / 628 | $3.39\times10^4$ | 80 | 0.29 | 0.24 | 61 | 9.58 | MeOH |
| **VM6** | 548 / 630 | $3.76\times10^4$ | 82 | 0.45 | 0.49 | 63 | 16.92 | DMSO |
| | 551 / 632 | $3.90\times10^4$ | 81 | 0.26 | 0.20 | 62 | 10.15 | MeOH |
| **VM8** | 546 / 629 | $3.81\times10^4$ | 83 | 0.43 | 0.47 | 64 | 16.40 | DMSO |
| | 549 / 630 | $4.05\times10^4$ | 81 | 0.25 | 0.19 | 63 | 8.73 | MeOH |
| **VM20** | 543 / 619 | $2.34\times10^4$ | 76 | 0.47 | 0.51 | 60 | 10.99 | DMSO |
| | 542 / 616 | $2.30\times10^4$ | 74 | 0.39 | 0.32 | 57 | 8.98 | MeOH |
| **VM25** | 543 / 620 | $4.52\times10^4$ | 77 | 0.44 | 0.46 | 60 | 19.88 | DMSO |
| | 544 / 617 | $4.22\times10^4$ | 73 | 0.37 | 0.31 | 56 | 15.60 | MeOH |
| **VM23** | 542 / 621 | $3.20\times10^4$ | 79 | 0.45 | 0.49 | 60 | 14.71 | DMSO |
| | 544 / 618 | $3.24\times10^4$ | 74 | 0.39 | 0.31 | 57 | 12.65 | MeOH |

*$\Phi_f$-R6G = 0.95 and $\Phi_f$-RB = 0.70 in EtOH

### *2.3.2 Spectroscopic characterization of Nile blue derivatives*

The optical properties of Nile blue derivatives in some solvents including DMSO and methanol were determined using spectroscopic techniques. These properties showed some similarities to those of Nile red derivatives. For example, the absorption and emission spectra in DMSO and methanol of monoalkylated derivatives (**VM41**, **VM44**, and **VM45**) were blue-shifted compared to those of dialkylated derivatives (NB, **VM47**, **VM38**, and **VM46**) of about 14-17 and 21-26 nm, respectively. This can be attributed to the presence of additional alkyl groups adding

more vibrational and rotational energy levels to the dye molecules. However, the absorbance and emission spectra of Nile blue derivatives showed a red shift in DMSO relative to those in methanol of about 11-14 and 14-19 nm, respectively. The maximum wavelengths of absorbance and emission are shifted to higher wavelength due to increasing solvent polarity on going from methanol to DMSO.[25] It was observed that absorption maximum of Nile blue is blue-shifted of 21 nm in triethylamine relative to a mixture of triethylamine and 1-chloronaphthalene (1:1000) due to solvent polarity increased from 0.14 in triethylamine to 0.71 in 1-chloronaphthalene.[26] The molar absorptivity values for Nile blue derivatives were good as indicated by the linear relationship between the absorbance and the dye concentration. Monoalkylated derivatives had similar Stokes shift values in both solvents, and they were smaller compared to those for dialkylated derivatives. Quantum yield values of dialkylated derivatives in DMSO were slightly higher relative to methanol due to the increase of hydrogen bonding of the solvent resulting in higher rate of internal conversion,[23] as mentioned previously in Nile red results but in a lesser extent with Nile blue derivatives. On the other hand, monoalkylated derivatives showed opposite behavior in methanol in which quantum yield values were higher in methanol compared to those in DMSO. Monoalkylated derivatives are less hydrophobic and have more hydrogen bond donors than dialkylated derivatives. The enhancement in quantum yield can be attributed to the formation of hydrogen bonds between the monoalkylated derivatives and methanol which breaks up the aggregation of dye. Frade and his coworkers reported an enhancement of quantum yield value of about 40% on going from the dialkylated derivative of Nile blue (**1c**) to the corresponding monoalkylated derivative (**1f**) in ethanol from 0.17 in the former dye to 0.41 in the latter dye.[27] Another indicator that monoalkylated derivatives experienced less aggregation is the small FWHM values relative to those for dialkylated derivatives. Furthermore, molecular brightness values for

monoalkylated derivatives were higher than those for dialkylated derivatives in both solvents particularly in methanol.

It was achievable to determine optical properties of some monoalkylated derivatives specifically **VM41** and **VM44** in 20 mM phosphate buffer pH 7.2. The absorbance spectra revealed the aggregation phenomenon of benzophenoxazine derivatives in which each compound showed the monomer form as indicated by the M-band. Moreover, the blue shoulder of the peak indicated the formation of the H-band due to the plane-to-plane stacking of the dye molecules in aqueous media. The optical properties summarized in Table 2.2 indicated that the two dyes had similar molar absorptivity and Stokes shift values. Quantum yield value of **VM41** was greater compared to that for **VM44** which could be attributed to the difference in the side chine groups attached to benzophenoxazine backbone. Moreover, the FWHM and molecular brightness values for **VM41** were smaller than that for **VM44**.

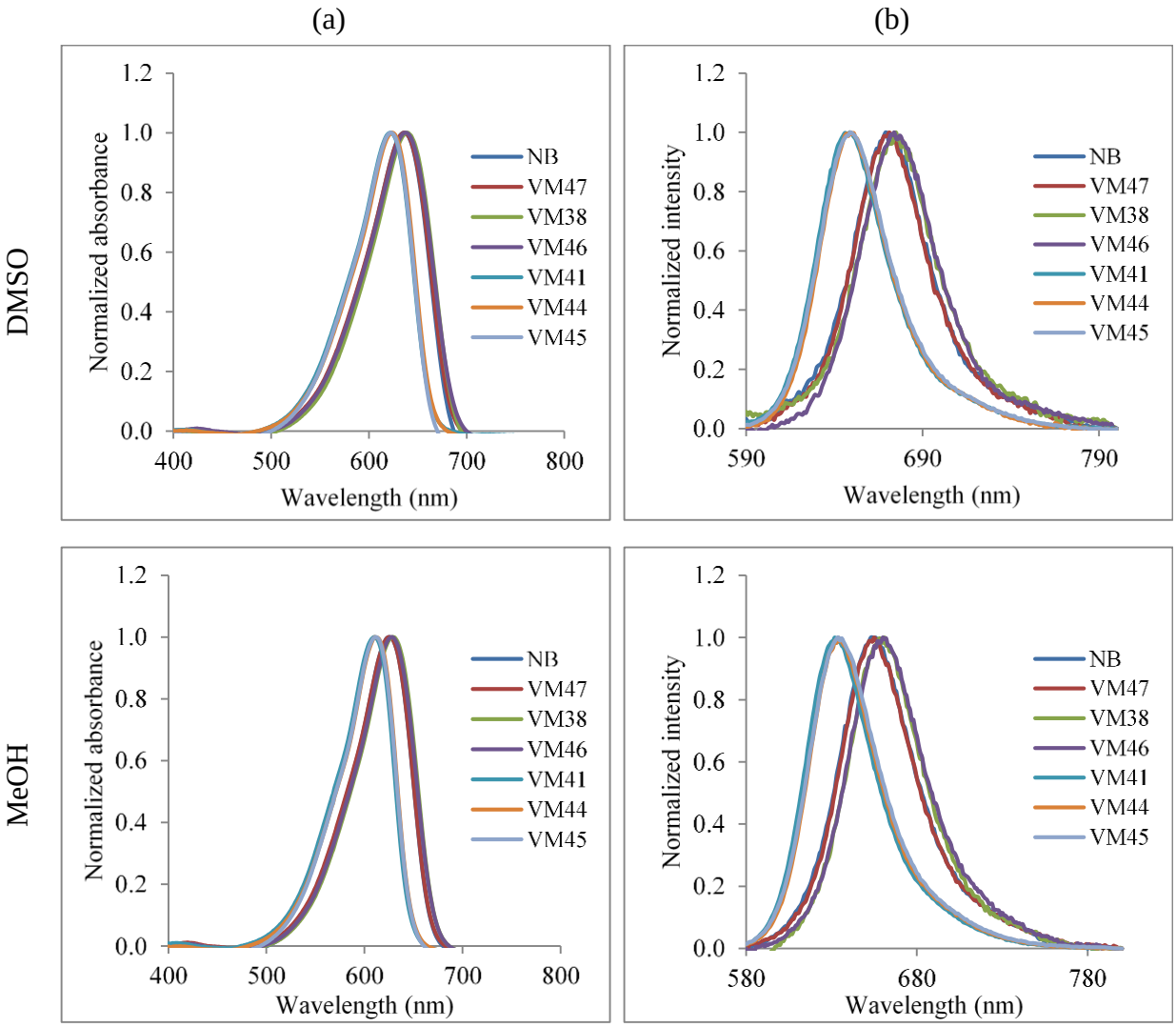


**Figure 2.4 (a) Absorbance and (b) emission spectra of Nile blue derivatives in in some solvents**

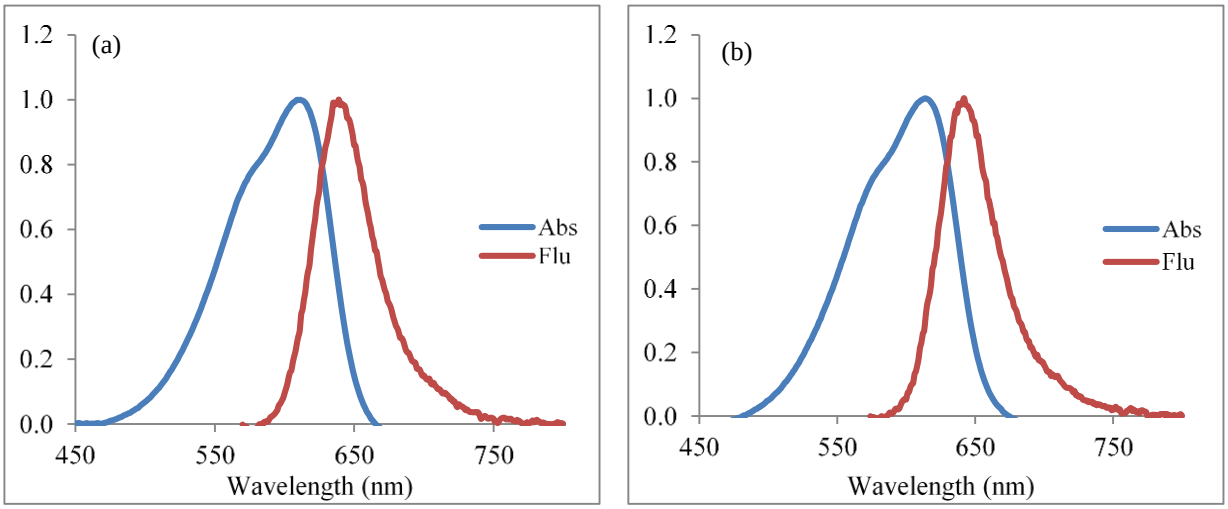


**Figure 2.5 Absorbance spectra (blue lines) and emission spectra (red lines) of: (a) VM41 and (b) VM44 in 20 mM phosphate buffer pH=7.2**

**Table 2.2 Optical properties of Nile blue derivatives in some solvents**

| Dye | $\lambda_{Abs}$ / $\lambda_{em}$ (nm) | ε ($M^{-1}cm^{-1}$) | Stokes shift (nm) | $\Phi_f$* | FWHM (nm) | MB ($M^{-1}cm^{-1}$) | Solvent |
|---|---|---|---|---|---|---|---|
| NB | 636 / 669 | $6.71\times10^4$ | 33 | 0.30 | 49 | 20.12 | DMSO |
| | 625 / 655 | $8.08\times10^4$ | 30 | 0.26 | 52 | 21.01 | MeOH |
| **VM47** | 636 / 671 | $7.00\times10^4$ | 35 | 0.27 | 49 | 18.91 | DMSO |
| | 625 / 655 | $7.76\times10^4$ | 30 | 0.25 | 52 | 19.39 | MeOH |
| **VM38** | 639 / 674 | $6.78\times10^4$ | 35 | 0.24 | 50 | 16.26 | DMSO |
| | 629 / 660 | $7.86\times10^4$ | 31 | 0.21 | 52 | 16.51 | MeOH |
| **VM46** | 638 / 674 | $6.90\times10^4$ | 36 | 0.29 | 50 | 20.02 | DMSO |
| | 628 / 660 | $7.47\times10^4$ | 32 | 0.27 | 53 | 20.17 | MeOH |
| **VM41** | 622 / 648 | $5.60\times10^4$ | 26 | 0.70 | 46 | 39.17 | DMSO |
| | 610 / 633 | $6.53\times10^4$ | 23 | 0.87 | 46 | 56.83 | MeOH |
| | 610 / 640 | $3.59\times10^4$ | 30 | 0.31 | 44 | 11.28 | PB |
| **VM44** | 624 / 649 | $6.16\times10^4$ | 25 | 0.65 | 46 | 40.02 | DMSO |
| | 612 / 634 | $6.93\times10^4$ | 22 | 0.80 | 46 | 55.40 | MeOH |
| | 614 / 642 | $3.63\times10^4$ | 28 | 0.26 | 48 | 9.47 | PB |
| **VM45** | 623 / 649 | $6.82\times10^4$ | 26 | 0.69 | 47 | 47.05 | DMSO |
| | 611 / 634 | $7.27\times10^4$ | 23 | 0.79 | 48 | 57.44 | MeOH |

*$\Phi_f$-NB = 0.27 in methanol

### *2.3.3 Photostability studies of benzophenoxazine derivatives*

Photostability is a fundamental characteristic of a good fluorophore to measure the extent of photodegradation that could happen during the illumination.[28] Photostability studies of benzophenoxazine derivatives were conducted in DMSO using two sets of experiments; one set was exposed to light whereas the other set was kept in the dark. The photostability analysis for all

Nile red derivatives revealed a descending trend in which $\lambda_{Abs}$ of dialkylated derivatives decreased about 40%, whereas for those monoalkylated derivatives diminished about 80% as shown in Figure 2.6 (a). Monoalkylated derivatives containing secondary amines were less stable in light than dialkylated derivatives containing tertiary amines because monoalkylated derivatives are less protected and more susceptible to degradation process than dialkylated derivatives. All these dyes remained stable when kept in the dark for the same period of time as shown in Figure 2.6 (b). In contrast, Nile blue derivatives containing secondary and tertiary amines were more stable in light in comparison to Nile red derivatives with only 10% reduction in the absorbance value over the 15 days as indicated in Figure 2.7 (a). The photostability of Nile blue derivatives could be attributed to the fact that the electrons are delocalized across the aromatic ring of the dye. Nile blue derivatives kept in the dark were relatively stable for the same period of time as shown in Figure 2.7 (b).

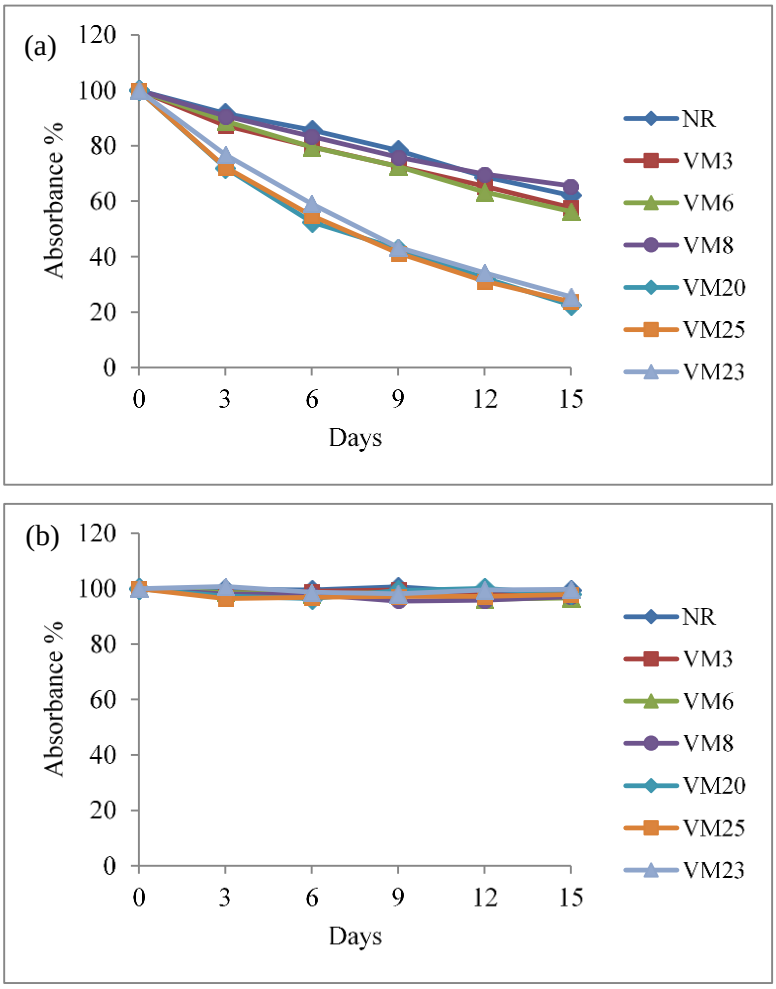


**Figure 2.6 Photostability studies of $1.5\times10^{-5}$ M Nile red derivatives in DMSO of (a) exposed light and (b) in the dark**

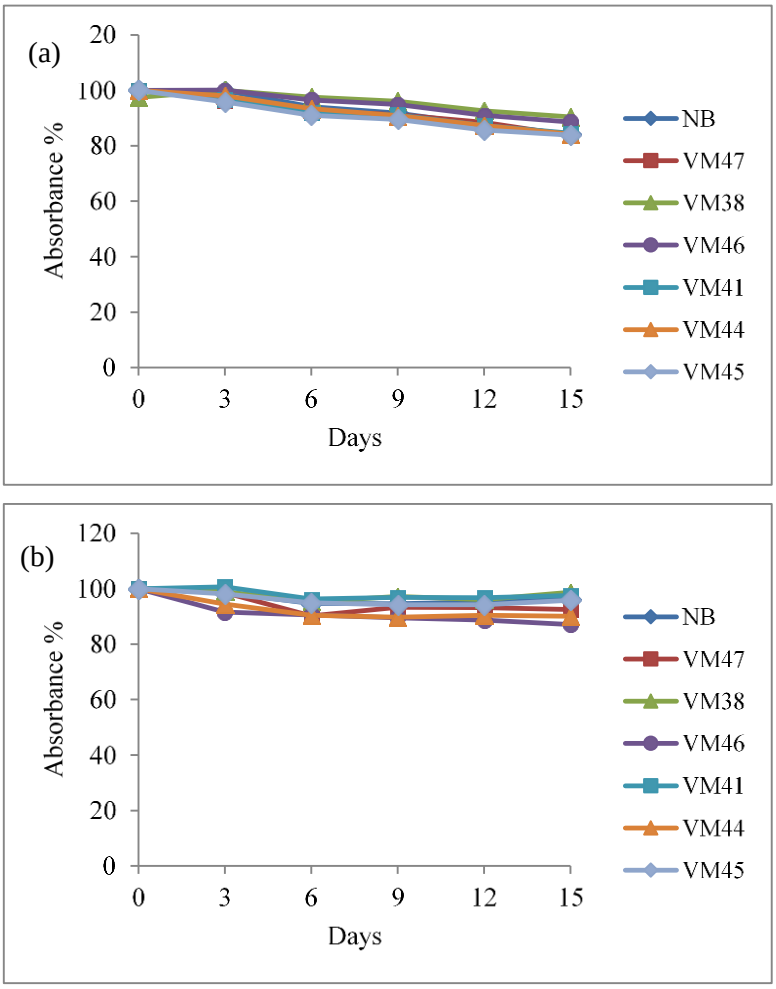


**Figure 2.7 Photostability studies of $1.0\times10^{-5}$ M Nile blue derivatives in DMSO of (a) exposed light and (b) in the dark**

## 2.4 Conclusions

The optical properties of two groups of benzophenoxazine dyes, Nile red and Nile blue derivatives, were determined in some organic solvents and phosphate buffer. Each group of the dyes can be divided into two classes dialkylated derivatives containing tertiary amines at the side chain of the position 9 and monoalkylated derivatives containing secondary amine at the same position. The results revealed that the derivatives could be considered as good fluorophores in

terms of molar absorptivity, quantum yield, Stokes shifts, molecular brightness, as well as photostability studies. The absorbance and emission wavelengths of Nile red derivatives were in the range of 540-550 and 615-630 nm, respectively, and for Nile blue derivatives were in the range of 620-630 and 655-670 nm, respectively. Monoalkylated derivatives of Nile red had higher quantum yield in MeOH about 10-13% compared to those derivatives with tertiary amines. Moreover, monoalkylated derivatives of Nile blue had higher quantum yield in both solvents DMSO and MeOH of about 40% and 60%, respectively compared to dialkylated derivatives. The increase in quantum yield is due to hydrogen bonding formed between the dye and the solvent which breaks up the aggregation. Nile blue derivatives were more stable after being irradiated by the light source than Nile red derivatives.

**References**


1. Phillip, G.; Eugene, P. M.; Stanley, D. F., Nile Red: A Selective Fluorescent Stain for Intracellular Lipid Droplets. *The Journal of Cell Biology* **1985,** (3), 965.
2. Fowler, S. D.; Greenspan, P., Application of Nile red, a fluorescent hydrophobic probe, for the detection of neutral lipid deposits in tissue sections: comparison with Oil Red O. *J. Histochem. Cytochem.* **1985,** *33* (8), 833-6.
3. Elsey, D.; Jameson, D.; Raleigh, B.; Cooney, M. J., Fluorescent measurement of microalgal neutral lipids. *J. Microbiol. Methods* **2007,** *68* (3), 639-642.
4. Montalbo-Lomboy, M.; Kantekin, M. N.; Wang, T., Lipid Estimation of Surfactant-Extracted Microalgae Oil Using Nile Red. *Journal of the American Oil Chemists' Society (JAOCS)* **2014,** *91* (4), 665-680.
5. Chen, W.; Zhang, C. W.; Song, L. R.; Sommerfeld, M.; Hu, Q., A high throughput Nile red method for quantitative measurement of neutral lipids in microalgae. *Journal of Microbiological Methods* **2009,** *77* (1), 41-47.
6. Jana, B.; Ghosh, S.; Chattopadhyay, N., Competitive binding of nile red between lipids and β-cyclodextrin. *Journal of Photochemistry & Photobiology, B: Biology* **2013,** *126*, 1-10.
7. Halder, A.; Saha, B.; Maity, P.; Kumar, G. S.; Sinha, D. K.; Karmakar, S., Lipid chain saturation and the cholesterol in the phospholipid membrane affect the spectroscopic properties of lipophilic dye nile red. *Spectroc. Acta Pt. A-Molec. Biomolec. Spectr.* **2018,** *191*, 104-110.

8. Chen, Q. G.; Li, D. H.; Zhao, Y.; Yang, H. H.; Zhu, Q. Z.; Xu, J. G., Interaction of a novel red-region fluorescent probe, Nile Blue, with DNA and its application to nucleic acids assay. *Analyst* **1999,** *124* (6), 901-906.

9. Zhao, G. C.; Zhu, J. J.; Chen, H. Y.; Wang, X. M.; Lu, Z. H., Spectroscopic and spectroelectrochemical studies of interaction of Nile Blue with DNA. *Chin. J. Chem.* **2002,** *20* (1), 57-62.

10. Mitra, R. K.; Sinha, S. S.; Pal, S. K., Interactions of Nile blue with micelles, reverse micelles and a genomic DNA. *Journal of Fluorescence* **2008,** *18* (2), 423-432.

11. Raju, B. R.; Naik, S.; Coutinho, P. J. G.; Goncalves, M. S. T., Novel Nile Blue derivatives as fluorescent probes for DNA. *Dyes and Pigments* **2013,** *99* (1), 220-227.

12. Krishna, M. M. G., Excited-state kinetics of the hydrophobic probe Nile red in membranes and micelles. *J. Phys. Chem. A* **1999,** *103* (19), 3589-3595.

13. Kurniasih, I. N.; Liang, H.; Mohr, P. C.; Khot, G.; Rabe, J. P.; Mohr, A., Nile Red Dye in Aqueous Surfactant and Micellar Solution. *Langmuir* **2015,** *31* (9), 2639-2648.

14. Das, K.; Jain, B.; Patel, H. S., Nile Blue in Triton-X 1-00/benzene-hexane reverse micelles: a fluorescence spectroscopic study. *Spectroc. Acta Pt. A-Molec. Biomolec. Spectr.* **2004,** *60* (8-9), 2059-2064.

15. Wagner, B. D.; Stojanovic, N.; Leclair, G.; Jankowski, C. K., A spectroscopic and molecular modelling study of the nature of the association complexes of Nile Red with cyclodextrins. *J. Incl. Phenom. Macrocycl. Chem.* **2003,** *45* (3-4), 275-283.

16. Briggs, M. S. J.; Bruce, I.; Miller, J. N.; Moody, C. J.; Simmonds, A. C.; Swann, E., Synthesis of functionalised fluorescent dyes and their coupling to amines and amino acids. *J. Chem. Soc.-Perkin Trans. 1* **1997,** (7), 1051-1058.

17. Raju, B. R.; Firmino, A. D. G.; Costa, A. L. S.; Coutinho, P. J. G.; Gonçalves, M. S. T., Synthesis and photophysical properties of side-chain chlorinated benzo[a]phenoxazinium chlorides. *Tetrahedron* **2013,** *69*, 2451-2461.

18. Jose, J.; Burgess, K., Syntheses and properties of water-soluble Nile Red derivatives. *J. Org. Chem.* **2006,** *71* (20), 7835-7839.

19. Jose, J.; Ueno, Y.; Burgess, K., Water-Soluble Nile Blue Derivatives: Syntheses and Photophysical Properties. *Chem.-Eur. J.* **2009,** *15* (2), 418-423.

20. Rudat, B.; Birtalan, E.; Vollrath, S. B. L.; Fritz, D.; Kölmel, D. K.; Nieger, M.; Schepers, U.; Müllen, K.; Eisler, H.-J.; Lemmer, U.; Bräse, S., Photophysical properties of fluorescently-labeled peptoids. *European Journal of Medicinal Chemistry* **2011,** *46* (9), 4457-4465.

21. Chao, J. B.; Song, K. L.; Zhang, Y. B.; Yin, C. X.; Huo, F. J.; Wang, J. J.; Zhang, T., A pyrene-based colorimetric and fluorescent pH probe with large stokes shift and its application in bioimaging. *Talanta* **2018,** *189*, 150-156.

22. Zhu, X.-Y.; Yao, H.-W.; Fu, Y.-J.; Guo, X.-F.; Wang, H., Effect of substituents on Stokes shift of BODIPY and its application in designing bioimaging probes. *Analytica Chimica Acta* **2019,** *1048*, 194-203.

23. Cser, A.; Nagy, K.; Biczok, L., Fluorescence lifetime of Nile Red as a probe for the hydrogen bonding strength with its microenvironment. *Chem. Phys. Lett.* **2002,** *360* (5-6), 473-478.

24. Karstens, T.; Kobs, K., Rhodamine B and rhodamine 101 as reference substances for fluorescence quantum yield measurements. *J. Phys. Chem.* **1980,** *84* (14), 1871-2.

25. Reichardt, C., *Solvents and solvent effects in organic chemistry*. Weinheim : Wiley-VCH, 3rd: 2003.

26. Douhal, A., Photophysics of Nile Blue A in Proton-Accepting and Electron-Donating Solvents. *Journal of Physical Chemistry* **1994,** *98* (50), 13131-13137.

27. Frade, V. H. J.; Coutinho, P. J. G.; Moura, J.; Goncalves, M. S. T., Functionalised benzo a phenoxazine dyes as long-wavelength fluorescent probes for amino acids. Tetrahedron 2007, 63 (7), 1654-1663.

28. Zhang, Y.; Autry, S. A.; McNamara, L. E.; Nguyen, S. T.; Le, N.; Brogdon, P.; Watkins, D. L.; Hammer, N. I.; Delcamp, J. H., Near-Infrared Fluorescent Thienothiadiazole Dyes with Large Stokes Shifts and High Photostability. *The Journal Of Organic Chemistry* **2017,** *82* (11), 5597-5606.

# 3 INTERACTION OF BENZOPHENOXAZINE DYES WITH HUMAN SERUM ALBUMIN

## 3.1 Introduction

Optical imaging is one of the most popular techniques for visualization cells and tissues. The technique enables studying cells in terms of their movement, growth, and functions offering a great opportunity to disease treatment, tumor detection, and drug design. In recent years, fluorescent dyes have gained much attention in such applications due to their unique properties. They emit in the long wavelength region of the electromagnetic spectrum which make them an excellent probe for cell imaging.[1] Few phenoxazine dyes have been used as imaging agents, one of which is oxazine 4. The dye is considered as a nerve-specific agent and has shown a great binding capability for nerve tissue as indicated by the enhancement in fluorescence intensity.[2] However, many nerve-specific fluorophores have the tendency to accumulate in other tissues of a similar composition such as adipose tissue. To overcome this issue, a study was conducted with the aim of synthesis several Nile red derivatives with different electron donating and withdrawing groups to be adipose-specific agents without nerve accumulation. It was demonstrated that among all the prepared fluorophores one derivative (NR5) with $CF_3SO_3$ substitute at the position 2 displayed adipose-specific contrast and decreased nerve uptake using ratiometric imaging. The study also included the use of dual fluorophore staining for improved visualization in which a mixture of oxazine 4, the nerve-specific dye, and dye NR5 provided enhanced nerve-to-adipose contrast in comparison to a mixture of oxazine 4 and Nile red.[3] In order to involve a large number of benzophenoxazine derivatives in the field of molecular imaging, tremendous efforts have been made to synthesize new analogs by structural modification. For example, a fluorescent probe of

Nile blue containing indomethacin (IMC) linked to the benzophenoxazine backbone via a hexanediamine linker was constructed for tumor imaging. The probe has shown to bind specifically to cyclooxygenase-2 (COX-2) that localized in Golgi of cancer cells.[4] Moreover, some Nile red derivatives were designed for intracellular imaging particularly as stains for mitochondria and Golgi.[5] Furthermore, a fluorescent probe based on Nile red-palladium was constructed to detect carbon monoxide in some tissue culture cells.[6] Also, biosensors based on Nile blue derivatives were designed as pH- sensitive probes and for imaging of tumor cells.[7] Besides the applications in tumor diagnosis and cell organelles, benzophenoxazine derivatives have been developed as a lysosomal probe for many types of live cells. A Nile blue derivative with a morpholine substituent was designed for such applications. Due to the high photostability and biocompatibility of the dye, it was used to track lysosomes during cell apoptosis and observe morphological changes of lysosomes during cell division.[8] Moreover, benzophenoxazine derivatives have been implemented for the design "turn-on" fluorescent probes that are selective and sensitive toward target analytes. For instance, "turn-on" probes based on Nile red or Nile blue derivative containing dinitrophenyl-ether group were examined for hydrogen sulfide detection. The purpose of the substituent was to quench fluorescence, but in the presence of hydrogen sulfide the dinitrophenyl group was removed, and the fluorescence signal is restored.[9]

In addition to the enormous use of benzophenoxazine derivatives in bioimaging applications, they have shown a great binding ability to proteins. Several studies have indicated that the Nile red and Nile blue have high affinity to different proteins such as human serum albumin, bovine serum albumin, $\alpha_1$-acid glycoprotein, β-lactoglobulin, ovomucoid, κ-casein, ovalbumin, and β-galactosidase (E. coli).[10-15] The results demonstrated the dyes bind to the hydrophobic areas of proteins, and emission maximum is shifted to shorter wavelengths upon the

interaction with the proteins. However, very few studies have investigated the binding constant of the dye-protein complex[14]. Since evaluation of binding constant is a key factor in non-covalent protein labeling, it is of great importance to fully understand the binding interactions of benzophenoxazine derivatives with a protein such as human serum albumin and compare their affinity to HSA based on binding constant values.

## 3.2 Experimental

### *3.2.1 Instrumentation*

Absorbance spectra were acquired using a Cary 3G UV-visible spectrophotometer (Varian Inc., Palo Alto, CA) interfaced to a PC. Fluorescence spectra were achieved using a K2 Spectrofluorometer (ISS Inc., Champaign, IL) interfaced to a PC. Excitation was achieved using a Xenon Arc lamp, model PS 300-1, (ILC Technology Inc., Sunnyvale, CA). All measurements were performed in 1.0 cm quartz cuvettes. Nanopure water was obtained using an ELGA Purelab.

### *3.2.2 Chemicals and reagents*

Nile red (NR) and Nile blue (NB) were obtained from Sigma-Aldrich (St. Louis, MO). Benzophenoxazine derivatives were provided by the research group of Dr. Maged Henary; synthesized by Vincent Martinez. The dyes have been designed with different substituent groups on the amine side chain at the 9-position. The derivatives can be classified as mentioned previously into two types according to the type of amine attached to benzophenoxazine backbone at the 9-position which are dialkylated and monoalkylated derivatives containing tertiary and secondary amine, respectively. The chemical structures of Nile red derivatives and Nile blue derivatives are

shown in the previous sections, Figures (2.1) and (2.2). Sodium phosphate monobasic and sodium phosphate dibasic obtained from Aldrich Chemical Company (Milwaukee, WI).

### *3.2.3 HSA binding interaction with benzophenoxazine derivatives*

The initial investigation of binding interaction between HSA and the dye involves using fluorescence spectroscopy to monitor a fixed concentration of the dye in phosphate buffer first. Then, the same concentration of the dye is mixed with a similar concentration of the protein assuming 1:1 stoichiometry in buffer and monitored by recording the fluorescence intensity. The dye concentration is determined in which the absorbance value should be below 0.1 units and to avoid inner filter effect or self-quenching. The use of fluorescence spectroscopy allows observing any changes that might occur in the maximum wavelength of emission (bathochromic or hypsochromic shift) or fluorescence intensity (hyperchromic or hypochromic shift) after the interaction between the dye and the protein. The fixed concentrations for the binding interaction with HSA for Nile red derivatives and Nile blue derivatives were $5.0\times10^{-6}$ M and $2.0\times10^{-6}$ M, respectively. These concentrations were selected based on the optical properties of the dyes and instrumentation limits. Therefore, for the interaction of Nile red derivatives with HSA, a solution containing $5.0\times10^{-6}$ M of the pure dye in 20 mM phosphate buffer pH 7.2 was recorded first. Then, a solution containing $5.0\times10^{-6}$ M of the dye with $5.0\times10^{-6}$ M of HSA in 20 mM phosphate buffer pH 7.2 was recorded. For the interaction of Nile blue derivatives with HSA, a solution containing $2.0\times10^{-6}$ M of the pure dye in 20 mM phosphate buffer pH 7.2 was recorded first. A solution containing $2.0\times10^{-6}$ M of the dye with $2.0\times10^{-6}$ M of HSA in 20 mM phosphate buffer pH 7.2 was recorded second. To confirm the HSA-dye binding ratio, Job's method was used to identify the stoichiometry as discussed in the following section.

### *3.2.4 Determination of HSA-dye stoichiometry using Job's method*

Job's method or the method of continuous variation is used to determine the stoichiometry of the predominant complex when multiple interactions can occur.[16] This method includes varying the number of moles for the protein and the dye whereas the total concentration of the solution remains constant. Fluorescence spectroscopy can be used to identify the predominant complex which corresponds to maximum fluorescence intensity as a function of the mole fraction of HSA. The total concentration of HSA-dye complex for Nile red derivatives except **VM25** was $10.0\times10^{-6}$ M while for Nile blue derivatives was $4.0\times10^{-6}$ M. The best result of Job's method for HSA-**VM25** complex was achieved when the total concentration kept low at $2.0\times10^{-6}$ M due to aggregation of the dye in aqueous solution.

### *3.2.5 Effect of time on HSA-dye complex*

The effect of time on HSA-dye complex with benzophenoxazine derivatives was investigated by fluorescence spectroscopy on a mixture of the dye and HSA of equal concentrations. The concentration of Nile red derivatives was $5.0\times10^{-6}$ M of the dye and HSA whereas for Nile blue derivatives was $2.0\times10^{-6}$ M of the dye and HSA in 20 mM phosphate buffer pH 7.2. The reaction for all benzophenoxazine derivatives was monitored by recording the fluorescence intensity every 5 min for 30 min at room temperature.

### *3.2.6 Determination of binding constant of HSA-dye complex*

Binding constant (K) was determined only for those dyes that showed affinity to HSA as indicated from Job's method. The HSA interaction was studied by preparing a series of samples containing a constant concentration of the dye and different concentrations of HSA in 20 mM

phosphate buffer pH 7.2. The dye concentration was $5.0\times10^{-6}$ and $2.0\times10^{-6}$ M for Nile red derivatives and Nile blue derivatives, respectively. The HSA-dye complex was vortexed for 30 seconds and then left for different time periods according to the results of effect time on HSA-dye complex. All working solutions contained only 1.0% (v/v) of DMSO to facilitate the dye dissolution and to avoid HSA denaturation. The binding constant (K) for those dyes binding to HSA in 1:1 stoichiometry was determined according to the equation:[17]

$$\frac{1}{\Delta F} = \frac{1}{k[\text{Dye}]} + \left(\frac{1}{k[\text{Dye}]K}\right)\frac{1}{[\text{HSA}]} \qquad (3.1)$$

where ΔF represents the change in maximum wavelength of emission of the HSA-dye complex and k is a constant dependent on the quantum efficiency of the process and the instrumentation.

For those dyes binding to HSA in different stoichiometry other than 1:1 ratio, the binding constant was determined according to the equation:[18]

$$\log\frac{(F - F_0)}{F} = \log K + n\log[\text{HSA}] \qquad (3.2)$$

where F and $F_0$ represent the emission intensity of the dye in the presence and absence of HSA, respectively, and n is the binding sites. Duplicate measurements were obtained, and the average binding constant values were reported.

## 3.3 Results and discussion

### *3.3.1 HSA binding interaction with benzophenoxazine derivatives*

Before studying the interaction of benzophenoxazine derivatives and HSA, the absorbance spectra of the pure dye in 20 mM phosphate buffer pH 7.2 were recorded. Each dye showed different spectral behavior in terms of maximum wavelength, peak intensity, and absorbance pattern due to the aggregation process and formation of dimers (and perhaps higher-order

polymers) of the dye in aqueous solution[19] as shown in Figure 3.1 (a). For Nile red derivatives, similar and broad absorption band was observed for NR and **VM3** with $\lambda_{Abs}$ of about 540 nm but higher absorbance value for NR even though the two dyes have similar chemical structures except that **VM3** has an extra hydroxyl group. The absorbance spectra of **VM6** and **VM8** showed identical spectral behavior with $\lambda_{Abs}$ of about 530 nm. The two dyes contain hydrophobic substituents of butyl and phenylpropyl groups, respectively. **VM20** and **VM25** had similar absorption shapes with a blue shift of about 100 nm compared to that in organic solvent with $\lambda_{Abs}$ of about 440 nm and higher absorbance for **VM25.** The absorption spectrum of **VM23** was broad and $\lambda_{Abs}$ was at 517 nm. There was a noticeable color change of the aqueous solutions of monoalkylated derivatives in which solutions of **VM20** and **VM25** appeared yellow and **VM23** turned to pale carmine as depicted Figure 3.1 (c). In the case of Nile blue derivatives, the effect of substituents on their spectral behavior in aqueous media was more pronounced than Nile red derivatives as shown in Figure 3.1 (b). An examination of the absorbance spectra of derivatives with ethyl and butyl substituents displayed the monomer form of the dye (M-band) as well as the formation of the blue-shifted shoulder (H-band) because of the aggregation behavior. Similar absorbance spectra were obtained for NB and **VM47** and **VM38** with $\lambda_{Abs}$ of about 635 nm but lower intensity value for **VM38**. The absorbance spectra of **VM41** and **VM44** were identical regarding the shape and maximum wavelength of about 610 nm. **VM46** and **VM45** containing phenylpropyl substitutions had broad absorption bands and the former dye had a wider band because two groups are attached to benzophenoxazine backbone whereas one group is attached to the latter dye. Moreover, the two dyes appeared in different colors than other dialkylated and monoalkylated derivatives as depicted in Figure 3.1 (d).

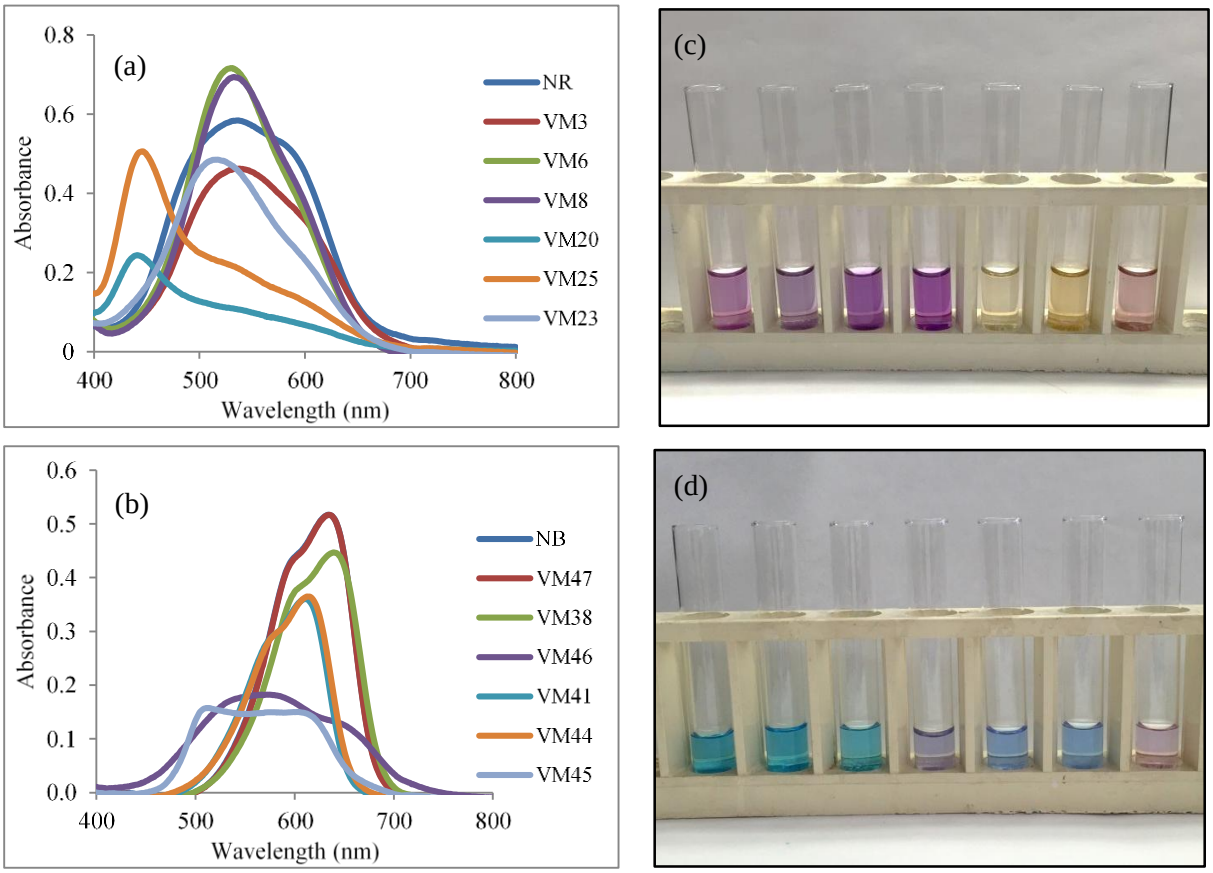


**Figure 3.1 Absorbance spectra of (a) $3.0\times10^{-5}$ M of Nile red derivatives and (b) $1.0\times10^{-5}$ M of Nile blue derivatives in 20 mM phosphate buffer pH 7.2, corresponding dyes color from left to right (c) NR, VM3, VM6, VM8, VM20, VM25, and VM23 and (d) NB, VM47, VM38, VM46, VM41, VM44, and VM45**

The interaction between HSA and the dye was investigated by observing the emission spectrum of the pure dye first. Then, the spectral behavior of the dye was compared to that of HSA-dye complex. In the case of Nile red derivatives (Figure 3.2), the maximum wavelength of emission of NR and **VM3** was at 663 nm. After the addition of HSA, a blue shift of about 30 nm in the emission spectrum was observed for both dyes. Moreover, there was an enhancement in fluorescence intensity for NR, but the intensity decreased for **VM3**. The hydrophobic derivatives,

**VM6** and **VM8**, did not fluoresce in phosphate buffer. However, interaction with HSA resulted in restoring fluorescence intensity due to the disruption of dye aggregation. The fluorescence intensity of monoalkylated derivatives decreased as the hydrophobicity of the dye increased in which the least hydrophobic dye **VM20** had the highest intensity whereas no fluorescence signal was observed for the most hydrophobic dye **VM23**. There was an increase in fluorescence intensity upon binding with HSA. Moreover, the yellow color of **VM20** and **VM25** changed to purple/pink color after the addition of HSA. Such change is of great significance and can be used for colorimetric and fluorometric detection.[20] Regarding Nile blue derivatives (Figure 3.3), only dialkylated derivatives showed potential for interaction with HSA. NB and **VM47** and **VM38** containing ethyl and butyl substitutions had $\lambda_{em}$ of 667 nm. They showed a blue shift of about 32 nm in the presence of HSA. Additionally, the fluorescence intensity of the formed complexes increased, and **VM38** had greater intensity increase compared to other dyes. The spectral shift toward shorter wavelength upon interaction with HSA was also observed in some Nile red derivatives containing ethyl and butyl substitutions, NR and **VM3**. Spectral changes such as shifting the emission maximum to shorter wavelengths and increasing fluorescence intensity are attributed to changes in the environment surrounding the dye due to interaction with the protein relative to that of the pure dye.[11-13] The most hydrophobic derivative, **VM46** did not fluoresce in aqueous solutions as was obtained with hydrophobic derivatives. Nonetheless, the loss of fluorescence intensity was restored when the dye binds to HSA. Monoalkylated derivatives, **VM41**, **VM44**, and **VM45**, had $\lambda_{em}$ of about 640 nm, and the intensity reduced as the hydrophobicity of the dye increased. However, no considerable changes were observed either in $\lambda_{em}$ or fluorescence intensity in the presence of HSA even though the pure dyes showed a fluorescence signal at about 640 nm.

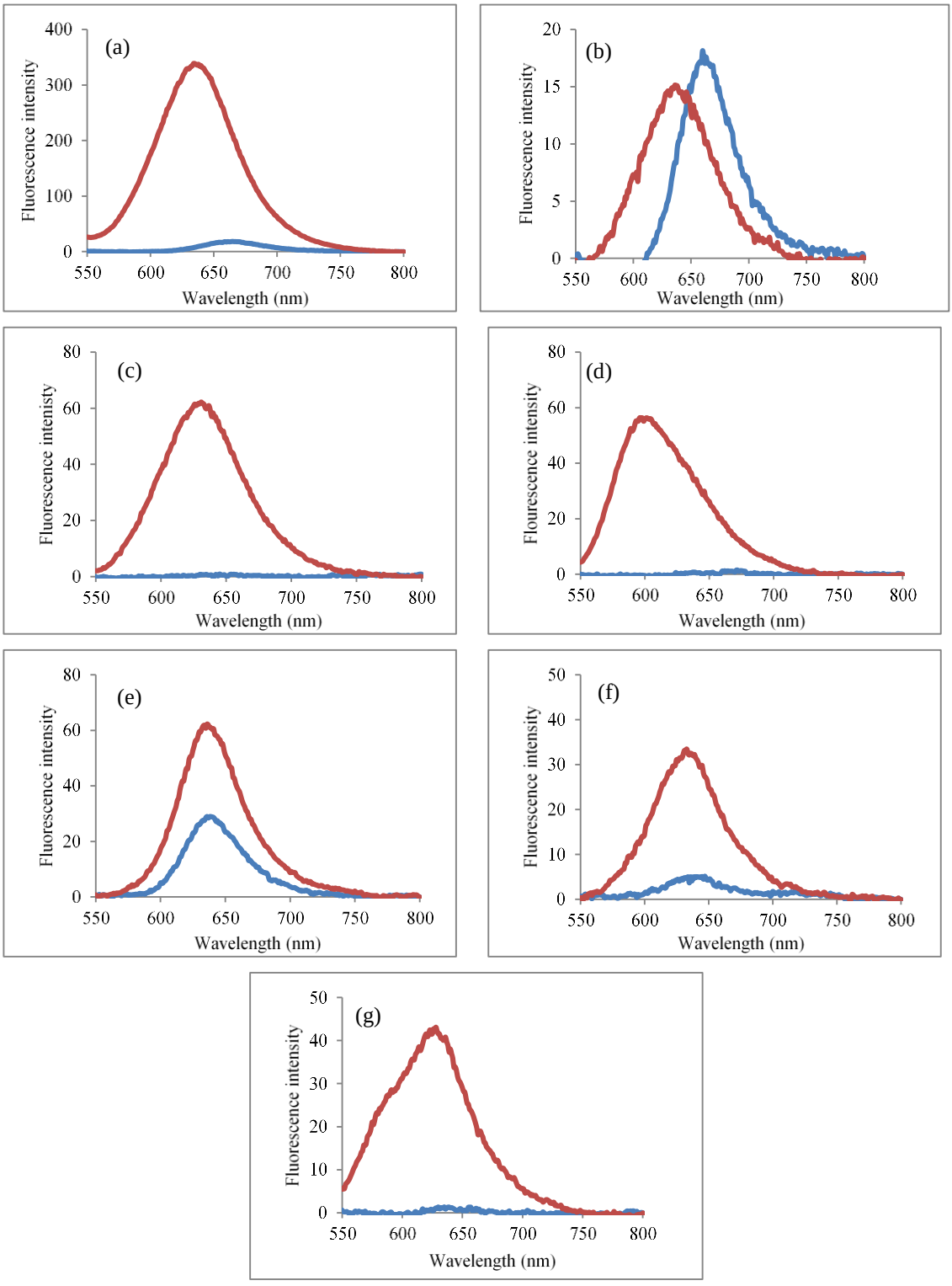


**Figure 3.2 Emission spectra of $5.0\times10^{-6}$ M dye (blue lines) and emission spectra of $5.0\times10^{-6}$M dye and $5.0\times10^{-6}$ M HSA (red lines) for ((a) NR, (b) VM3, (c) VM6, (d) VM8, (e) VM20, (f) VM25, and (g) VM23 in 20 mM phosphate buffer pH 7.2, excited at 500 nm**

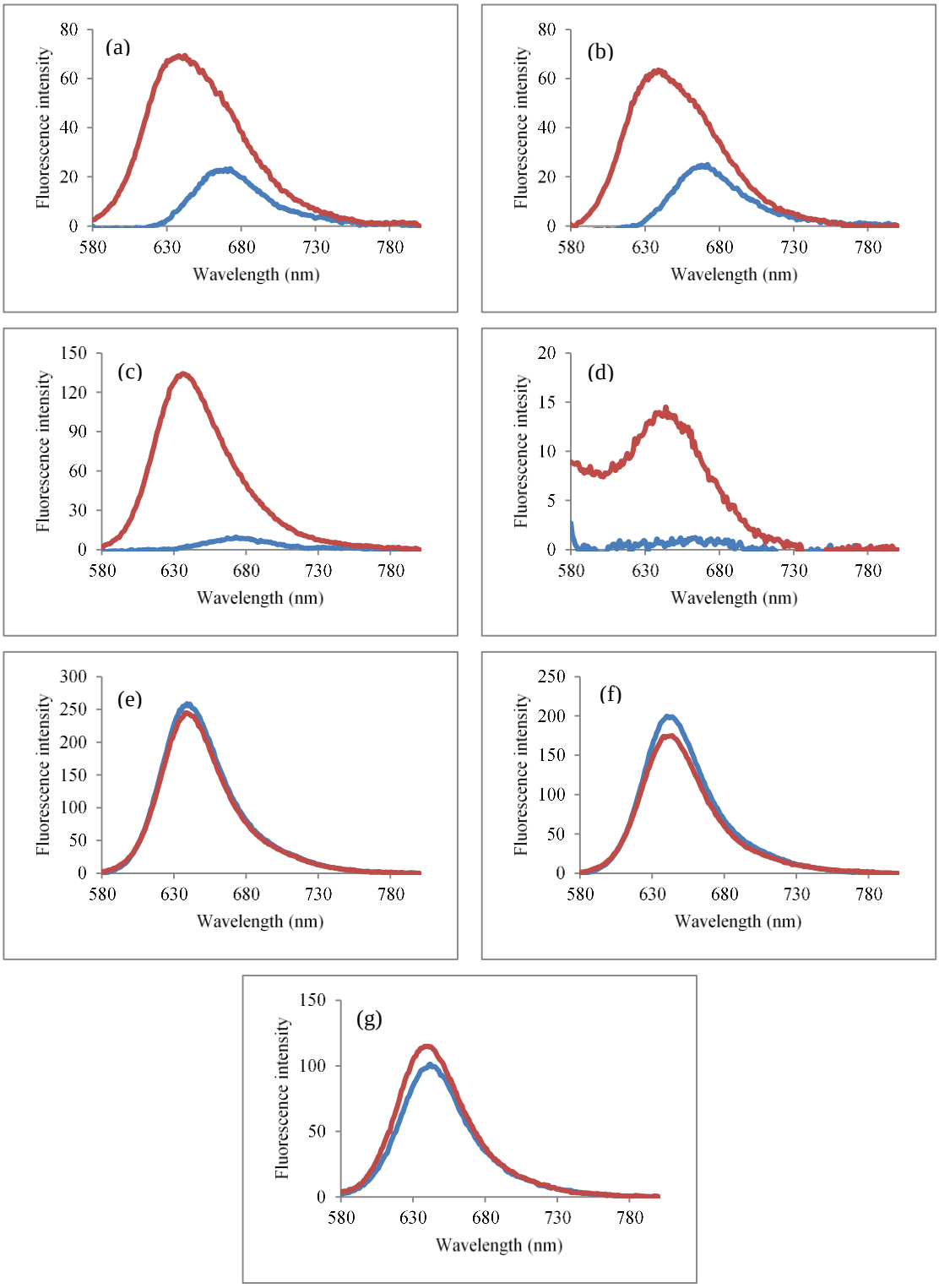


**Figure 3.3 Emission spectra of $2.0\times10^{-6}$ M dye (blue lines) and emission spectra of $2.0\times10^{-6}$M dye and $2.0\times10^{-6}$ M HSA (red lines) for (a) NB, (b) VM47, (c) VM38, (d) VM46, (e) VM41, (f) VM44, and (g) VM45 in 20 mM phosphate buffer pH 7.2, excited at 560 nm**

### *3.3.2 Determination of HSA-dye stoichiometry using Job's method*

Job's method (method of continuous variation) was used to determine the stoichiometry of the binding interaction between HSA and benzophenoxazine derivatives. Thus, variation of the number of moles for HSA with Nile red derivatives (Figure 3.4) resulted in a maximum mole fraction of 0.50 for HSA-dye complex with NR, **VM6**, **VM8**, **VM25**, and **VM23** which corresponds to a 1:1 binding stoichiometry. **VM20** displayed a maximum mole fraction at 0.33 indicating the formation of HSA-dye complex with 1:2 stoichiometry. Variation of the number of moles for HSA with **VM3** resulted in straight line meaning that the dye did not have any potential to interact with HSA. Therefore, Job's method provided another evidence that the dye did not bind to HSA. In the case of Nile blue derivatives (Figure 3.5), the maximum intensity was observed at a mole fraction of 0.50 for HSA-dye complex with dialkylated derivatives (NB, **VM47**, **VM38**, and **VM46**) corresponding to 1:1 binding ratio. Variation of the number of HSA moles of monoalkylated derivatives (**VM41**, **VM44**, and **VM45**) did not show any maximum intensity corresponding to a specific binding ratio. Nonetheless, there was a linear decrease in fluorescence intensity as the mole fraction of HSA increased or the mole fraction of dye decreased. Job' method confirmed that no binding interaction occurs between HSA and monoalkylated derivatives.

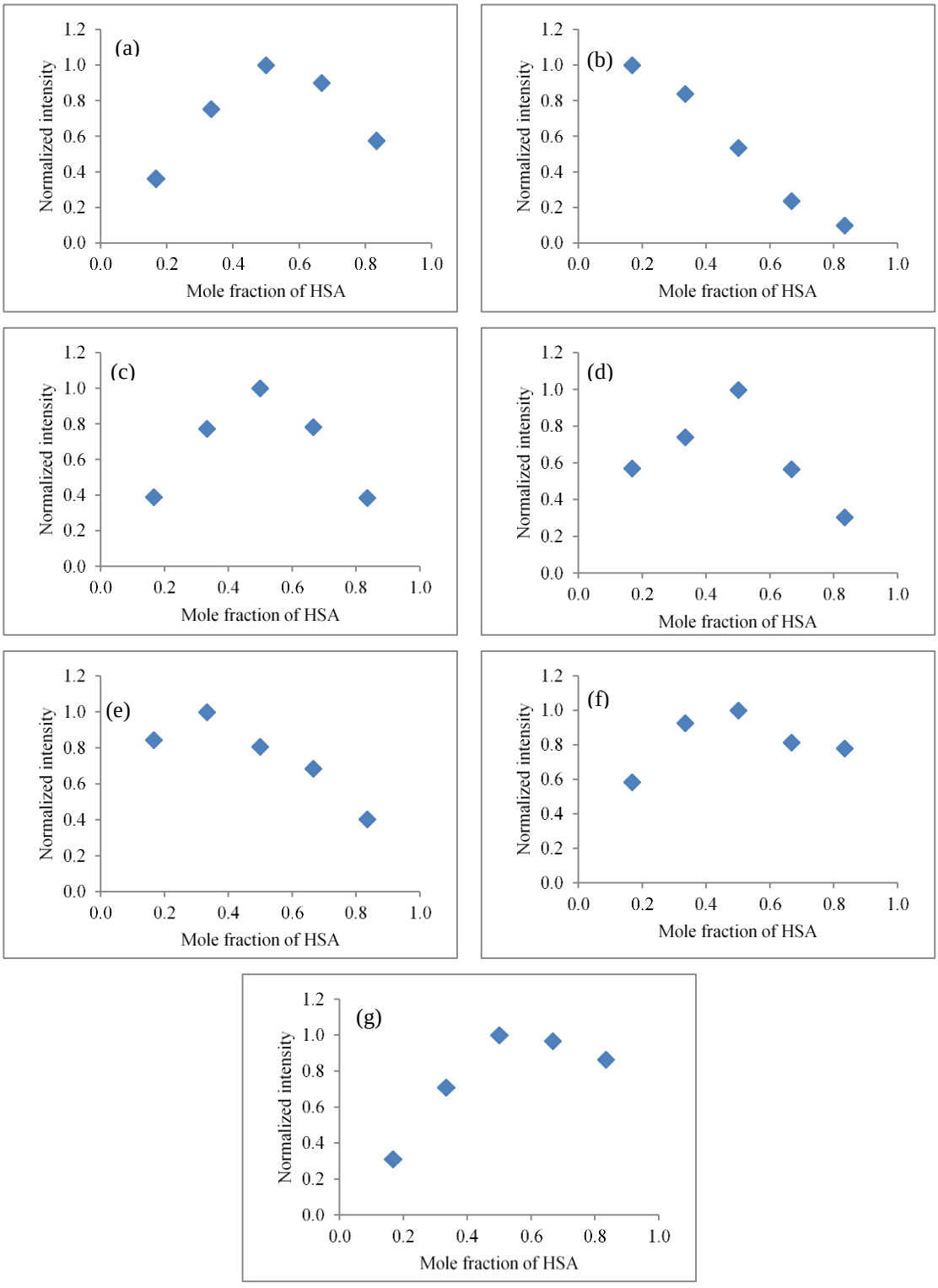


**Figure 3.4 Job's method of HSA-dye complex for (a) NR, (b) VM3, (c) VM6, (d) VM8, (e) VM20, (f) VM25, and (g) VM23 in 20 mM phosphate buffer pH 7.2, excited at 500 nm**

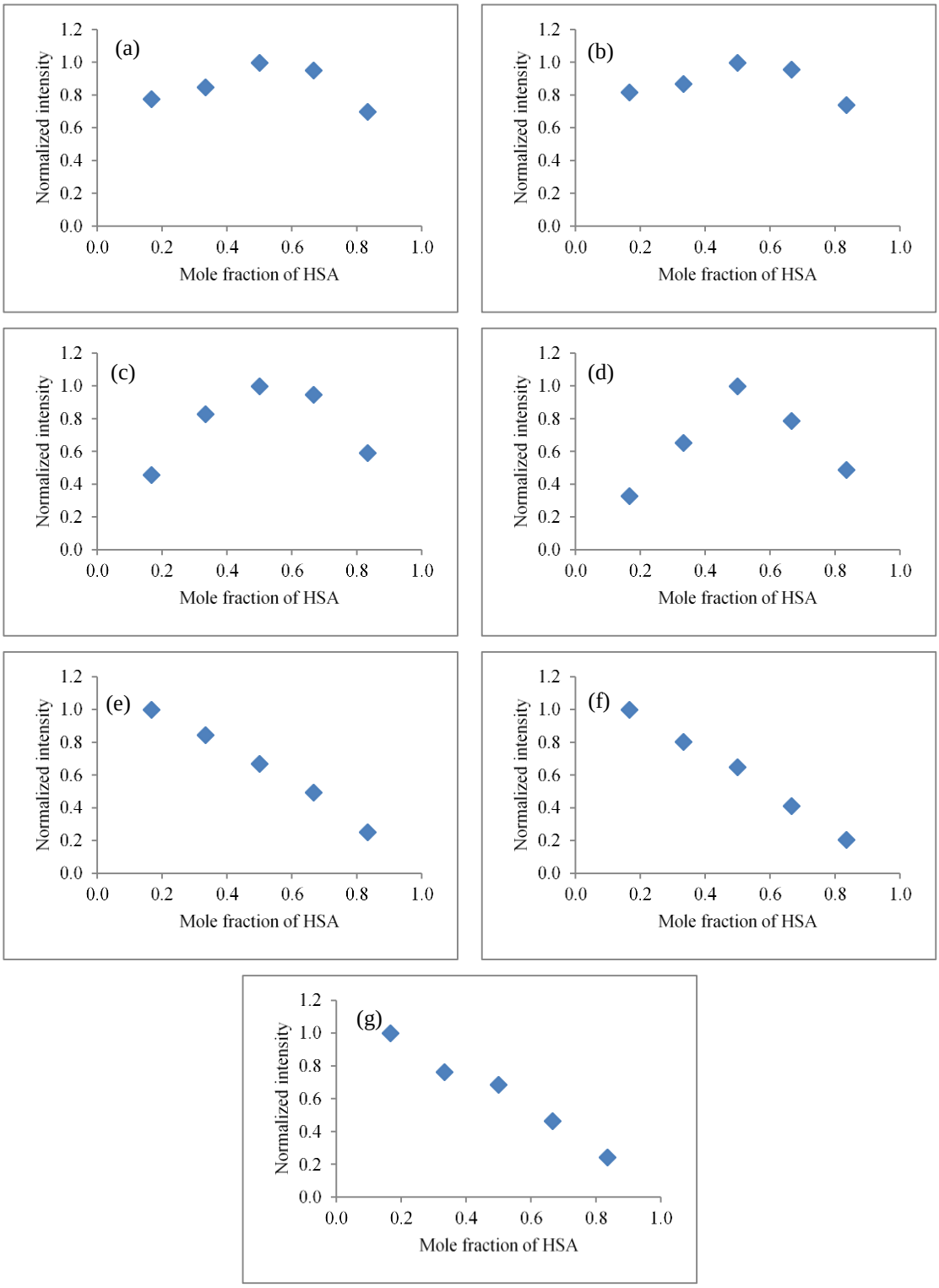


**Figure 3.5 Job's method of HSA-dye complex for (a) NB, (b) VM47, (c) VM38, (d) VM46, (e) VM41, (f) VM44, and (g) VM45 in 20 mM phosphate buffer pH 7.2, excited at 560 nm**

### *3.3.3 Effect of time on HSA-dye complex*

Determination of the time needed for the dye to fully interact with the protein is a key factor to investigate the binding affinity.[21] The effect of time on HSA-dye complex with benzophenoxazine derivatives was studied by measuring fluorescence intensity every 5 min for 30 min at room temperature. For Nile red derivatives fluorescence intensity was recorded on a solution containing $5.0\times10^{-6}$ M of the dye and $5.0\times10^{-6}$ M of HSA in 20 mM phosphate buffer pH 7.2 as shown in Figure 3.6 (a). The interaction between HSA and NR, **VM6**, and **VM23** was rapid reaching the equilibrium fast whereas it was slow with **VM8** and the intensity increased over time. The slow kinetics of **VM8** to interact with HSA could be attributed to the steric hindrance effect due to the dipropylphenyl groups attached to the benzophenoxazine backbone. On the other hand, HSA interaction with **VM20** and **VM25** was not stable over time due to the decomposition of the formed complex. Therefore, the fluorescence intensity of Nile red derivatives with HSA in binding constant determination was recorded after 10 min for NR, **VM6**, and **VM23**, after 30 min for **VM8**, and immediately for **VM20** and **VM25**. In the case of Nile blue derivatives, the effect of time was investigated on a solution containing $2.0\times10^{-6}$ M of dye and $2.0\times10^{-6}$ M of HSA in 20 mM phosphate buffer pH 7.2 as indicated in Figure 3.6 (b). The reaction between HSA and dialkylated derivatives (NB, **VM47**, **VM38**, and **VM46)** reached the equilibrium fast. Thus, the fluorescence intensity of Nile blue derivatives was measured after 5 min for determination of binding constant. The effect of time was conducted too in monoalkylated derivatives (**VM41**, **VM44**, and **VM45)** even though they did not interact with HSA as mentioned in previous sections. This was performed to allow adequate time for these dyes to bind to HSA if there was any interaction.

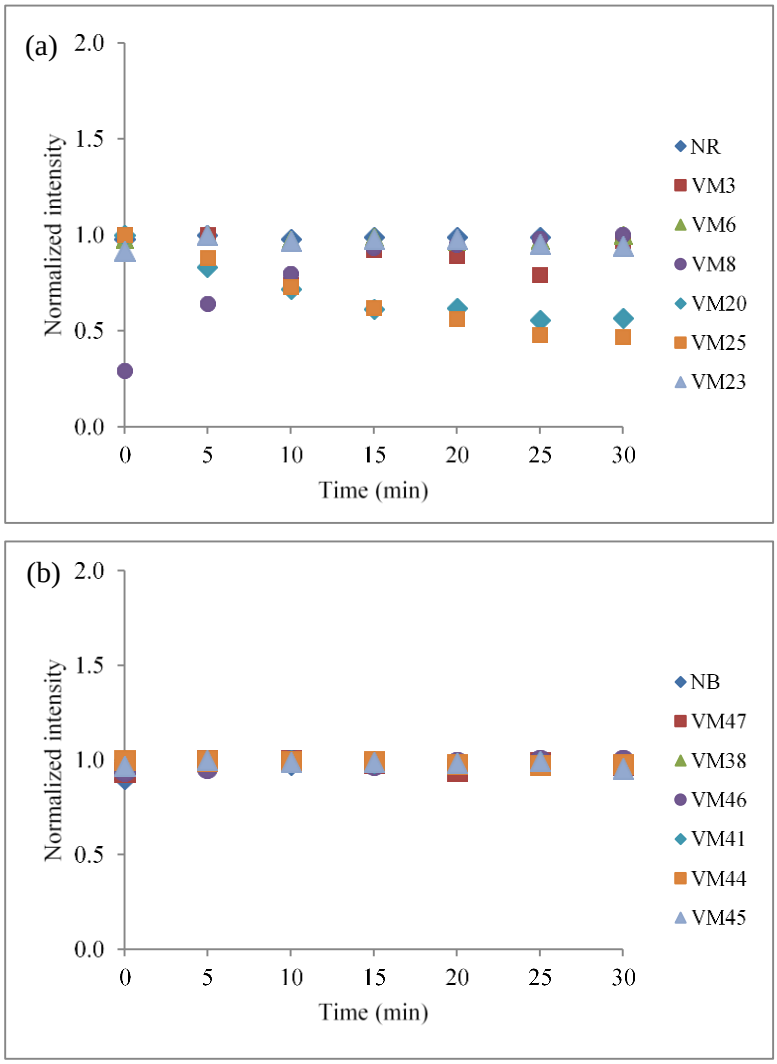


**Figure 3.6 Effect of time on interaction between the dye and HSA (a) Nile red derivatives and (b) Nile blue derivatives**

### *3.3.4 Determination of binding constant of HSA-dye complex*

The binding constant of the complex for those dyes binding to HSA in 1:1 and 1:2 stoichiometry was evaluated using equations (3.1) and (3.2), respectively. In order to understand the binding nature between HSA and benzophenoxazine derivatives, distribution coefficient

(logD) values were determined. The results indicated that the binding affinity to HSA is mainly influenced by the dye hydrophobicity. However, other factors such as steric hindrance and electrostatic interaction play a role too. At the experimental condition of pH 7.2, the net charge of HSA is negative as indicated by isoelectric point of 4.7,[22-23] whereas Nile red is neutral and dialkylated and monoalkylated derivatives are negatively charged due to the deprotonation of the hydroxyl group as indicated by $pK_a$ values. It has been known that the more hydrophobic a molecule is, the stronger binding interaction with HSA is. This binding pattern was confirmed by the highest binding constant of Nile red due to the great hydrophobicity of the dye as indicated by logD value (Table 3.2). Moreover, the least hydrophobic derivative **VM20** as indicated by logD value had the constant value. In addition, the binding of **VM25** to HSA was greater than that of **VM20** due to increase the dye hydrophobicity from 1.24 in **VM20** to 2.21 in **VM25**. However, the most hydrophobic dialkylated and monoalkylated derivatives (**VM8** and **VM23**) respectively did not show the highest binding affinity to HSA. This result can be attributed to steric hindrance of the bulky aromatic system due to phenylpropyl substituents. It was mentioned that steric hinderance can affect the interaction between the protein and the dyes.[17, 24] For Nile blue derivatives (NB, **VM47**, **VM38**, and **VM46**) the binding interaction is mostly hydrophobicity dependent. The binding constant increased as hydrophobicity of the dye increased on going from NB to **VM38**. Nonetheless, increasing the dye hydrophobicity beyond a certain point did not increase binding affinity to HSA as indicated by the constant value of the most hydrophobic **VM46** due to the significance of steric factors.

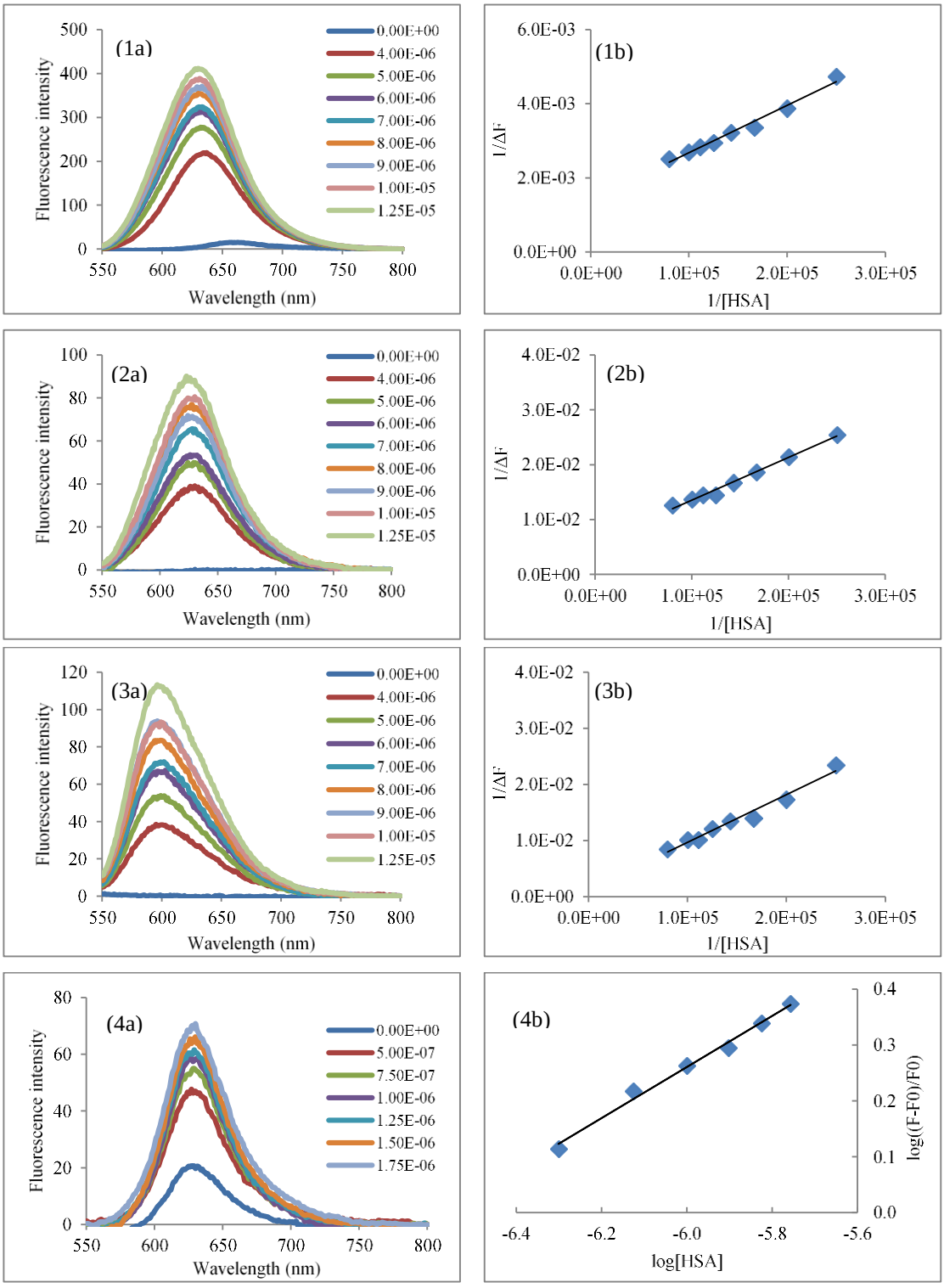


**Figure 3.7 (a) Emission spectra of $2.0\times10^{-6}$ M of dye at different concentrations of HSA (left) and (b) corresponding linear plot (right) of (1) NR (2) VM6, (3) VM8, (4) VM20, (5) VM25 and (6) VM23 in 20 mM phosphate buffer pH 7.2**

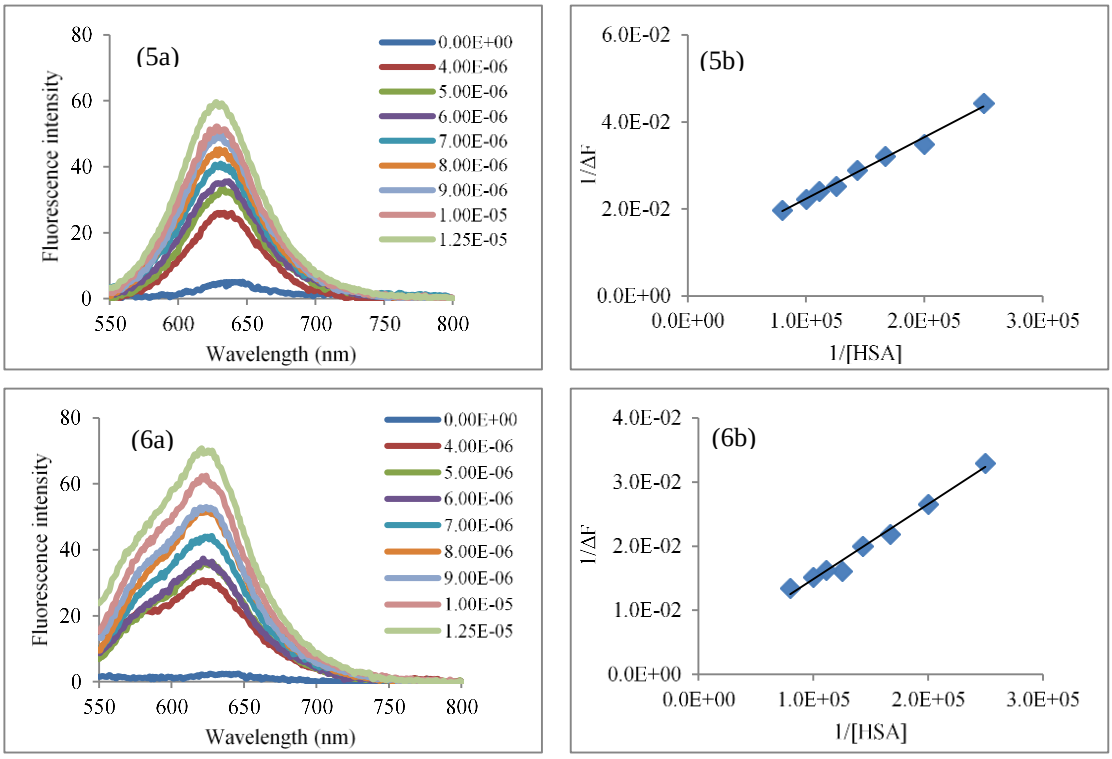


**Figure 3.7 Continue**

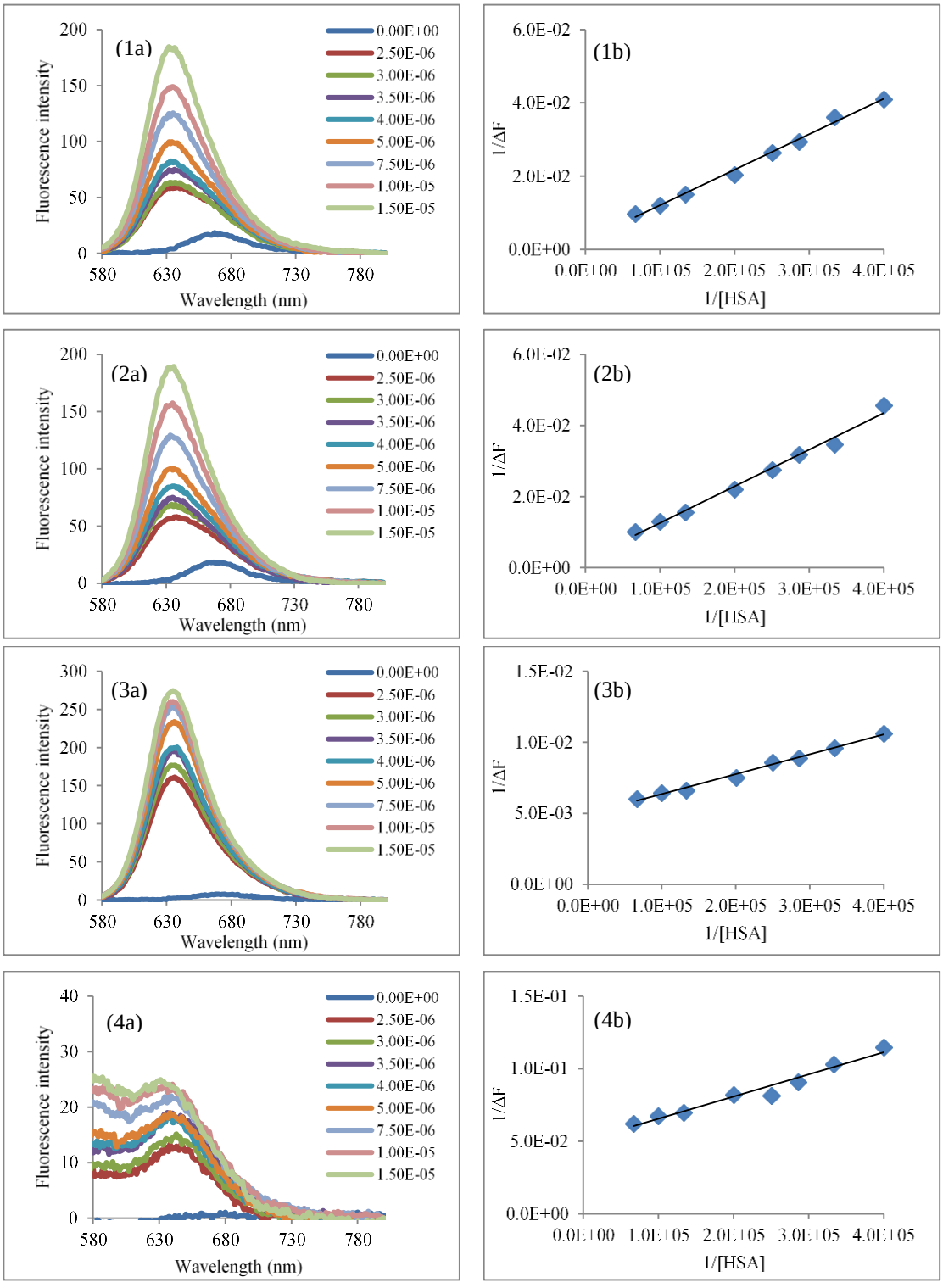


**Figure 3.8 (a) Emission spectra of $2.0\times10^{-6}$ M of dye at different concentrations of HSA (left) and (b) corresponding linear plot (right) of (1) NB, (2) VM47, (3) VM38, and (4) VM46 in 20 mM phosphate buffer pH 7.2**

**Table 3.1 Binding constant values of Nile blue derivatives in 20 mM phosphate buffer pH 7.2**

| Dye | K ($M^{-1}$) | LogD* at pH 7.4 | $pK_a$* (amine) | $pK_a$* (OH) |
|---|---|---|---|---|
| NR | $1.10\times10^{5}$ | 3.83** | 3.90 | _____ |
| **VM6** | $7.64\times10^{4}$ | 3.65 | 4.31 | 5.37 |
| **VM8** | $1.58\times10^{4}$ | 5.92 | 4.36 | 5.37 |
| **VM20** | $1.01\times10^{3}$ | 1.24 | 4.03 | 5.35 |
| **VM25** | $6.55\times10^{4}$ | 2.21 | 4.14 | 5.35 |
| **VM23** | $3.62\times10^{4}$ | 3.34 | 4.21 | 5.36 |

* Calculated by ChemAxon
** logP

**Table 3.2 Binding constant values of Nile blue derivatives in 20 mM phosphate buffer pH 7.2**

| Dye | K ($M^{-1}$) | LogD* at pH 7.4 | $pK_a$* (amine at 9-position) | $pK_a$* (amine at 5-position) |
|---|---|---|---|---|
| NB | $2.63\times10^{4}$ | 0.60 | 3.44 | 11.14 |
| **VM47** | $2.30\times10^{4}$ | 0.60 | 3.44 | 11.14 |
| **VM38** | $3.56\times10^{5}$ | 2.53 | 3.89 | 11.14 |
| **VM46** | $3.47\times10^{5}$ | 4.80 | 3.95 | 11.14 |

* Calculated by ChemAxon

## 3.4 Conclusions

Interaction of benzophenoxazine derivatives with human serum albumin was investigated in 20 mM phosphate buffer pH 7.2. The pure dyes displayed different spectral patterns and absorbance intensity in aqueous solution. An increase in fluorescence intensity and/or a blue shift was observed after the addition of HSA to the dye. Nile red derivatives except **VM3** and dialkylated Nile blue derivatives only showed great binding affinity to HSA. Those dyes interact with the protein in different mole fractions such as 0.33 or 0.50 as indicated by the method of continuous variation (Job's method) corresponding to a complex formation of 1:2 or 1:1, respectively. The results obtained by the study of effect of time on HSA-dye complex revealed that the interaction between HSA and most benzophenoxazine derivatives was fast and stable over time. However, HSA interaction with some Nile red derivatives such as **VM20** and **VM25** were not stable over time whereas the interaction with **VM8** was slow and took a long time to reach equilibrium. The binding constant values of HSA-dye complex were evaluated using spectroscopic techniques. The binding nature of the dye with HSA is hydrophobicity dependent, but it is affected by other factors such as steric hindrance and electrostatic interaction.

**References**


1. Hassan, M.; Klaunberg, B. A., Biomedical applications of fluorescence imaging in vivo. *Comparative Medicine* **2004,** *54* (6), 635-644.
2. Park, M. H.; Hyun, H.; Ashitate, Y.; Wada, H.; Park, G.; Lee, J. H.; Njiojob, C.; Henary, M.; Frangioni, J. V.; Choi, H. S., Prototype Nerve-Specific Near-Infrared Fluorophores. *Theranostics* **2014,** *4* (8), 823-833.
3. Korber, J. R.; Barth, C. W.; Gibbs, S. L., Nile Red derivatives enable improved ratiometric imaging for nerve-specific contrast. *Journal of Biomedical Optics* **2018,** *23* (7), 13.
4. Wang, B. H.; Fan, J. L.; Wang, X. W.; Zhu, H.; Wang, J. Y.; Mu, H. Y.; Peng, X. J., A Nile blue based infrared fluorescent probe: imaging tumors that over-express cyclooxygenase-2. *Chemical Communications* **2015,** *51* (4), 792-795.
5. Jose, J.; Loudet, A.; Ueno, Y.; Barhoumi, R.; Burghardt, R. C.; Burgess, K., Intracellular imaging of organelles with new water-soluble benzophenoxazine dyes. *Org. Biomol. Chem.* **2010,** *8* (9), 2052-2059.
6. Liu, K. Y.; Kong, X. Q.; Ma, Y. Y.; Lin, W. Y., Preparation of a Nile Red-Pd-based fluorescent CO probe and its imaging applications in vitro and in vivo. *Nature Protocols* **2018,** *13* (5), 1020-1033.
7. Madsen, J.; Canton, I.; Warren, N. J.; Themistou, E.; Blanazs, A.; Ustbas, B.; Tian, X. H.; Pearson, R.; Battaglia, G.; Lewis, A. L.; Armes, S. P., Nile Blue-Based Nanosized pH Sensors for Simultaneous Far-Red and Near-Infrared Live Bioimaging. *Journal of the American Chemical Society* **2013,** *135* (39), 14863-14870.

8. Fan, J. L.; Dong, H. J.; Hu, M. M.; Wang, J. Y.; Zhang, H.; Zhu, H.; Sun, W.; Peng, X. J., Fluorescence imaging lysosomal changes during cell division and apoptosis observed using Nile Blue based near-infrared emission. *Chemical Communications* **2014,** *50* (7), 882-884.

9. Liu, X. D.; Fan, C.; Sun, R.; Xu, Y. J.; Ge, J. F., Nile-red and Nile-blue-based near-infrared fluorescent probes for in-cellulo imaging of hydrogen sulfide. *Anal. Bioanal. Chem.* **2014,** *406* (28), 7059-7070.

10. Brown, M. B.; Edmonds, T. E.; Miller, J. N.; Seare, N. J., Use of Nile Red as a long-wavelength fluorophore in dual-probe studies of ligand-protein interactions. *J. Fluoresc.* **1993,** *3* (3), 129-30.

11. Davis, D. M.; Birch, D. J., Extrinsic fluorescence probe study of human serum albumin using Nile red. *Journal Of Fluorescence* **1996,** *6* (1), 23-32.

12. Sackett, D. L.; Wolff, J., Nile red as a polarity-sensitive fluorescent probe of hydrophobic protein surfaces. *Analytical Biochemistry* **1987,** *167* (2), 228-234.

13. Salomi, B. S. B.; Mitra, C. K.; Gorton, L., Electrochemical and spectrophotometric studies on dyes and proteins labelled with dyes. *Synth. Met.* **2005,** *155* (2), 426-429.

14. Lee, S. H.; Suh, J. K.; Li, M., Determination of bovine serum albumin by its enhancement effect of Nile blue fluorescence. *Bulletin of the Korean Chemical Society* **2003,** *24* (1), 45-48.

15. Sutter, M.; Oliveira, S.; Sanders, N. N.; Lucas, B.; van Hoek, A.; Hink, M. A.; Visser, A.; De Smedt, S. C.; Hennink, W. E.; Jiskoot, W., Sensitive spectroscopic detection of large and denatured protein aggregates in solution by use of the fluorescent dye Nile red. *Journal of Fluorescence* **2007,** *17* (2), 181-192.

16. Harris, D. C., *Quantitative Chemical Analysis*. Eighth ed.; W.H. Freeman and Company: New York, 2010.

17. Beckford, G.; Owens, E.; Henary, M.; Patonay, G., The solvatochromic effects of side chain substitution on the binding interaction of novel tricarbocyanine dyes with human serum albumin. *Talanta* **2012,** *92*, 45-52.

18. Sadeghi, M.; Bayat, M.; Cheraghi, S.; Yari, K.; Heydari, R.; Dehdashtian, S.; Shamsipur, M., Binding studies of the anti-retroviral drug, efavirenz to calf thymus DNA using spectroscopic and voltammetric techniques. *Luminescence: The Journal Of Biological And Chemical Luminescence* **2016,** *31* (1), 108-117.

19. Brown, M. B.; Edmonds, T. E.; Miller, J. N.; Riley, D. P.; Seare, N. J., Novel Instrumentation and Biomedical Applications of Very Near Infrared Fluorescence. *Analyst* **1993,** *118* (4), 407-410.

20. Sun, H.; Xiang, J.; Zhang, X.; Chen, H.; Yang, Q.; Li, Q.; Guan, A.; Shang, Q.; Tang, Y.; Xu, G., A colorimetric and fluorometric dual-modal supramolecular chemosensor and its application for HSA detection. *The Analyst* **2014,** *139* (3), 581-584.

21. Ramezani, A. M.; Manzoori, J. L.; Amjadi, M.; Jouyban, A., Spectrofluorimetric Determination of Human Serum Albumin Using Terbium-Danofloxacin Probe. *Scientific World Journal* **2012**, 9.

22. Vlasova, I. M.; Saletsky, A. M., Study of the denaturation of human serum albumin by sodium dodecyl sulfate using the intrinsic fluorescence of albumin. *Journal of Applied Spectroscopy* **2009,** *76* (4), 536-541.

23. Tramarin, A.; Tedesco, D.; Naldi, M.; Baldassarre, M.; Bertucci, C.; Bartolini, M., New insights into the altered binding capacity of pharmaceutical-grade human serum albumin:

site-specific binding studies by induced circular dichroism spectroscopy. *Journal of Pharmaceutical and Biomedical Analysis* **2019,** *162,* 171-178.

23. Pisoni, D. S.; Todeschini, L.; Borges, A. C. A.; Petzhold, C. L.; Rodembusch, F. S.; Campo, L. F., Symmetrical and Asymmetrical Cyanine Dyes. Synthesis, Spectral Properties, and BSA Association Study. *J. Org. Chem.* **2014,** *79* (12), 5511-5520.

# 4 INTRODUCTION TO FINGERPRINT DETECTION

## 4.1 Introduction

Identifying fingerprints are considered one of the most valuable evidence in forensic science. Forensic investigators use both terms, fingerprints and fingermarks, interchangeably even though there is a slight difference between the two terms. Fingerprints are the impressions made intentionally by an individual's hand using ink or digital imaging. They contain complete ridge details of fingertips and palm and are collected for identification purposes. Fingermarks are the residues deposited by a person's hand when touching a surface. These marks are usually incomplete in fingertips details and left by unknown individuals. Fingerprints found in a crime scene are categorized into three forms: patent, latent, and plastic prints. A patent print is a visible print that can be observed simply by the naked eye such as a fingerprint left on a glass. The patent print can be classified into two types: a positive print when the fingertip is contaminated by a colored substance such as blood or ink; or a negative print when the fingertip clears away some of the surface materials such as dust. A latent print is a hidden or unseen print that requires a special process for visualization like a fingerprint deposited on porous surfaces such as paper. It is considered the most common form found in criminal cases. Detection of this form of fingerprints is a major challenge in forensic investigation due to its invisibility. A plastic print is formed when the surface in pliable enough at the contact time to create three-dimensional image of the print such as candle wax or putty. Detection of fingerprints can be obtained through several enhancement methods: (1) physical adherence of the reagent to sticky components of fingerprint deposit.; (2) chemical reaction of the reagent with fingerprint residue; or (3) physico-chemical process between the reagent and specific fingerprint components. The basic principle of detection

methods is to create a great visual contrast between the developed prints and the underlying substrate without distorting fingerprint ridges. To achieve good contrast, the reagent should interact specifically with fingerprint components and not with the substrate.[1, 2]

## 4.2 Fingerprint composition

Fingerprint residue is a complex mixture of several substances originating from the epidermis, the secretory glands in the dermis, intrinsic components such as medication and drug level, and extrinsic contaminants such as blood, make-up, food, moisturizers, and dirt.[3, 4] The epidermis is the outer layer of skin while the dermis is the bottom layer of the skin that contains five million secretory glands including eccrine, sebaceous, and apocrine glands responsible for body secretion:[5]

- Eccrine glands are distributed throughout the body and in high density on the hand palms and feet soles. The main component of eccrine secretion is water (99%) in addition to some organic and inorganic compounds as summarized in Table 4.1. Studies have identified 20 amino acids in fingerprint residue using different analytical techniques.[6-8] The first amino acid found in eccrine secretion is serine. The abundance of amino acids in fingerprint deposition relative to serine[9-11] is shown in Table 4.2.
- Sebaceous glands are found on the body parts that contain hair follicles as well the face and scalp. The secretion of these glands is called sebum which is composed of several organic compounds. The major compound of sebum is lipids[6] such as triglycerides, fatty acids, wax esters, squalene, and cholesterol as indicated in Figure 4.1 and Table 4.3.
- Apocrine glands are located mainly in the axillary regions (armpits and genital areas). The compounds secreted from these glands do not contribute to fingerprint composition due to

their locations. However, analysis of apocrine secretion might be crucial in some sexual crimes.[3]

However, fingerprint residue predominantly consists of secretions from eccrine and sebaceous glands. Lipids from the epidermis also contribute to fingerprints residue.[3, 5]

**Table 4.1 A summary of the composition of eccrine secretions**

| Organic (major) | Amount | Organic (trace) | Inorganic (major) | Amount | Inorganic (trace) |
|---|---|---|---|---|---|
| Amino acids | 1.45 mg/L | Creatine | Chloride | 3.5 g/L | Magnesium |
| Proteins | 200 mg/L | Creatinine | Sodium | 3.3 g/L | Zinc |
| Glucose | 3.50 mg/L | Glycogen | Potassium | 0.2 g/L | Copper |
| Lactate | 3.15 mg/L | Uric acid | Iron | 3.5 mg/L | Cobalt |
| Urea | 0.75 mg/L | Vitamins | Calcium | 2.0 mg/L | Lead |
| Pyruvate | 0.079 mg/L | | Bicarbonate | 107 mg/L | Manganese |
| Lipids: | | | Sulphate | 10 mg/L | Molybdenum |
| Fatty acids | 0.005 mg/L | | Phosphate | 1.4 mg/L | Tin |
| Sterols | 0.065 mg/L | | Fluoride | 69 μg/L | Mercury |
| | | | Bromide | 35 μg/L | |
| | | | Iodide | 0.85 μg/L | |

**Table 4.2 The relative abundance of amino acids (percentage to serine) in fingerprint residue**

| Amino acids | Hadorn et al. [9] | Hamilton [10] | OrÓ and Skewes [11] |
|---|---|---|---|
| Serine | 100 | 100 | 100 |
| Glycine | 54 | 67 | 59 |
| Ornithine | 45 | 32 | 45 |
| Alanine | 35 | 27 | 28 |
| Aspartic acid | 11 | 22 | 22 |
| Threonine | 9 | 17 | 18 |
| Histidine | 13 | 17 | 14 |
| Valine | 10 | 12 | 9 |
| Leucine | 7 | 10 | 10 |
| Isoleucine | 6 | 8 | 8 |
| Glutamic acid | 12 | 8 | 5 |
| Lysine | 5 | 10 | — |
| Phenylalanine | 5 | 7 | 5 |
| Tyrosine | 3 | 6 | 5 |

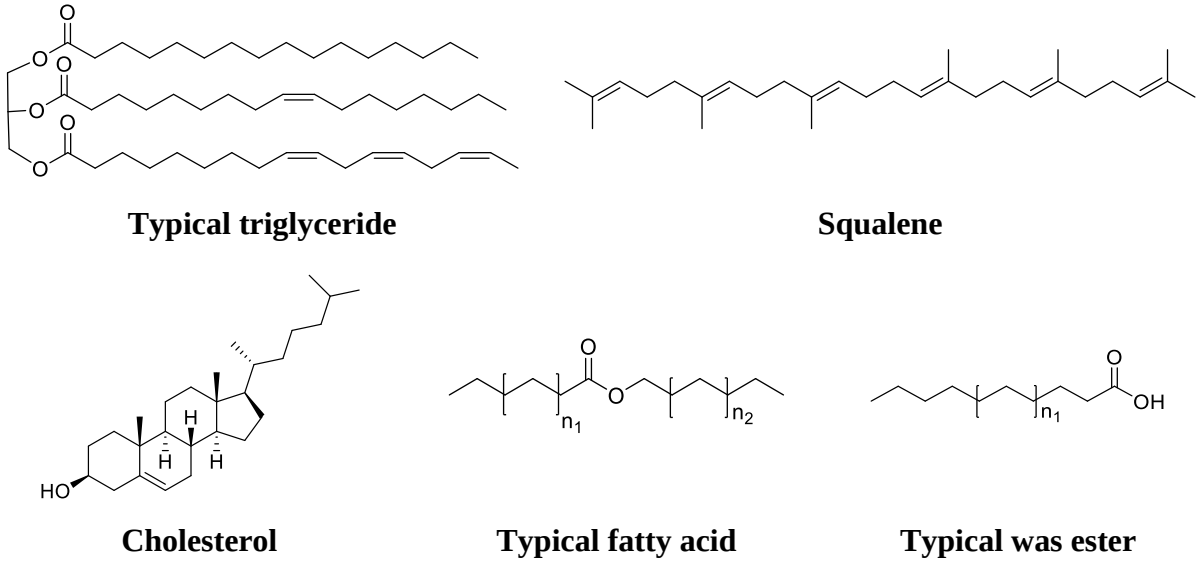


**Figure 4.1 Chemical structures of some sebaceous secretion compounds**

**Table 4.3 A summary of the composition of sebaceous secretions**

| Organic (major) | Amount | Organic (trace) |
|---|---|---|
| Triglycerides | 30-40% | Aldehydes |
| Fatty acids: | 15-25% | Ketones |
| saturated | 50% | Amines |
| monounsaturated | 48% | Amides |
| polyunsaturated | 2% | Alkanes |
| Wax esters | 20-25% | Alkenes |
| Squalene | 10-12% | Alcohols |
| Cholesterol | 1-3% | Phospholipids |
| Cholesterol esters | 2-3% | Pyrroles |
| | | Pyridines |
| | | Piperidines |
| | | Pyrazines |
| | | Furans |
| | | Haloalkanes |
| | | Mercaptans |
| | | Sulphides |

## 4.3 Variability of fingerprint composition

Fingerprint composition is affected by several factors such as personal characteristics, environmental factors, fingerprint age, and type of substrate. It is of great interest to explore the influence of these factors on fingerprint residue as the composition is highly variable.

Fingerprint residue can vary between donors due to the differences in their personal characteristics including age, gender, race, and diet, as well as medications and drugs. The composition is influenced by the donor's age in that it alters among children, adolescents, adults, and elderly. Studies have explored the chemical difference in fingerprints between children and

adults as a determination method for the age of a person based on FTIR analysis.[12-14] The results indicated a difference in fingerprint composition between children and adults was obtained considering lipid components in that the former contain high amount of cholesterol, cholesteryl esters, and straight-chain fatty acids while the latter contain squalene, wax esters, and branched fatty acids.[12] Fingerprint composition can be influenced by gender, although contrary results were observed. Studies have shown that fingerprint components such as fatty acids or amino acids were found to vary between male and female donors. However, the variation was not significant due to the small scale of individuals involved in the studies.[15, 16] Moreover, results have indicated that the relative amount of ten fingerprint components relative to squalene displayed a minor gender difference for only three components in a small group of donors. However, when the study included a large group of donors, no statistical differences in fingerprint composition among male and female donors were obtained.[17] The influence of race on fingerprint residue has been studied. A small-scale study revealed that the ratio of some fatty acids and their methyl esters could be used to differentiate individuals from various ethnic groups in which the highest difference in the ratio was between Caucasian and African American males. It was concluded, however, further study including larger donors is required to support the obtained data.[16] In addition to the donor's age, gender, and race, diet may affect fingerprint composition. Fatty acids and amino acids such as alanine, glycine, and serine were found in high levels in the vegetarian donors, but no significant difference was observed due to the small size of the study.[18]

The composition of fingerprints is affected by environmental conditions including light exposure, temperature, and humidity levels. Studies have shown that exposure to light affects fingerprint composition. For example, squalene concentration decreases much faster when stored in the light than in the dark. It was observed that squalene was not detected in prints after 9 days

storage in light condition whereas in dark condition it was still detectable after 33 days storage.[19] Moreover, a reduction in lactic acid concentration was obtained after 2 days of sunlight exposure. On the contrary, amino acids and urea were found to be resistant to light even after long exposure time.[20] Exposure to high temperature is another factor that has an impact on fingerprint composition. FTIR analysis showed that a degradation process of esters occurred rapidly at high temperature. However, acid salts were not affected by high temperature, and they still could be detected even after heating at 70 °C for 72 hours.[14] Findings have indicated that exposure to high temperature increased the degradation of amino acids.[8, 20] Other components of fingerprint residue such as urea was found to decompose at high temperature.[20] Moreover, exposure to elevated temperature increases the rate of water loss from fingerprint residue. The effect of humidity on fingerprint composition has not been investigated directly. Nonetheless, studies have been conducted to explore the effect of humidity on developing methods. Fingerprints developed by amino-acid reagents such as ninhydrin and 1,2-indanedione are more affected by humidity level compared to DFO development.[21] A study by Paine et al. indicated that efficiency of cyanoacrylate fuming for fingerprint development varies with humidity levels as 80% relative humidity is the optimum level. It was concluded that eccrine components of fingerprint residue are more influenced by variation in relative humidity than sebaceous components.[22]

Fingerprint residue undergo changes occurring over time by means of chemical, physical, or biological processes resulting in the aged composition of fingerprints. These changes include disappearance or conversion in the initial composition through various processes such as degradation, evaporation, metabolism, drying, migration, oxidation or polymerization.[3, 4] The effect of aging on eccrine components is water loss as water is the main compound of eccrine secretion. As the fingerprint ages, amino acids remain stable over a long period of time on porous

substrates under normal environmental conditions (relative humidity <80%). A study of ninhydrin analogues for fingerprint detection demonstrated that good stability of amino acids is because of their high affinity for cellulose as they do not migrate or diffuse through dry paper. Thus, very old fingerprints (up to 40 years) can be revealed with good quality by amino acid reagents.[1, 23] Concerning the effect of aging on proteins, a study of fingerprint visualization on porous surfaces using antibody with albumin indicated that both fresh and old fingerprints (up to 130 days) were detected with good ridge details.[24] Regarding inorganic components such as chloride, however, it tends to diffuse through the substrate over time which is significantly affected by environmental conditions such as humidity. Therefore, developing old fingerprints by some enhancement methods targeting chloride ions such as sliver nitrate results in blurred images.[1, 4] The concentration of sebaceous components such as squalene, cholesterol, fatty acids, and wax ester decreases over time. These compounds undergo several decomposition and degradation processes resulting in formation of small oxidized molecules. Squalene, for example, decomposes very quickly in the first day and cannot be detected on old fingerprints after one week of deposition on glass substrate. However, the decomposition occurs at a much lower rate on microfilters and squalene still is detectable after 30 days.[25] The concentration of cholesterol decreases at a slow rate on glass while no change in the concentration was observed on microfilters even after 30 days of deposition.[25] It was observed that short-chain fatty acids were detected in aged fingerprints whereas long-chain fatty acids were found in fresh fingerprints. This is probably due to the decomposition reaction of long fatty acids forming the short ones.[19] Saturated lipids such as wax ester and saturated fatty acids remain longer in fingerprint deposition than unsaturated compounds. The explanation for this behavior is saturated compounds do not contain functional groups for degradation process.[4]

The effect of substrate on fingerprint composition depends on the characteristics of the substrate such as porosity, texture, curvature, physico-chemical structure, temperature, electrostatic forces, and surface tension.[3] Results have shown that penetration of fingerprint components into the substrate is proportional to the degree of porosity.[26] The more porous the substrate is, the higher fingerprint residue penetrates to the substrate. In general, substrates baring fingerprints can be classified according to their porosity into three types: porous, semi-porous, and non-porous substrates. Fingerprint residue reacts differently with each type of substrate. Porous substrates such as paper and cardboard absorb eccrine components quickly within few seconds after deposition while sebaceous components take longer time to be absorbed (about 12 hours to one day). Semi-porous substrates such as glossy paper and plastics absorb eccrine components slowly within few minutes to one hour after deposition whereas sebaceous components stay on the surface for longer time before absorption occurs in a day or several days. In non-porous substrates such as glass and metals, no fingerprint secretions are absorbed. In fact, fingerprint components stay on the surface and become very fragile over time and susceptible to degradation process.[1, 27]

In addition to the number of factors affecting fingerprint residue listed above, the composition is influenced by deposition conditions such as deposition pressure, contact time with substrate, and how often the donor washes his hands. Also, fingerprints may contain some contaminations such as blood, make-up, food, and dirt that may be present in hand. Moreover, fingerprint composition of the same donor varies from day to day as well as at different periods of the same day.[4, 19]

## 4.4 Fingerprint detection methods

A wide variety of techniques have been used to develop fingerprints on different types of surfaces. The most popular fingerprint detection methods such as physical developer, cyanoacrylate fuming, and powder dusting are demonstrated in this section.

### *4.4.1 Physical developer*

Physical developer (PD) is a latent fingerprint technique that was introduced first by Morris and Wells in 1979.[28] It has been used since then as a standard method in many forensic laboratories to develop fingerprints on porous surfaces that have been wet such as paper. It is recommended to use physical developer at the end of treatment sequence if no fingerprints were detected by amino-acid sensitive reagents in order to obtain additional details of fingerprints. Given the fact that amino acid-sensitive reagents such as ninhydrin, DFO, indanedione detect the water-soluble components of fingerprint reside, there is an assumption that physical developer targets the water-insoluble components such as lipids. The assumption of physical developer targeting the lipids secreted from sebaceous glands or originated from the epidermis has been investigated as well as another assumption of physical developer targeting the eccrine secretion components. It was concluded from the studies that PD does not specifically target lipids, but it may target eccrine components or a mixture of both lipids and eccrine secretion.[29, 30]

There are two types of developers: chemical developer and physical developer. Chemical developer process involves the use of reducing agent such as pyrogallol or metal, whereas reducing agent in physical developer process is ferric and ferrous ions. Both developers are a photographic process to form a silver image. The most common developer uses ferrous/ferric redox solution for fingerprint development because of its reversibility and stability. Beside the reducing agent, other

solutions are involved in physical developer process including silver nitrate solution and surfactant solution such as n-dodecylamine acetate along with prewash acidic solution. The most accepted mechanism of physical developer is that silver ions are reduced to metallic silver forming black colloidal particles on the surface bearing fingerprints and ferrous ions are oxidized to ferric ions according to the reaction:[31, 32]

$$Ag^{+}_{(aq)} + Fe^{2+}_{(aq)} \rightleftharpoons Ag_{(s)} + Fe^{3+}_{(aq)}$$

The fingerprints treated by physical developer sometimes are weak or have poor contrast particularly on dark surfaces. Some research groups have attempted to improve the contrast of developed fingerprints by means of modification of the procedure. For instance, distilled water used in the original formulation has been replaced by more purified reverse osmosis/deionized water. As a result, concentrations of working solution such as silver nitrate, surfactant, ferrous solution, and citric acid are reduced because the deionized water is less ionic than distilled water. Moreover, malic acid was introduced to the new formulation at different concentrations, and the effect of acid type from malic to maleic acid was investigated too. The performance of the new formulation was comparable or better than the original formulation at low cost.[33] Another research group has studied the effect of various formulations of stock solutions on the efficiency of physical developer such as changing the order of reagents addition, omitting surfactants or citric acid, and substitution a reagent with another one. It was concluded that no specific order for reagent addition is required, but some alterations in concentrations may lead to insufficient fingerprint detection.[34] Other studies have been conducted in attempts to modify physical developer procedure in terms of longevity and stabilty of working solutions.[35, 36] On the other hand, several methods can be used to enhance the background contrast between the prints and the substrate including optical methods, scanning electron and x-ray methods, digital imaging methods, and chemical methods.[32] However,

physical developer has some disadvantages; the technique has been known as expensive, complex, and time consuming. Moreover, working solutions have a short shelf-life and are highly sensitive to contamination which requires meticulous cleaning of glassware. Additionally, the paper can be damaged during processing due to prewash with maleic acid and serial immersion in aqueous solutions. Regardless of these limitations, physical developer is the most reliable method to detect latent fingerprints on wet porous surfaces.

### *4.4.2 Cyanoacrylate fuming*

Cyanoacrylate fuming is a fingerprint technique that was first used in the late 1970's.[37] Since then, it has become the most common process for detection on non-porous surfaces such as glass and plastic. The fuming process includes the use of colorless monomeric liquid known as Superglue, a rapid high strength glue. When cyanoacrylate is heated to the boiling point, the monomeric vapor reacts by polymerization with some fingerprint residue such as sebaceous and eccrine components but not with the background surface. Lipid and greasy (sebaceous) components show high sensitivity to the vapor although cyanoacrylate interacts with moisture and some water-soluble (eccrine) components. The polymerization process produces a white solid polymer (polycyanoacrylate) developing fingerprint ridges as shown in Figure 4.2. Because of the vapor toxicity and health hazardous, the fuming is performed in a closed chamber where exposure to the vapor can be minimized, and heating process can be controlled.[38]

However, the main disadvantage of the technique is the poor contrast from the background due to the white color of polymer particularly on light-colored surfaces. The contrast of cyanoacrylate-developed fingerprints can be improved by post-treatment using several methods such as combining fuming with the ninhydrin/zinc chloride method and laser illumination,[39]

dusting using fluorescent powder,[40] and imaging using an infrared spectral mapping.[41] The most common improvement method is staining using fluorescent dyes followed by laser illumination or light source such as Nile red, Nile blue, acid fuchsin, rhodamine 6G, basic yellow 40, basic red 28, and Styryl 7 [42-44]. The success of the staining process depends on the choice of the dye and its optical properties as well as the nature of the background such as color and luminescence properties.[44] Khuu et al. proposed a one-step procedure to enhance cyanoacrylate-developed fingerprints using CN Yellow Crystals, PolyCyano UV and PECA Multiband as an alternative method to the conventional post-treatment methods.[45] The procedure was evaluated for fingerprints deposited on non-porous and semi-porous surfaces and aged for up to 8 weeks.

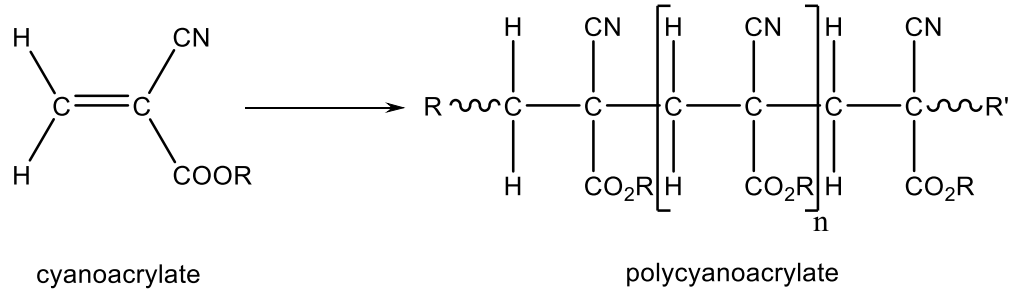


**Figure 4.2 Polymerization reaction of cyanoacrylate during fuming process**

### *4.4.3 Powder method*

Powder method is one of the most popular techniques for developing fingerprints on non-porous surfaces. The first use of fingerprint powders was in the early nineteenth century, and it still is commonly used at a crime scene. The technique is simple and can be applied by dusting the powder onto the surface using a brush, so the powder adheres physically to moisture and oily components of fingerprint residue. When using powder method for fingerprint identification, some aspects should be taken into consideration with respect to surface and powder properties such as

size and color. The surface bearing the fingerprints must be appropriate for dusting action and not interact with the powder. Concerning the powder properties, the particle size of the powder must be suitable for adhesion process to yield satisfactory results. Moreover, the powder should adhere sufficiently to fingerprint residue to provide clear patterns. In addition, the powder color should be dissimilar than the surface color so good contrast of fingerprints from the surface can be achievable. Despite the simplicity of the use of powder method for fingerprint development, some disadvantages have been reported. For instance, contact of the brush with the surface bearing the prints results in destroying fingerprint ridges, so care should be taken by the fingerprint expert to avoid destructive effect.[46, 47]

In general, there are three types of fingerprint powders: regular, luminescent, and metallic or magnetic powders. The first type of fingerprint powder is regular powder; it contains a polymeric resin for adhesion process and coloration compounds to ensure background contrast. Many powder formulas have been reported for fingerprint detection. For example, black powder such as ferric oxide powder and lampblack powder is used for light-colored surfaces. On the other hand, white powder such as titanium oxide powder is applied to dark-colored surfaces. However, some of the regular fingerprint powders contain toxic heavy elements including lead, mercury, bismuth, or antinomy. Therefore, they are no longer in use due to potential health hazards.[2, 46] The second type of fingerprint powder is luminescent powder; it consists of natural or synthetic chemicals that fluoresce upon exposure to UV light, laser light, or light source. This type of powder is beneficial for revealing fingerprints left on dark surfaces. In addition, the performance of weak fingerprints developed by the regular powder can be enhanced by the luminescent powder due to its great sensitivity. Some common fluorescent dyes have been used in luminescent powder compositions including acridine orange, acridine yellow, crystal violet, Nile blue, coumarin 6,

rhodamine B, and rhodamine 6G.[47] The third type of fingerprint powder is magnetic powder; it is a fine ferromagnetic powder containing mainly iron oxide or iron powder dust as well as a colorant. It can be applied using a standard magnetic applicator. Unlike the regular powder, magnetic powder is effective for developing fingerprints deposited on non-porous surfaces such as paper of different colors and textured surface.[48] Several formulas of magnetic flake powders reported for fingerprint development have shown equal or superior detection results compared to commercial aluminum powders on smooth and rough surfaces, respectively.[49]

## 4.5 Fingerprint developing reagents

Several reagents have been investigated for fingerprint development. Each reagent reacts with specific components of fingerprint residue and works the best on a particular substrate. The most common reagents such as fluorescent dyes, ninhydrin, 1,8-diazafluoren-9-one (DFO), and 1,2-indanedione are described in this section.

### *4.5.1 Fluorescent dyes*

Fluorescent dyes are organic molecules that absorb light, and upon excitation they emit it at long wavelengths. They react mostly with sebaceous secretions of fingerprints deposited on porous and non-porous surfaces. Fluorescent dyes have been used extensively in forensic investigation as main reagents or complementary agents due to their ability to develop fingerprints that are difficult to detect by regular reagents, particularly on dark-colored surfaces. Thus, good contrast and clear fingerprints with more ridge details are obtained by these dyes due to their luminescence properties. It was stated that the sensitivity of luminescence methods is significantly superior to those of absorption methods up to four orders of magnitude.[50] As discussed earlier,

fluorescent dyes have been applied as dusting agents such as acridine orange, acridine yellow, crystal violet, coumarin 6, and rhodamine B.[47] Some fluorescent dyes such as acid fuchsin, basic yellow 40, basic red 28, and Styryl 7 have been used as an enhancement method for the fingerprints developed by cyanoacrylate fuming,[43, 44] as mentioned previously. Moreover, some dyes have been involved in post-treatment process as well as main reagents. For instance, Nile red was initially used to improve the performance of cyanoacrylate fuming and then has been studied as a primary reagent for fingerprint detection.[42, 51] Moreover, Nile blue has contributed to fingerprint investigation in such different ways: secondary treatment of cyanoacrylate, powdering, and an aqueous solution.[43, 47, 52] Besides its use as a fingerprint powder, rhodamine 6G has been introduced to the post-treatment process of two different methods: cyanoacrylate fuming and staining with Oil Red O for enhancement purposes.[44, 47, 53] Other dyes such as eosin-blue dye have been used in two different fingerprints developing techniques: powder dusting and in a formulation based on phase transfer catalyst.[54, 55] In addition to the fluorescent dyes, some dyes have been used widely in fingerprint detection even though they are not fluorescent such as Oil Red O and solvent black 3. The two dyes are lysochrome used in histology as lipids and phospholipids stains. Fingerprints developed by Oil Red O and solvent black 3 appear as visible red and dark blue impressions, respectively.[2] The chemical structure of most dyes used as fingerprint reagents is shown in Figure 4.3.

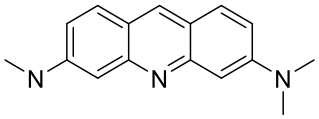

**Acridine orange**

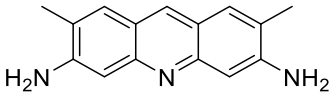

**Acridine yellow**

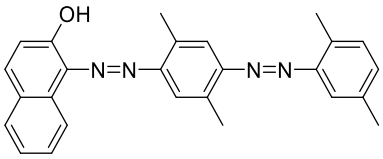

**Oil Red O**

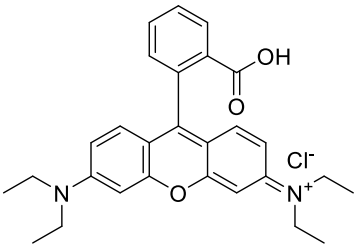

**Rhodamine B**

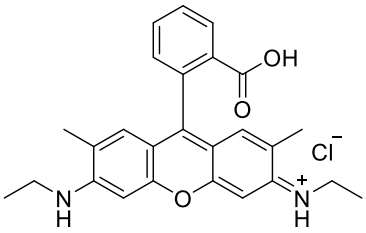

**Rhodamine 6G**

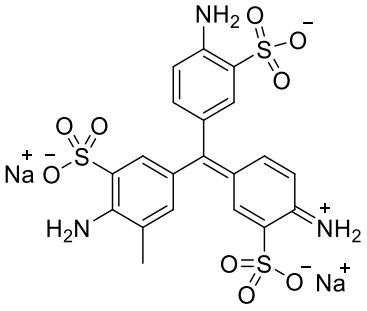

**Acid fuchsin**

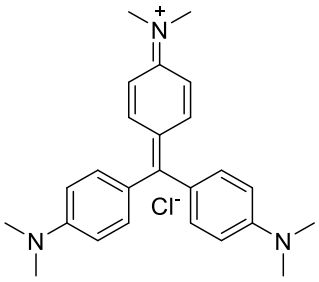

**Crystal violet**

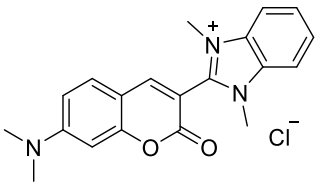

**Basic yellow 40**

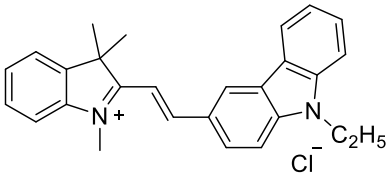

**Basic red 28**

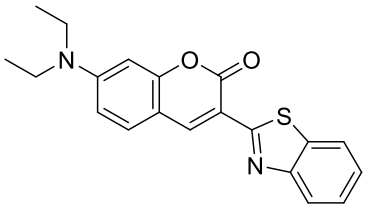

**Coumarin 6**

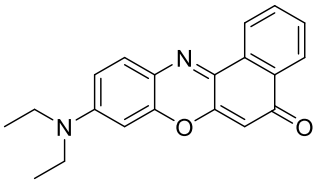

**Nile red**

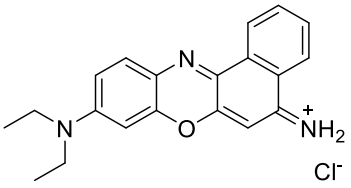

**Nile blue**

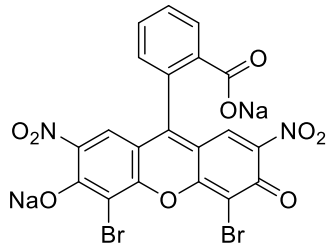

**Eosin-blue dye**

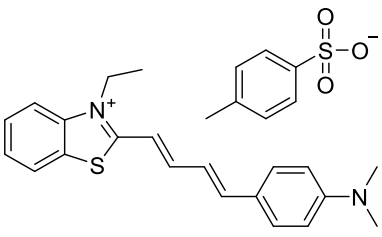

**Styryl 7**

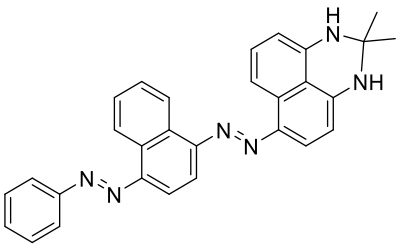

**Solvent black 3**

**Figure 4.3 Chemical structures of some dyes used as fingerprint reagents**

### *4.5.2 Ninhydrin*

Ninhydrin (2,2-dihydroxy-1,3-indanedione) is the most popular reagent for developing latent fingerprints on porous surfaces. It was first synthesized by Ruhemann in 1910 to react with amino acids forming a deep blue or purple product named "Ruhemann's purple".[56] The initial use of ninhydrin as a developing agent in forensic science was in 1954 by Oden and von Hofsten.[57] Many studies have been examined the reaction mechanism of ninhydrin with amino acids. Ruhemann claimed that both α- and β- amino acids react with ninhydrin to form the purple product. However, it has been reported by other groups that only α-amino acids produce the purple compound upon reaction with ninhydrin.[58] The formation of Ruhemann's purple includes three general steps: the first step involves the initial attack of the amine group on ninhydrin; the second step is oxidation and reduction steps leading to intermediate compounds, and the third step is the formation of purple product from the intermediates.[58] The mechanistic description of Ruhemann's purple resulting from the reaction between ninhydrin and amino acid[59] is shown in Figure 4.4 (a).

When using ninhydrin in forensic investigation, fingerprints appear as visible purple marks on light-colored substrates. Many studies have been conducted to improve the performance of ninhydrin by optimizing the experimental conditions such as exposure time, solvent formulation, temperature, and humidity.[50] Despite the fact that ninhydrin is the common amino acid reagent for fingerprint detection, the contrast of the developed fingerprints and the substrate is week particularly on dark-colored surfaces. Therefore, efforts have been made to overcome this limitation and enhance the sensitivity of the reagent by post-treatment with metal salts. It was reported that fingerprints developed by ninhydrin produced a fluorescent complex when treated with salts of the group 12 metals of the periodic table.[60-62] The reaction of Ruhemann's purple with the salt of certain metals such as zinc and cadmium formed an orange and red complex,

respectively under illumination mode. The fluorescence properties of the complex increase when cooling to the temperature of liquid nitrogen (77K). Moreover, Almog et al. proposed a one-step process of fingerprint detection by ninhydrin instead of the two-step process (post-treatment).[63] It was concluded that the quality of developed fingerprints by the one-step was as efficient as those developed by the two-step process. The reaction mechanism of Ruhemann's purple with metal salts to form a complex ion[64] is shown in Figure 4.4 (b).

### *4.5.3 1,8-Diazafluoren-9-one*

1,8-Diazafluoren-9-one (DFO) is amino-acid reagent used widely for detecting latent fingerprints on porous surfaces such as paper. It was first synthesized by Druey and Schmidt in 1950;[65] however, the first use of the reagent for fingerprint development was in 1990 by Grigg and Pounds.[66] DFO reacts with amino acids in a similar pathway of ninhydrin to give a faint purple product (lighter than the color obtained with ninhydrin). However, the reaction product is very fluorescent without any post-treatment forming red-colored prints.[67] DFO is extremely more sensitive than ninhydrin due to its luminescence properties. Unlike the ninhydrin reaction, heat is required for the reaction to proceed using either an oven or ironing press.[68] The formation mechanism of the fluorescent compound is shown in Figure 4.5. First, DFO reacts with amino acids present in fingerprint deposition to form an imine intermediate. Then, the intermediate undergoes decarboxylation and hydrolysis process to form an aromatic amine. Lastly, the amine reacts with excess DFO molecules producing the red fluorescent compound.[69] Although fingerprints developed by DFO are fluorescent, studies have been continued to improve the reagent sensitivity and contrast from the background substrate. For instance, the effect of secondary treatment with metal salts on the luminescence properties of the fingerprints was investigated. It

was concluded that only a slight enhancement in luminescence of the developed prints was obtained when treatment with zinc chloride, while no improvement was observed with the salts of other metals such as cadmium, ruthenium or europium.[70] Currently, DFO is considered the best fluorescent reagent to reveal fingerprints on porous surfaces.

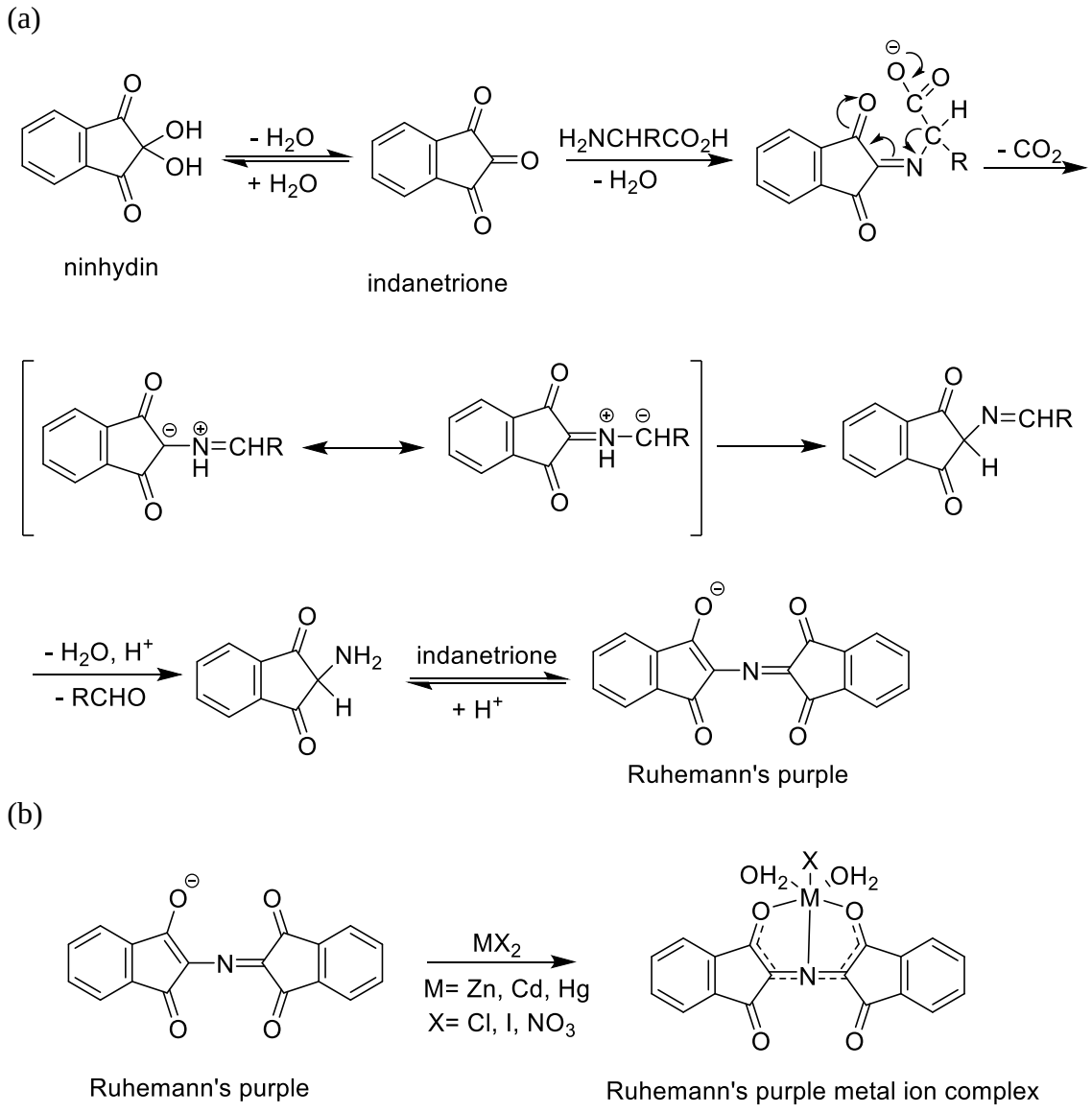


**Figure 4.4 Reaction mechanism of: (a) ninhydrin with amino acids to form Ruhemann's purple and (b) Ruhemann's purple with metal salts to form a complex ion**

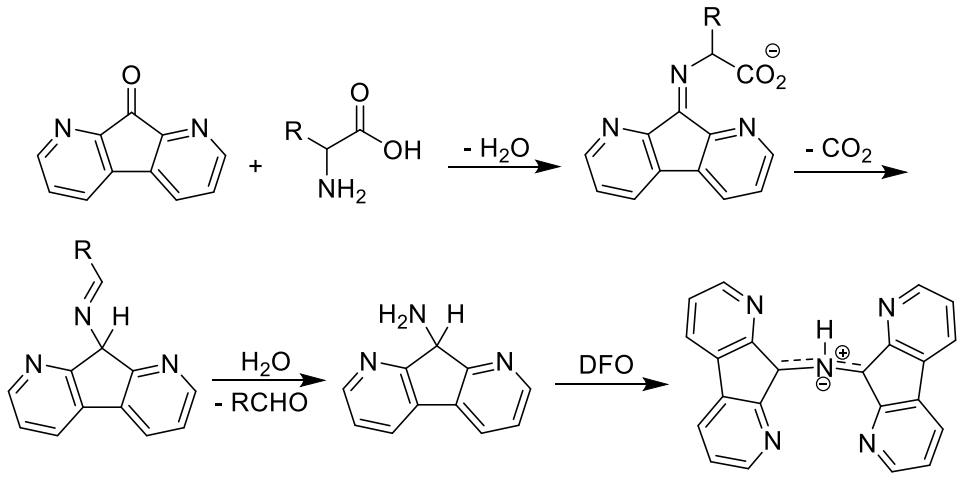


**Figure 4.5 Proposed reaction mechanism of DFO with amino acids**

### *4.5.4 1,2-Indanedione*

1,2-Indanedione is a developing reagent targeting amino acids present in latent fingerprints deposition. In 1997, Ramotowski and co-workers proposed a new class of ninhydrin analogous:1,2-indanedione to be used for fingerprint visualization.[71, 72] Similar to DFO, 1,2-indanedione detects fingerprints that appear light pink with intense fluorescent upon illumination. Significant studies have been reported on optimization the reagent in term of formulation, carrier solvents, and development conditions. [73-75] Moreover, these studies involved a comparative evaluation of reagent performance with the most conventional reagents for fingerprint detection on paper: ninhydrin and DFO. Even though the prints developed by 1,2-indanedione are fluorescent without post-treatment, the addition of metal salt has been investigated. It was shown that introducing of zinc chloride to 1,2-indanedione solution before sample treatment the increased the luminescence of the detected prints.[76, 77] The reaction mechanism of 1,2-indanedione with amino acids is indicated in Figure 4.6. First, 1,2-indanedione reacts with amino acids to form imines. Then, decarboxylation and Strecker degradation occur to produce 2-amino-1-indanone

which reacts after that with excess of 1,2-indanedione to produce 1,3-dipole the luminescent compound.[78]

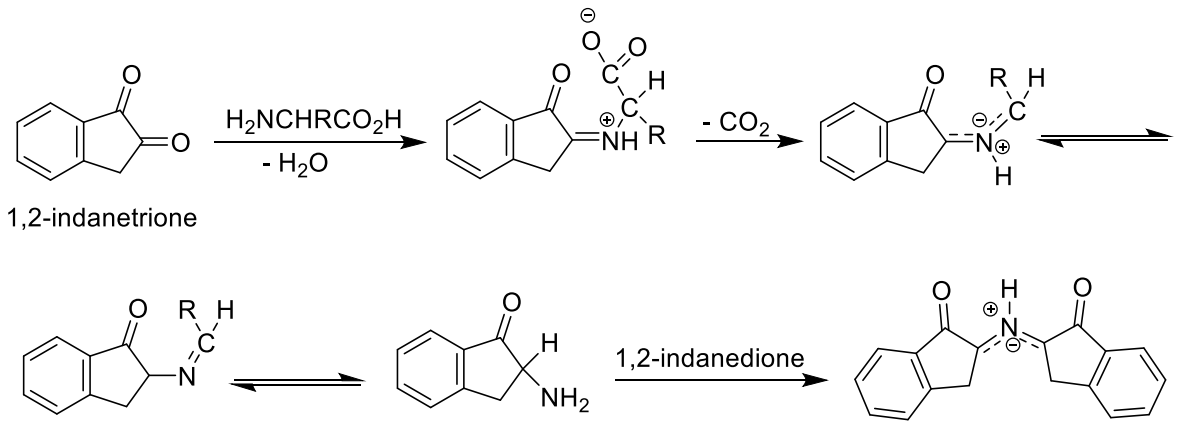


**Figure 4.6 Proposed reaction mechanism of 1,2-indanedione with amino acids**

## 4.6 Fingerprint reagents classification

Fingerprint reagents can be classified based on the targeting components of fingerprint residue into two types: water-soluble component and water-insoluble component reagents. An example of water-soluble component reagent is silver nitrate which detects the chloride ions present in fingerprint residue. The reagent interacts with chloride ions to form silver chloride converting into black metallic silver upon exposure to light.[46] Another example of water-soluble component reagent is ninhydrin which is the most suitable reagent for detecting amino acids in fingerprint residue. Fingerprints developed by ninhydrin appear as purple impression because of the formation of Ruhemann's purple.[50] Oil Red O is an example of water-insoluble components reagent in which this reagent detects the insoluble portion of fingerprint residue such as lipids and fatty acid. Using Oil Red O for fingerprint detection results in red impressions and slight pink coloration occurs for the underlying substrate.[2]

Another classification of fingerprint reagents can be based on the appearance of developed fingerprints after enhancement techniques into three types: visible-fingerprint reagents, luminescent-fingerprint reagents, and dual-fingerprint reagents or visible and luminescent fingerprint reagents. Visible-fingerprint reagent binds to fingerprint components, and the resulting impression can be seen only with the naked eye. All the mentioned above examples (silver nitrate, ninhydrin, and Oil Red O) are visible-fingerprint reagents. Even though these reagents interact with different components of fingerprint residue, fingerprints developed by silver nitrate, ninhydrin, and Oil Red O appear as black, purple, and red impressions, respectively. Visible-fingerprint reagent is easy to use because there is no need for a forensic laser system or light source. Luminescent-fingerprint reagent is a reagent that interacts with fingerprint residue to produce fluorescent impressions can be seen only under the illumination process. For instance, DFO is considered luminescent-fingerprint reagent in which the reagent reacts with amino acids present in fingerprint residue producing red-colored prints. The use of luminescent-fingerprint reagent is much more sensitive than visible fingerprint-reagent as more fingerprint details and good contrast can be obtained even on multicolored surfaces. Dual-fingerprint reagent, as the name suggests, produces fingerprint impressions that are both visible and luminescent. Few reagents have been known as dual-fingerprint reagent, one of which is Genipin. The reagent detects amino acids in fingerprint residues to produce visible blue impressions and red impressions under illumination process.[79]

## 4.7 Summary

Detection of fingerprints is considered one of the most important tools used in forensic science for identification purposes. There are three types of fingerprints at a crime scene: patent,

latent, and plastic prints. Detection techniques can be achieved through physical adherence, chemical reaction, or physico-chemical process between the reagent and fingerprint deposition. Fingerprints contain numerous substances from the epidermis and the secretory glands in the dermis as well as intrinsic and extrinsic compounds. The composition of fingerprints is highly complex as they include organic compounds such as proteins, amino acids, and lipids (triglycerides, fatty acids, wax esters, squalene, and cholesterol) and some inorganic substances such as sodium, potassium, and chloride. Fingerprint residue is affected by many factors such as donor characteristics, environmental conditions, fingerprint age, and substrate nature. Several developing methods such as physical developer, cyanoacrylate fuming, and powder dusting are presented. A brief description of each method is included as well as its advantages, limitations, and improvement efforts for successful detection. A number of developing reagents such as fluorescent dyes, ninhydrin, 1,8-diazafluoren-9-one, and 1,2-indanedione are mentioned. The reaction mechanism of each reagent with amino acids and the properties of developed fingerprints are explained. Fingerprint reagents are categorized into different types based on fingerprint components such as water-soluble components and water-insoluble components reagents or based on the optical properties of the developed fingerprints such as visible-fingerprint, luminescent-fingerprint, and dual-fingerprint reagents.

**References**


1. Champod, C.; Lennard, C.; Margot, P.; Stoilovic, M., *Fingerprints and Other Ridge Skin Impressions*. CRC Press: Boca Raton, 2004.
2. Becue, A.; Moret, S.; Champod, C.; Margot, P., Use of stains to detect fingermarks. *Biotechnic & Histochemistry* **2011,** *86* (3), 140-160.
3. Girod, A.; Ramotowski, R.; Weyermann, C., Composition of fingermark residue: A qualitative and quantitative review. *Forensic Science International* **2012,** *223,* 10-24.
4. Cadd, S.; Islam, M.; Manson, P.; Bleay, S., Fingerprint composition and aging: A literature review. *Science & Justice* **2015,** *55,* 219-238.
5. Ramotoeski, R. S., Composition of Latent Print Reside. In *Advances in Fingerprint Technology*, Lee, H. C.; Gaensslen, R. E., Eds. Boca Raton, Fla: CRC Press, 2nd ed.: 2001.
6. Croxton, R. S.; Baron, M. G.; Butler, D.; Kent, T.; Sears, V. G., Development of a GC-MS Method for the Simultaneous Analysis of Latent Fingerprint Components. *Journal of Forensic Sciences* **2006,** *51* (6), 1329-1333.
7. Atherton, T.; Croxton, R.; Baron, M.; Gonzalez-Rodriguez, J.; Gámiz-Gracia, L.; García-Campaña, A. M., Analysis of amino acids in latent fingerprint residue by capillary electrophoresis-mass spectrometry. *Journal Of Separation Science* **2012,** *35* (21), 2994-2999.
8. Richmond-Aylor, A.; Bell, S.; Callery, P.; Morris, K., Thermal degradation analysis of amino acids in fingerprint residue by pyrolysis GC-MS to develop new latent fingerprint developing reagents. *Journal Of Forensic Sciences* **2007,** *52* (2), 380-382.

9. Hadorn, B.; Hanimann, F.; Anders, P.; Curtius, H. C.; Halverson, R., Free amino-acids in human sweat from different parts of the body. *Nature* **1967,** *215* (5099), 416-417.

10. Hamilton, P. B., Amino acids on hands. *Nature (London, U. K.)* **1965,** *205* (4968), 284-5.

11. OrÓ, J.; Skewes, H. B., Free Amino-Acids on Human Fingers: The Question of Contamination in Microanalysis. *Nature* **1965,** *207* (5001), 1042.

12. Antoine, K. M.; Mortazavi, S.; Miller, A. D.; Miller, L. M., Chemical differences are observed in children's versus adults' latent fingerprints as a function of time. *J. Forensic Sci.* **2010,** *55* (2), 513-518.

13. Hemmila, A.; McGill, J.; Ritter, D., Fourier transform infrared reflectance spectra of latent fingerprints: a biometric gauge for the age of an individual. *Journal Of Forensic Sciences* **2008,** *53* (2), 369-376.

14. Williams, D. K.; Brown, C. J.; Bruker, J., Characterization of children's latent fingerprint residues by infrared microspectroscopy: Forensic implications. *Forensic Science International* **2011,** *206* (1), 161-165.

15. de Puit, M.; Ismail, M.; Xu, X., LCMS Analysis of Fingerprints, the Amino Acid Profile of 20 Donors. *J. Forensic Sci.* **2014,** *59* (2), 364-370.

16. Michalski, S.; Shaler, R.; Dorman, F. L., The evaluation of fatty acid ratios in latent fingermarks by gas chromatography/mass spectrometry (GC/MS) analysis. *J. Forensic Sci.* **2013,** *58* (S1), S215-S220.

17. Asano, K. G.; Bayne, C. K.; Horsman, K. M.; Buchanan, M. V., Chemical composition of fingerprints for gender determination. *J. Forensic Sci.* **2002,** *47* (4), 805-807.

18. Croxton, R. S.; Baron, M. G.; Butler, D.; Kent, T.; Sears, V. G., Variation in amino acid and lipid composition of latent fingerprints. *Forensic Science International* **2010,** *199* (1), 93-102.

19. Archer, N. E.; Charles, Y.; Elliott, J. A.; Jickells, S., Changes in the lipid composition of latent fingerprint residue with time after deposition on a surface. *Forensic Science International* **2005,** *154* (2), 224-239.

20. De Paoli, G.; Lewis Sr, S. A.; Schuette, E. L.; Lewis, L. A.; Connatser, R. M.; Farkas, T., Photo- and Thermal-Degradation Studies of Select Eccrine Fingerprint Constituents. *Journal of Forensic Sciences* **2010,** *55* (4), 962-969.

21. Azoury, M.; Gabbay, R.; Cohen, D.; Almog, J., ESDA processing and latent fingerprint development: the humidity effect. *J. Forensic Sci.* **2003,** *48* (3), 564-570.

22. Paine, M.; Bandey, H. L.; Bleay, S. M.; Willson, H., The effect of relative humidity on the effectiveness of the cyanoacrylate fuming process for fingermark development and on the microstructure of the developed marks. *Forensic Science International* **2011,** *212*, 130-142.

23. Hansen, D. B.; Joullie, M. M., The development of novel ninhydrin analogues. *Chem. Soc. Rev.* **2005,** *34* (5), 408-417.

24. Reinholz, A. D.; Scientist, F., Albumin development method to visualize friction ridge detail on porous surfaces. *Journal of Forensic Identification* **2008,** *58* (5), 524.

25. Weyermann, C.; Roux, C.; Champod, C., Initial results on the composition of fingerprints and its evolution as a function of time by GC/MS analysis. *J. Forensic Sci.* **2011,** *56* (1), 102-108.

26. Almog, J.; Azoury, M.; Elmaliah, Y.; Berenstein, L.; Zaban, A., Fingerprints' third dimension: The depth and shape of fingerprints penetration into paper - Cross section examination by fluorescence microscopy. *Journal of Forensic Sciences* **2004,** *49* (5), 981-985.

27. Bobev, K., Fingerprints and factors affecting their condition. *Journal of Forensic Identification* **1995,** *45* (2), 176-183.

28. Morris, J. R.; Wells, J. M., Patent: 154014. **1979**.

29. de la Hunty, M.; Moret, S.; Chadwick, S.; Lennard, C.; Spindler, X.; Roux, C., Understanding physical developer (PD): Part I – Is PD targeting lipids? *Forensic Science International* **2015,** *257*, 481-487.

30. de la Hunty, M.; Moret, S.; Chadwick, S.; Lennard, C.; Spindler, X.; Roux, C., Understanding Physical Developer (PD): Part II – Is PD targeting eccrine constituents? *Forensic Science International* **2015,** *257*, 488-495.

31. Cantu, A. A.; Johnson, J. L., Silver Physical Development of Latent Prints. In *Advances in Fingerprint Technology*, Lee, H. C.; Gaensslen, R. E., Eds. Boca Raton, Fl: CRC Press, 2nd ed.: 2001.

32. Cantu, A. A., Silver physical developers for the visualization of latent prints on paper. *Forensic Sci Rev* **2001,** *13* (1), 29-64.

33. Burow, D.; Seifert, D.; Cantu, A. A., Modifications to the silver physical developer. *Journal of Forensic Sciences* **2003,** *48* (5), 1094-1100.

34. Sauzier, G.; Frick, A. A.; Lewis, S. W., Investigation into the performance of physical developer formulations for visualizing latent fingerprints on paper. *Journal of Forensic Identification* **2013,** *63* (1), 70-89.

35. Houlgrave, S.; Andress, M.; Ramotowski, R., Comparison of different physical developer working solutions - part I: longevity studies*. *Journal of Forensic Identification* **2011,** *61* (6), 621-639.

36. Houlgrave, S.; Ramotowski, R., Comparison of different physical developer working solutions - Part II: reliability studies. *Journal of Forensic Identification* **2011,** *61* (6), 640-651.

37. Lee, H. C.; Gaensslen, R. E., Cyanoacrylate fuming - theory and procedures. *Identification News* **1984,** *34* (6), 8-14.

38. Fingerprint Detection Techniques. In *Fingerprints and Other Ridge Skin Impressions*, Champod, C.; Lennard, C.; Margot, P.; Stoilovic, M., Eds. CRC Press: Boca Raton, 2004.

39. Menzel, E.; Burt, J.; Sinor, T.; Tubach-Ley, W.; Jordan, K., Laser Detection of Latent Fingerprints: Treatment with Glue Containing Cyanoacrylate Ester. **1983**.

40. Kerr, F. M.; Barron, I. W.; Haque, F.; Westland, A. D., Organic-Base Fluorescent Powders for Latent Fingerprint Detection on Smooth Surfaces: Part II. *Canadian Society of Forensic Science Journal* **1983,** *16* (1), 39-44.

41. Sonnex, E.; Almond, M. J.; Bond, J. W., Enhancement of Latent Fingerprints on Fabric Using the Cyanoacrylate Fuming Method Followed by Infrared Spectral Mapping. *Journal Of Forensic Sciences* **2016,** *61* (4), 1100-1106.

42. Day, K. J.; Bowker, W., Enhancement of Cyanoacrylate Developed Latent Prints Using Nile Red. *Journal of Forensic Identification* **1996,** *46* (2), 183-187.

43. Chesher, B. K.; Stone, J. M.; Rowe, W. F., Use of the Omniprint™ 1000 alternate light source to produce fluorescence in cyanoacrylate-developed latent fingerprints stained

with biological stains and commercial fabric dyes. *Forensic Science International* **1992,** *57* (2), 163-168.

44. Mazzella, W. D.; Lennard, C. J., An additional study of cyanoacrylate stains. *Journal of Forensic Identification* **1995,** *45* (1), 5-18.

45. Khuu, A.; Chadwick, S.; Spindler, X.; Lam, R.; Moret, S.; Roux, C., Evaluation of one-step luminescent cyanoacrylate fuming. *Forensic Science International* **2016,** *263*, 126-131.

46. Lee, H. C.; Gaensslen, R. E., Methods of Latent Fingerprint Development. In *Advances in Fingerprint Technology*, Lee, H. C.; Gaensslen, R. E., Eds. Boca Raton, Fla. : CRC Press, 2nd ed.: 2001.

47. Sodhi, G. S.; Kaur, J., Powder method for detecting latent fingerprints: a review. *Forensic Science International* **2001,** *120*, 172-176.

48. Wilshire, B.; Hurley, N., Development of latent fingerprints on paper using magnetic flakes. *Journal of Forensic Sciences* **1995,** *40* (5), 838-842.

49. James, J. D.; Pounds, C. A.; Wilshire, B., Magnetic flake powders for fingerprint development. *Journal of Forensic Sciences* **1993,** *38* (2), 391-401.

50. Almog, J., Fingerprint Development by Ninhydrin and Its Analogues. In *Advances in Fingerprint Technology*, Lee, H. C.; Gaensslen, R. E., Eds. Boca Raton, Fl: CRC Press, 2nd ed.: 2001.

51. Braasch, K.; de la Hunty, M.; Deppe, J.; Spindler, X.; Cantu, A. A.; Maynard, P.; Lennard, C.; Roux, C., Nile red: Alternative to physical developer for the detection of latent fingermarks on wet porous surfaces? *Forensic Science International* **2013,** *230*, 74-80.

52. Frick, A. A.; Busetti, F.; Cross, A.; Lewis, S. W., Aqueous Nile blue: a simple, versatile and safe reagent for the detection of latent fingermarks. *Chemical Communications* **2014,** *50* (25), 3341-3343.

53. Beaudoin, A., Fingerprint Staining Technique on Dark and Wetted Porous Surfaces: Oil Red O and Rhodamine 6G. *Journal of Forensic Identification* **2012,** *62* (4), 315-329.

54. Sodhi, G. S.; Gupta, G. P.; Kaur, J., A novel, cost-effective, organic fingerprint powder based on fluorescent eosin-blue dye. *Res. Pract. Forensic Med.* **1997,** *40*, 121-123.

55. Sodhi, G. S.; Kaur, J., Fingermarks detection by eosin-blue dye. *Forensic Science International* **2001,** *115*, 69-71.

56. Ruhemann, S., CCXII.—Triketohydrindene hydrate. *Journal of the Chemical Society, Transactions* **1910,** *97*, 2025.

57. Oden, S.; Von Hofsten, B., Detection of fingerprints by the ninhydrin reaction. *Nature* **1954,** *173* (4401), 449-450.

58. Joullié, M. M.; Thompson, T. R.; Nemeroff, N. H., Ninhydrin and ninhydrin analogs. Syntheses and applications. *Tetrahedron* **1991,** *47* (42), 8791-8830.

59. Friedman, M.; David Williams, L., Stoichiometry of formation of Ruhemann's purple in the ninhydrin reaction. *Bioorganic Chemistry* **1974,** *3*, 267-280.

60. Herod, D. W.; Menzel, E. R., Laser detection of latent fingerprints: ninhydrin followed by zinc chloride. *J Forensic Sci* **1982,** *27* (3), 513-8.

61. Kobus, H. J.; Stoilovic, M.; Warrener, R. N., A simple luminescent post-ninhydrin treatment for the improved visualisation of fingerprints on documents in cases where ninhydrin alone gives poor results. *Forensic Science International* **1983,** *22* (2), 161-170.

62. Stoilovic, M.; Kobus, H. J.; Margot, P. A. J. L.; Warrener, R. N., Improved enhancement of ninhydrin developed fingerprints by cadmium complexation using low temperature photoluminescence techniques. *J. Forensic Sci.* **1986,** *31* (2), 432-45.

63. Almog, J.; Levinton-Shamuilov, G.; Cohen, Y.; Azoury, M., Fingerprint reagents with dual action: color and fluorescence. *Journal Of Forensic Sciences* **2007,** *52* (2), 330-334.

64. Davies, P. J.; Kobus, H. J.; Taylor, M. R.; Wainwright, K. P., Synthesis and structure of the zinc(II) and cadmium(II) complexes produced in the photoluminescent enhancement of ninhydrin developed fingerprints using group 12 metal salts. *J. Forensic Sci.* **1995,** *40* (4), 565-9.

65. Druey, J.; Schmidt, P., Phenanthroline quinones and diazafluorenes. *Helv. Chim. Acta* **1950,** *33,* 1080-7.

66. Pounds, C. A.; Grigg, R.; Mongkolaussavaratana, T., The use of 1,8-diazafluoren-9-one (DFO) for the fluorescent detection of latent fingerprints on paper. A preliminary evaluation. *J. Forensic Sci.* **1990,** *35* (1), 169-75.

67. Grigg, R.; Mongkolaussavaratana, T.; Anthony Pounds, C.; Sivagnanam, S., 1,8-diazafluorenone and related compounds. A new reagent for the detection of (α-amino acids and latent fingerprints. *Tetrahedron Letters* **1990,** *31* (49), 7215-7218.

68. Stoilovic, M., Improved method for DFO development of latent fingerprints. *Forensic Sci. Int.* **1993,** *60* (3), 141-53.

69. Wilkinson, D., Study of the reaction mechanism of 1,8-diazafluoren-9-one with the amino acid, l-alanine. *Forensic Science International* **2000,** *109* (2), 87-103.

70. Conn, C.; Ramsay, G.; Roux, C.; Lennard, C., The effect of metal salt treatment on the photoluminescence of DFO-treated fingerprints. *Forensic Sci. Int.* **2001,** *116* (2-3), 117-123.

71. Ramotowski, R.; Cantu, A. A.; Joullie, M. M.; Petrovskaia, O., 1,2-Indanediones: a preliminary evaluation of a new class of amino acid visualizing compounds,. *Fingerprint Whorld,* **1997,** *23,* 131-140.

72. Hauze, D. B.; Petrovskaia, O.; Taylor, B.; Joullie, M. M.; Ramotowski, R.; Cantu, A. A., 1,2-Indanediones: new reagents for visualizing the amino acid components of latent prints. *J. Forensic Sci.* **1998,** *43* (4), 744-747.

73. Wallace-Kunkel, C.; Lennard, C.; Stoilovic, M.; Roux, C., Optimisation and evaluation of 1,2-indanedione for use as a fingermark reagent and its application to real samples. *Forensic Science International* **2007,** *168* (1), 14-26.

74. Bicknell, D. E.; Ramotowski, R. S., Use of an optimized 1,2-indanedione process for the development of latent prints*. *J Forensic Sci* **2008,** *53* (5), 1108-16.

75. Serrano, E.; Sturelle, V., Modification and evaluation of a 1,2-indanedione-zinc chloride formula using petroleum ether as a carrier solvent. *J. - Can. Soc. Forensic Sci.* **2010,** *43* (3), 108-116.

76. Stoilovic, M.; Lennard, C.; Wallace-Kunkel, C.; Roux, C., Evaluation of a 1,2-indanedione formulation containing zinc chloride for improved fingermark detection on paper. *Journal of Forensic Identification* **2007,** *57* (1), 4-18.

77. Russell, S. E.; John, G. L.; Naccarato, S. L., Modifications to the 1,2-indanedione/zinc chloride formula for latent print development. *Journal of Forensic Identification* **2008,** *58* (2), 182-192.

78. Petrovskaia, O.; Taylor, B. M.; Hauze, D. B.; Carroll, P. J.; Joullie, M. M., Investigations of the Reaction Mechanisms of 1,2-Indanediones with Amino Acids. *J. Org. Chem.* **2001,** *66* (23), 7666-7675.

79. Almog, J.; Cohen, Y.; Azoury, M.; Hahn, T. R., Genipin - A novel fingerprint reagent with colorimetric and fluorogenic activity. *Journal of Forensic Sciences* **2004,** *49* (2), 255-257.

# 5 INVESTIGATION OF BENZOPHENOXAZINE DERIVATIVES FOR THE DETECTION OF LATENT FINGERPRINTS ON POROUS SURFACES

In this report, two classes of benzophenoxazine dyes, Nile red and Nile blue derivatives, were evaluated for the detection of latent fingerprints on porous surfaces. The efficiency to develop fingerprints is influenced by the physical properties of the dye molecules including hydrophobicity as characterized by distribution coefficient value (logD), and other factors such as chemical structure of the dye and hydrogen bonds. Both Nile red and the basic form of Nile blue showed excellent to acceptable ability to detect fingerprints due to their great hydrophobicity at 515 and CSS setting of the forensic light source. Higher hydrophobicity derivatives of Nile red and Nile blue (in the basic form) improved both quality and sensitivity of fingerprint detection in comparison with their corresponding parent dyes. They developed strong luminescent and visible fingerprints, and better contrast was achieved between impressions and the background surface suggesting the potential use of these compounds in forensic investigation. Therefore, the hydrophobic derivatives are considered dual-fingerprint reagents because the developed prints can be seen by the naked eye and under illumination process. However, lower hydrophobicity derivatives of Nile red and Nile blue and derivatives with different substituents developed weak or non-luminescent fingerprints with poor contrast. A complete analysis of what dye properties are the most important in fingerprint detection is discussed along with chemical structures for improved performance.

## 5.1 Introduction

Fingerprint identification is considered one of the most crucial clues of physical evidence in forensic investigation. The common form of fingerprints found at a crime scene is latent fingerprints, the invisible residue deposited by a person's hand when touching a surface. Due to the complexity of fingerprint residue, revealing the prints requires physical or chemical treatment to enable their detection. Several developing reagents have been used for fingerprint detection that target various components such as amino acids or lipids in fingerprint residue. Amino acid-sensitive reagents such as ninhydrin, 1,8-diazafluoren-9-one (DFO), and 1,2-indanedione are insufficient for revealing fingerprints on porous surfaces that have been wetted or found in humid conditions.[1-3] In this case, amino acids are likely to be dissolved or washed away due to their solubility in water. Therefore, lipid-sensitive reagent is the reagent of choice to detect fingerprints on wet porous substance. Physical developer (PD) is the standard technique for developing fingerprints in such applications. However, this technique has been recognized as a complex and time-consuming process due to high sensitivity to contaminations and the need for freshly prepared working solutions.[4] Many studies have been conducted on alternative lipid sensitive reagents such as dyes.[5-7] Oil Red O is a diazo dye used in histological staining for lipidic compounds and belongs to the family of Sudan dyes. It has been studied extensively for recovering fingerprints as red visible prints on wet porous surfaces due to the high affinity of the dye to lipids.[8-9] Solvent black 3 is another diazo dye that comes from the same family of Sudan dyes. Similarly, the dye has been investigated in revealing fingerprints but to a lesser extent than Oil Red O. Solvent black 3 is more effective in developing fingerprints on greasy contaminated substances.[10]

Fingerprints developed by the previously mentioned reagents are visible to the naked eye which limit their applications to light-colored surfaces. However, the use of organic dyes that

fluoresce upon exposure to the light source has the advantage of revealing fingerprints with sufficient contrast on dark-colored surfaces. The fluorescent dye eosin-blue with a phase transfer catalyst was used to detect fingerprints on many surfaces.[11] Moreover, a formulation based on Coomassie brilliant blue G-250 dye has been proposed as a developing reagent to differentiate between male and female fingerprints.[12] Furthermore, several fluorescent dyes have been reported as dusting agents for detecting fingerprints including acridine orange, acridine yellow, crystal violet, coumarin 6, and rhodamine B.[13] In addition, micro-structured fluorescent powders based on benzazole dyes have applied for the development of latent fingerprints on many surfaces.[14] Moreover, the fluorescence properties of such compounds enhance the sensitivity of fingerprints developed with regular reagents. Rhodamine 6G, for example, was used as post-treatment of fingerprints developed with Oil Red O on dark porous surfaces.[15]

Recently, benzophenoxazine dyes such as Nile red and Nile blue have been applied in the field of fingerprint detection. Nile red is a neutral fluorescent dye used in histology for staining of some lipid compounds such as triacylglycerols, phospholipids, cholesteryl esters, and lipoproteins.[16] Nile blue is a cationic dye used in the histological staining of neutral fats, phospholipids, and fatty acids.[17] These compounds are present in fingerprint residue as a result of sebaceous gland secretions.[18] The optical properties of Nile red and Nile blue are highly influenced by the solvent polarity and dielectric constant. In non-polar media, the fluorescence spectrum of both dyes is in the visible to the near-infrared region, and high quantum yield values are recorded. In polar media, however, the fluorescence spectrum shows a red shift with low quantum yield values due to hydrogen bonding.[19-21] The early use of Nile red in fingerprint detection was a post-treatment for cyanoacrylate fuming. It was reported that the performance of Nile red for the enhancement of cyanoacrylate-developed latent fingerprint was considerably superior to that for rhodamine 6G.[22]

Similarly, Nile blue was initially used to improve the contrast of latent fingerprints developed by cyanoacrylate.[23] Both dyes have been used for the detection of latent lip prints on multicolored surfaces, and Nile red performed better than Nile blue especially with old prints.[24] Nile red has been used effectively to develop fingerprints on different porous surfaces in a methanolic-aqueous formulation. In addition, Nile red performance was compared to that of PD with fresh and aged fingerprints.[25] On the other hand, an aqueous solution of Nile blue has been proposed as an alternative fingerprint reagent to the previous formulation of Nile red. The procedure was described as simple, less toxic, and less cost and can be applied on different surfaces.[26] The efficiency of this solution is due to the small presence of Nile red resulting from the spontaneous hydrolysis of Nile blue.[27] The presence of the two dyes in one formulation stains both neutral lipids and acidic moieties.[17] Recently, an aqueous microemulsion of Nile red has been developed for visualizing both natural and charged fingerprints. The performance of the solution was comparable to the methanolic-aqueous formulation of Nile red and superior to the aqueous solution of Nile blue.[28] More recently, Nile red has been encapsulated into mesoporous silica nanoparticles for developing fingerprints on thermal paper without the need of organic solvents.[29]

Most fluorescent dyes used in forensic detection as developing reagents are hydrophobic. The hydrophobicity of a compound is measured by the partition coefficient (logP) or the distribution coefficient (logD). Both terms describe the ratio of the concentration of a compound in organic and aqueous phases (octanol and water) at equilibrium. However, logD is more extensively used than logP to express such property because logP deals with unionized form only while logD takes into consideration both ionized and unionized forms. Moreover, logD is pH-dependent whereas logP is pH-independent.[30-31] LogP value was first mentioned in forensic science as an indication of the great hydrophobicity of Oil Red O explaining the extensive use of

the dye in histological staining.[9] The hydrophobicity characterized by logD for common developing reagents is summarized in Table 5.1.

**Table 5.1 LogD values of some fluorescent dyes at pH 7.4**

| Dye | LogD[a] |
|---|---|
| Oil Red O | 9.52 |
| Solvent black 3 | 8.13 |
| Eosin-blue | 6.08 |
| Acidine orange | 2.93 |
| Acidine yellow | 1.85 |
| Crystal violet | 1.39 |
| Coomassie brilliant blue | 5.86 |
| Rhodamine B | 2.34 |
| Rhodamine 6G | 1.45 |
| Coumarin 6 | 4.79 |
| Nile red | 3.83 |
| Nile blue | 0.60 |

[a] Calculated by ChemAxon

Fingerprint reagents can be classified based on the appearance of fingerprints after treatment process into three types: visible-fingerprint reagent, luminescent-fingerprint reagent, and dual-fingerprint reagent. Visible-fingerprint reagents such as ninhydrin, and Oil Red O bind to fingerprint components and the resulting impression can be seen only by the naked eye. Luminescent-fingerprint reagents such as Nile red and Nile blue interact with fingerprint residue

to produce fluorescent impressions which can be seen only upon exposure to a light source. Dual-fingerprint reagents produce fingerprint impressions that are both visible and luminescent. Few reagents have been known as dual-fingerprint reagents, one of which is a natural pigment called Genipin. It is extracted from gardenia fruit and produces blue color with various amino acids.[32] This reagent detects amino acids in fingerprint residue to produce visible blue impressions and red impressions under illumination.[33] Our preliminary results indicated that some benzophenoxazine derivatives synthesized by our group were dual reagents as they developed colored and luminescent fingerprints.

To the best of our knowledge, most of the fingerprint detection reports have studied the common developing reagents and compared their performance with new analogous compounds for enhanced detection.[34-37] However, very few reports have studied the relationship of the chemical structure of a reagent and its efficiency for fingerprint development. The purpose of our work was to compare the performance of two fingerprint reagents Nile red and Nile blue (in the basic form) in terms of their chemical and physical properties such as hydrophobicity. The study aimed also to evaluate several modified structures of benzophenoxazine derivatives as reagents for fingerprint detection with respect to the two parent reagents. The use of benzophenoxazine derivatives in forensic investigation has the advantage of revealing luminescent fingerprints on porous surfaces. In addition, some derivatives of higher hydrophobicity developed visible and luminescent prints and thus are considered as dual-fingerprint reagents.

## 5.2 Materials and methods

### *5.2.1 Chemicals and reagents*

Nile red (NR) and Nile blue (NB) were obtained from Sigma-Aldrich (St. Louis, MO). The synthesis of all Nile red and Nile blue derivatives except **NR1** and **NR2** will be illustrated in

Martinez et al. (in preparation). The chemical synthesis of **NR1** and **NR2** is described in the following section. The chemical structures of all dyes are shown in Figure 5.1. Ethanol (200 proof ethanol) was obtained from Pharmco-AAPER (Brookfield, CT). Sodium hydroxide (99%) was obtained from Fisher Scientific (Fair Lawn, NJ). Absorbance spectra were acquired using a Cary 3G UV-visible spectrophotometer (Varian Inc., Palo Alto, CA) interfaced to a PC. All measurements were performed in disposable plastic cuvette with a path length of 1.0 cm. Nanopure water was obtained using an ELGA Purelab Classic water purification system. The nuclear magnetic resonance spectra were obtained by high quality Kontes NMR tubes (Kimble Chase, Vineland, N*J*) rated to 500 MHz and were recorded on a Bruker Avance 400 MHz spectrometer interfaced to a PC using Topspin 3.1. High-resolution accurate mass spectra were obtained at the Georgia State University Mass Spectrometry Facility using a Waters Q-TOF micro (ESI-Q-TOF) mass spectrometer.

(a)

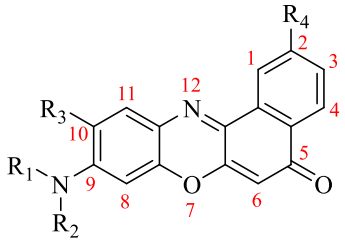


NR: $R_1 = R_2 = C_2H_5$ , $R_3 = R_4 = H$
**NR1:** $R_1 = R_2 = C_4H_9$ , $R_3 = R_4 = H$
**NR2:** $R_1 = R_2 = (C_6H_5)C_3H_6$ , $R_3 = R_4 = H$
**NR3:** $R_1 = R_2 = C_2H_5$ , $R_3 = H$, $R_4 = OH$
**NR4:** $R_1 = R_2 = C_4H_9$ , $R_3 = H$, $R_4 = OH$
**NR5:** $R_1 = R_2 = (C_6H_5)C_3H_6$ , $R_3 = H$, $R_4 = OH$
**NR6:** $R_1 = C_4H_9$ , $R_2 = H$, $R_3 = CH_3$ , $R_4 = OH$
**NR7:** $R_1 = (C_6H_5)C_3H_6$ , $R_3 = H$, $R_3 = CH_3$ , $R_4 = OH$

(b)

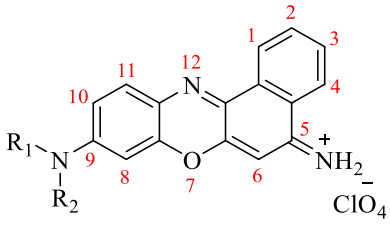


NB: $R_1 = R_2 = C_2H_5$
**NB1:** $R_1 = R_2 = C_4H_9$
**NB2:** $R_1 = R_2 = (C_6H_5)C_3H_6$
**NB3:** $R_1 = C_2H_5$ , $R_2 = H$
**NB4**: $R_1 = C_4H_9$ , $R_2 = H$

**Figure 5.1 Chemical structures of (a) Nile red derivatives and (b) Nile blue derivatives**

### *5.2.2 Synthesis of the dialkylated Nile red derivatives (NR1 and NR2)*

All chemical reactions were maintained under a positive pressure of nitrogen unless otherwise stated. The reaction progress was monitored using silica gel 60 F254 thin layer chromatography plates (Merck EMD Millipore, Darmstadt, Germany). Open column chromatography was utilized for the purification of all final compounds using 60−200 μm, 60A classic column silica gel (Dynamic Adsorbents, Norcross, GA).

According to Scheme 1, compounds (**2a-b**) were prepared by dissolving 3-aminophenol, compound **1**, (2.00 g) with two molar equivalents of potassium carbonate in isopropanol/water (1:1, v/v). Two molar equivalents of iodobutane were added to the mixture of **2a** and two molar equivalents of 1-bromo-3-phenylpropane were added to the mixture of **2b**, both mixtures were heated to 70°C for 3 h. The **2b** solution was evaporated under reduced pressure then extracted with ethyl acetate. For both compounds, the organic layer was separated and concentrated under reduced pressure to yield brown oil. This was purified by regular phase column chromatography using hexane /ethyl acetate (95:5, v/v). 0.6 g of Compounds (**2a-b**) were dissolved in isopropanol (2.0 mL) to facilitate its dissolution. Then 4.0 mL (32% HCl) and 8.0 g of crushed ice were added. The mixture was chilled in an ice bath and a solution of $NaNO_2$ (0.4 g in 6.0 mL water) was added dropwise over one hour. This was continuously stirred for 3 additional hours at 0º C. For compound **2a**, the liquid medium had changed color to dark orange which was then concentrated under reduced pressure. The nitroso product, compound **3a**, was dried under reduced pressure and used in the next step without further purification due its instability. For compound **2b**, a yellow-orange precipitate had formed by this time. This precipitate was filtered and dried under reduced pressure. Due to instability of nitroso compounds, the product was used in the next step without purification. Compounds (**4a-b**) were prepared by dissolving compounds (**3a-b**) and one molar equivalent of

1-hydroxynaphthalene in 15.0 mL ethanol. The mixture was heated to 70°C for 3 h to afford a highly impure dye. The solution was neutralized with ammonium hydroxide and then extracted with $CH_2Cl_2$. The organic layer was separated and then removed under reduced pressure. This was purified by regular phase column chromatography using $CH_2Cl_2$/methanol (99:1, v/v) and (90:10, v/v) for compounds **4a** and **4b,** respectively.

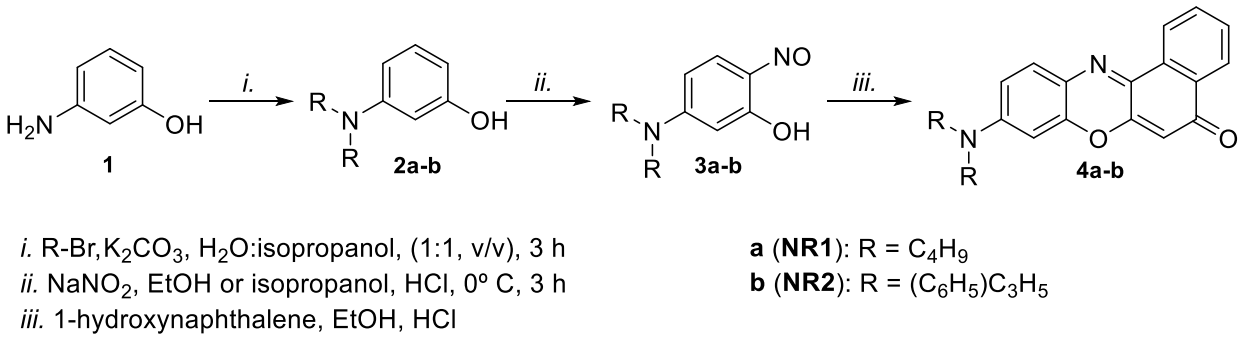


**Scheme 1 Synthetic route for the preparation of the Nile red derivatives, NR1 and NR2**

9-(dibutylamino)-5H-benzo[a]phenoxazin-5-one (**NR1**): 41% yield. $^1$H NMR (400 MHz, $CDCl_3$) δ 8.68 (d, 1H, *J* = 8 Hz), 8.33 (d, 1H, *J* = 8 Hz), 7.75 (t, 1H, *J* = 7.6 Hz ), 7.70 (t, 1H, *J* = 7.6 Hz), 7.63 (d, 1H, *J* = 8.8 Hz), 6.65 (d, 1H, *J* = 8.8 Hz), 6.48 (s, 1H), 6.42 (s, 1H), 3.43 (t, 4H, *J* = 8 Hz), 1.69 (m, 4H, *J* = 8 Hz), 1.44 (m, 4H, *J* = 8 Hz), 1.03 (t, 6H, *J* = 8 Hz); MS (ESI): 375 ($M^+$); m.p. >210 °C.

9-(bis(3-phenylpropyl)amino)-5H-benzo[a]phenoxazin-5-one (**NR2**): 23% yield. $^1$H NMR (400 MHz, $CDCl_3$) δ 8.68 (d, 1H), 8.33 (d, 1H), 7.74 (t, 1H), 7.68 (t, 1H), 7.58 (t, 2H), 7.31-7.39 (m, 4H), 7.21-7.30 (m, 5H), 6.48 (d, 1H), 6.41 (s, 1H), 6.26 (s, 1H), 3.40 (t, 4H), 2.71 (t, 4H), 2.00 (m, 4H); MS (ESI): 499 ($M^+$); m.p. >220 °C.

### *5.2.3 Classification of benzophenoxazine derivatives*

Nile red derivatives can be classified into three types according to the substituents attached to benzophenoxazine backbone in two positions: the 2-position and the 9-position. The first type is dialkylated derivatives containing a tertiary amine at the 9-position including **NR1** and **NR2**, the second type is 2-hydroxy-dialkylated derivatives containing a hydroxyl group at the 2-position and a tertiary amine at the 9-position including **NR3**, **NR4** and **NR5**, and the third type is 2-hydroxy-monoalkylated derivatives containing a hydroxyl group at the 2-position and a secondary amine at the 9-position including **NR6** and **NR7** as shown in Figure 5.1(a). Nile blue derivatives can be classified into two types according to the type of amine attached to benzophenoxazine backbone at the 9-position. The first type is dialkylated derivatives containing a tertiary amine at the 9-position including **NB1** and **NB2**, and the second type is monoalkylated derivatives containing a secondary amine at the 9-position including **NB3** and **NB4** as shown in Figure 5.1(b).

### *5.2.4 Preparation of working solutions*

Stock solutions of Nile red and Nile blue and their derivatives ($4.0\times10^{-4}$ M) were prepared in ethanol and sonicated for 15 minutes to ensure complete dissolution of the dye. Sodium hydroxide solution (0.01 M, pH 12.0) was prepared in deionized water. Working solution was prepared by slowly adding 15.0 mL of sodium hydroxide solution to 15.0 mL of the dye with constant stirring and used immediately after preparation. Final concentration of the dye in the working solution was $2.0\times10^{-4}$ M in ethanol: aqueous sodium hydroxide (1:1, *v/v*).

### *5.2.5 Fingerprints detection procedure*

This work aims to provide a better understanding of the effect of chemical structure of the dye on fingerprint development. Therefore, one donor and one porous substrate (paper) were selected for the study. Fingerprints were collected on a white copy paper from a 26-year-old male donor and left 24 hours before treatment. Fingerprints were deposited after the donor was instructed to wipe his fingers with his nose prior to fingerprint collection. The donor was asked not to wash his hands within the previous two hours. Fingerprints were obtained using the three middle fingers holding for 8 seconds. The paper was cut in half before treatment, then the left side of the paper was developed using derivatives of Nile red or Nile blue and the right side of the paper was developed using the corresponding parent dye (Nile red or Nile blue) for comparison purposes. The sample was first immersed in deionized water for 5 minutes, then it was removed and immersed in the working solution for 30 minutes. The excess solution was removed by immersing the sample in deionized water for 5 minutes. The sample was left to dry for about one hour on a paper towel at room temperature in a dark place.

### *5.2.6 Sample visualization and evaluation*

The sample was visualized by the forensic light source (FLS), Mini-CrimeScope 400, (MCS-400) (Spex Forensics, Edison, NJ) at an excitation wavelength of 515 nm for Nile red derivatives, CSS for Nile blue derivatives, and white light for all dyes. The two halves for each sample were placed side by side and photographed together using a digital camera (Nikon D3300) with a 550 nm long-pass barrier filter. University of Canberra (UC) scale [38] was used to compare the performance of the two detection methods: A and B in which A is the proposed method and B is the reference method. In this study, method A is the derivatives of Nile red or Nile blue and

method B is the corresponding parent dye, Nile red or Nile blue. Samples were given scores between (-2) and (+2) depending on the improvement in detection performance including fingerprint ridge details and/or contrast between the fingerprint impressions and background substrate. UC scores: (+2) Half fingerprint developed by method A shows far greater improvement in detection performance compared to half fingerprint developed by method B; (+1) Half fingerprint developed by method A shows slightly greater improvement in detection performance compared to half fingerprint developed by method B; (0) No significant difference between the two half fingerprints; (-1) Half fingerprint developed by method B shows slightly greater improvement in detection performance compared to half fingerprint developed by method A; (-2) Half fingerprint developed by method B shows far greater improvement in detection performance compared to half fingerprint developed by method A.[37]

## 5.3 Results and discussion

### *5.3.1 Photophysical properties of benzophenoxazine derivatives*

The absorbance spectra of Nile red and Nile blue is influenced by the surrounding environment as shown in Figure 5.2. The presence of sodium hydroxide (1:1, *v/v*) in the working solution resulted in a red shift of absorbance spectrum of Nile red of about 30 nm. However, the absorbance spectrum of Nile blue displayed a blue shift of about 100 nm due to the deprotonation of the amine group at the 5-position ($pK_a$ = 11.14) and formation the basic form of the dye. The deprotonation process co-occurs with a color change of Nile blue solution from blue color in pure ethanol to red color in the working solution, ethanol: sodium hydroxide (1:1, *v/v*). The high pH of the working solution was selected as indicated in previous studies [9, 24] and to increase logD value for benzophenoxazine derivatives. Moreover, improvement of fingerprint detection is observed for

hydrophobic dyes due to interaction with sebaceous secretions in fingerprint residue as discussed in the following sections. Given the fact that logD is pH dependent, the hydrophobicity of Nile blue alters by pH changes whereas that of Nile red does not. Therefore, Nile blue is more hydrophobic in alkaline solution at pH 12.0 (logD = 3.79) compared to neutral solution at pH 7.4 (logD = 0.60).

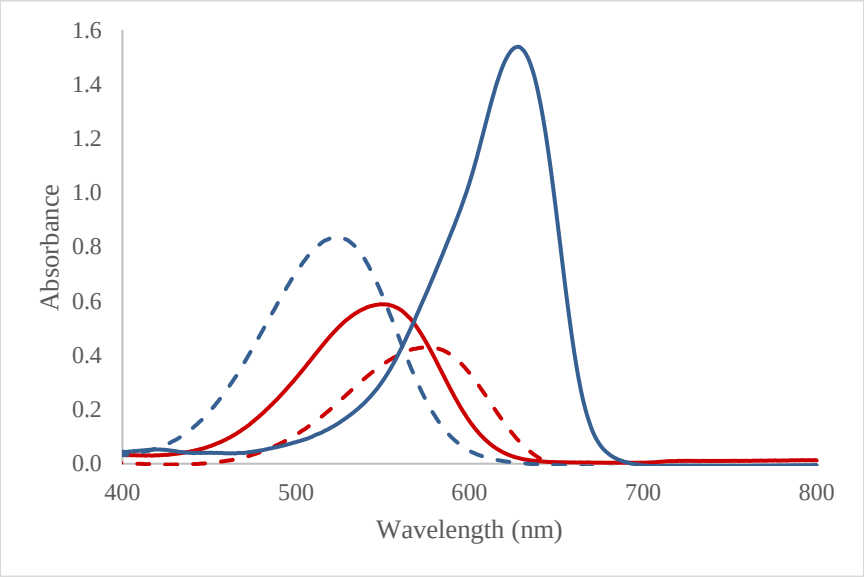


**Figure 5.2 Absorbance spectra of $2.0\times10^{-5}$ M Nile red (red line) and Nile blue (blue line) in ethanol (solid line) and in the working solution [ethanol: sodium hydroxide (1:1, v/v)] (dashed line)**

The chemical structure and physical properties such as hydrophobicity have an impact on spectroscopic studies of Nile red and Nile blue derivatives. A general and small blue shift in the absorption spectra was observed across Nile red derivatives (Figure 5.3a) and the order of shifting was Nile red, dialkylated derivatives **NR1** and **NR2**, 2-hydroxy-dialkylated derivatives **NR3**, **NR4**, and **NR5**, and 2-hydroxy-monoalkylated derivatives **NR6** and **NR7**. Similarly, the absorption spectra of Nile blue and dialkylated derivatives **NB1** and **NB2** showed a blue shift compared to

those monoalkylated derivatives **NB3** and **NB4** (Figure 5.3b). A similar behavior was observed for Nile blue derivatives after the addition of sodium hydroxide. There was a noticeable color change of the working solutions from blue to red color due to deprotonation of the amine group at the 5-position ($pK_a$ = 11.14) and formation the basic form of the dye.

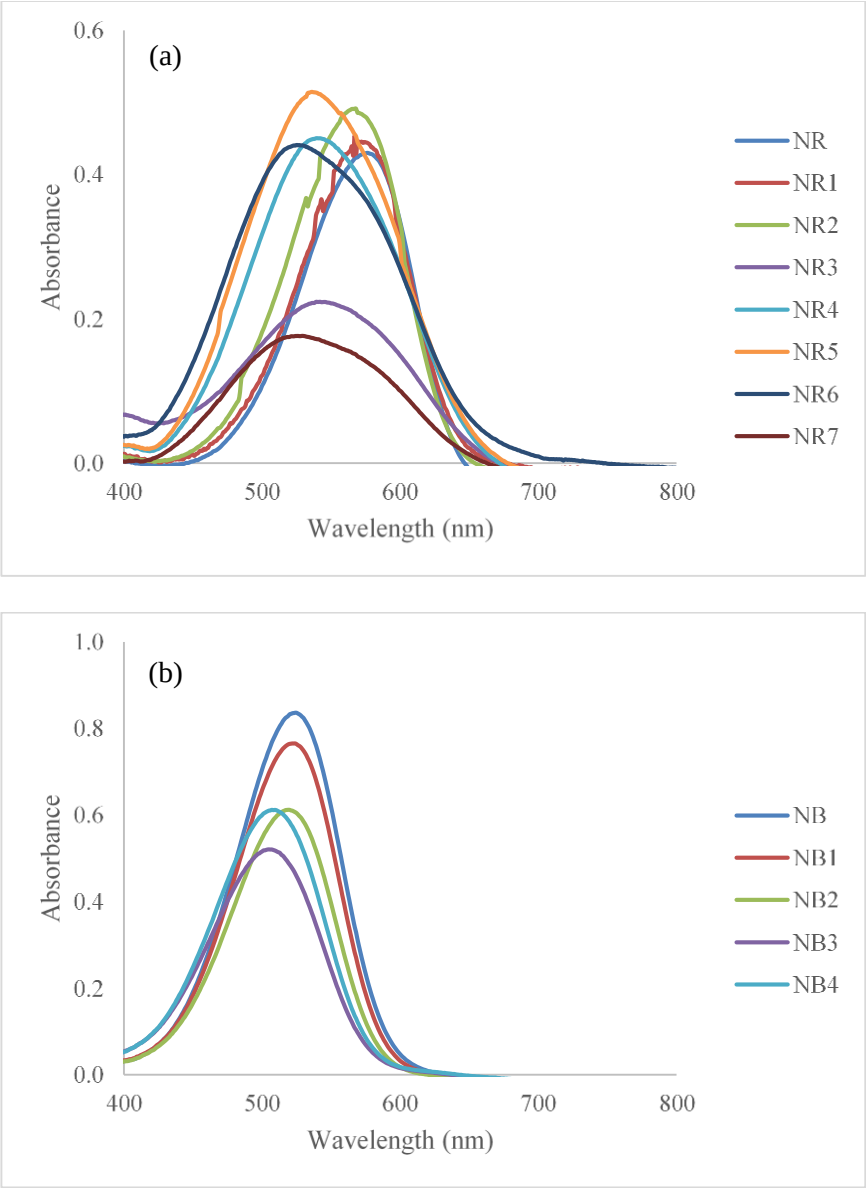


**Figure 5.3 Absorbance spectra of $2.0\times10^{-5}$ M of (a) Nile red derivatives and (b) Nile blue derivatives in the working solution [ethanol: sodium hydroxide (1:1, *v/v*)]**

### *5.3.2 Comparison between Nile red and Nile blue for fingerprint detection*

To investigate the detection efficiency of the two benzophenoxazine dyes, the working solution of Nile red and Nile blue (basic form) was used for developing fingerprints on a porous surface (paper) as shown in Figure 5.4. The sample treated by Nile red produced fingerprints more luminescent than those with Nile blue at two settings of FLS, 515 nm and CSS, both viewed with 550 nm long-pass barrier filter. Although both dyes have similar hydrophobicity at pH 12.0 (logD for Nile red and Nile blue is 3.83 and 3.79, respectively), the efficiency of fingerprint detection is attributed to the difference of chemical structure of the dyes. Both molecules have similar benzophenoxazine backbone except the attached groups at the 5-position, a carbonyl group and an amine group for Nile red and Nile blue, respectively. The amine group is a hydrogen bond donor forming hydrogen bonds with hydroxide ions present in the working solution. The hydrogen bonds weaken the hydrophobic interaction of Nile blue with sebaceous portion of fingerprint residue resulting in weak development.

FLS setting is an important factor to develop fingerprints with clear ridge details and good contrast, especially for comparison purposes. Nile red developed luminescent fingerprints and clear ridges in both settings of FLS as shown in Figure 5.4 (left half). However, at CSS the background appeared more bright providing poor contrast. Consequently, excitation wavelength at 515 nm is considered the optimum condition of fingerprint visualization for performance comparison of Nile red and its derivatives. On the other hand, weak fingerprint detection and poor contrast were observed for Nile blue in both settings of FLS as shown in Figure 5.4 (right half). Moreover, the sample treated by Nile blue at 515 nm seemed more pale due to lack of contrast between fingerprints and the substrate. Therefore, CSS setting of FLS could be the best for fingerprints visualization for performance comparison of Nile blue and its derivatives.

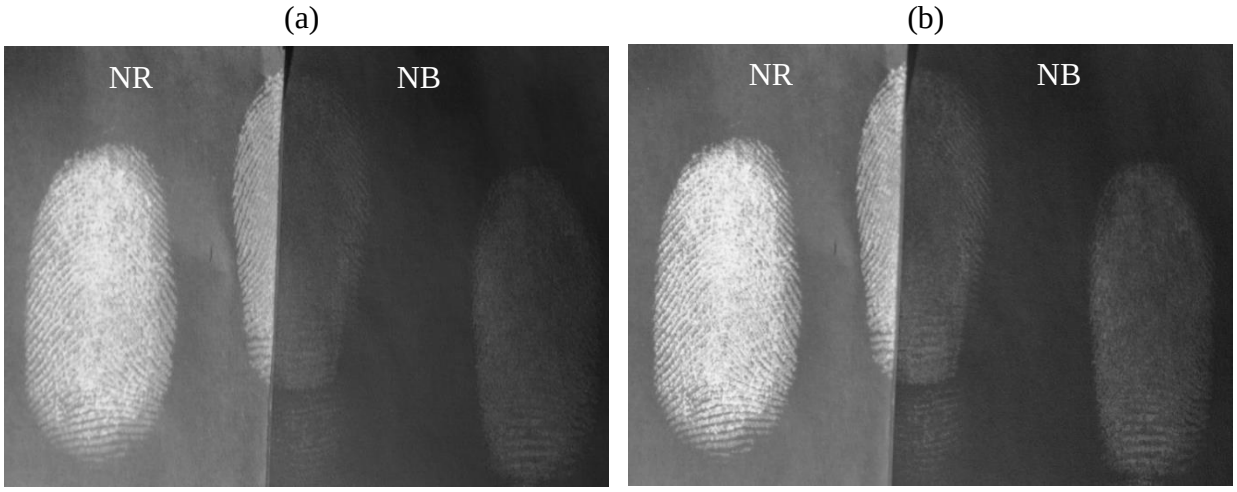


**Figure 5.4 Comparison of fingerprints developed by NR (left half) and NR (right half) at different FLS settings: (a) 515 nm excitation wavelength and (b) at CSS, both viewed with 550 nm long-pass barrier filter**

### *5.3.3 Application of Nile red derivatives to fingerprint devolvement*

Fingerprints developed by the dialkylated derivatives **NR1** and **NR2** were compared to those developed by Nile red as shown in Figure 5.5. Both dyes as well as Nile red showed excellent ability to detect fingerprint in which luminescent impressions and detailed ridges were observed at excitation wavelength of 515 nm of the FLS, and Nile red result is consistent with the work of Braasch et al.[25] Moreover, the underlying substrate of the sample treated by **NR1** was darker compared to Nile red providing more contrast between the prints and background and thus improvement in fingerprint detection. When using white light of FLS, fingerprints appeared as pink impressions with complete ridge details for **NR1** and **NR2**, whereas the prints were not visible for Nile red (Figure 5.5b). However, solid particles were precipitated on the background of the sample treated by **NR2** which could be due to the aqueous nature of the working solution and the great hydrophobicity of the dye. Nonetheless, the precipitation process did not prevent fingerprint

development. The improvement in fingerprint detection is attributed to the fact that both compounds are more hydrophobic than Nile red as indicated by logD values in Table 5.2. It has been hypothesized that Nile red tended to interact with lipids secreted by sebaceous glands and not with epidermal lipids.[25, 28] Therefore, the hydrophobic interaction of **NR1** and **NR2** with sebaceous secretions of fingerprint residue is stronger relative to Nile red making the two derivatives dual-fingerprint reagents developing visible prints seen by the naked eye (pink impressions) and luminescent prints (yellow-orange impressions) when using FLS.

The use of the 2-hydroxy dialkylated derivatives of Nile red resulted in fingerprints that produced various degree of luminescence according to their chemical and physical properties (Figure 5.6). Blurred and non-luminescent fingerprints were obtained by the less hydrophobic derivative, **NR3** due to the weak interaction with fingerprint components. On the other hand, fingerprints developed by **NR4** and **NR5** exhibited comparable results in which fingerprints were luminescent with clear ridge details. However, fingerprints developed by Nile red displayed a higher degree of luminescence, ridge details, and clarity. Despite the fact that **NR4** and **NR5** are hydrophobic and the latter dye is more hydrophobic than Nile red (Table 5.2), there was no improvement in the developing of fingerprints. This could be due to the unwanted interaction of the dye molecules with the working solution. At pH 12.0, the hydroxyl group at the 5-position is deprotonated ($pK_a$ = 5.37) and the negatively charged hydroxide ion can form a bond with positively charged sodium ions present in the working solution. Therefore, the hydrophobic interaction of both dyes with fingerprint secretions is weakened by interference effect. The ability of the dye to develop fingerprints is mainly influenced by its hydrophobicity and other factors such as type of substituents attached to benzophenoxazine backbone as indicated from the results of dialkylated derivatives and 2-hydroxy dialkylated derivatives. The chemical structures of Nile red,

**NR1** and **NR2** are analogous to those for **NR3**, **NR4** and **NR5**, respectively with the exception that the latter derivatives contain a hydroxyl group at the 2-position. The presence of hydroxyl group decreases the hydrophobicity of dyes and has adverse impact on fingerprints development.

Fingerprints developed by the 2-hydroxy monoalkylated derivatives were faint and appeared as smudged prints compared to those developed by Nile red (Figure 5.7). The inefficiency of **NR6** and **NR7** is referred to the low hydrophobicity as characterized by logD resulting in weak interaction with fingerprint residue and poor detection.

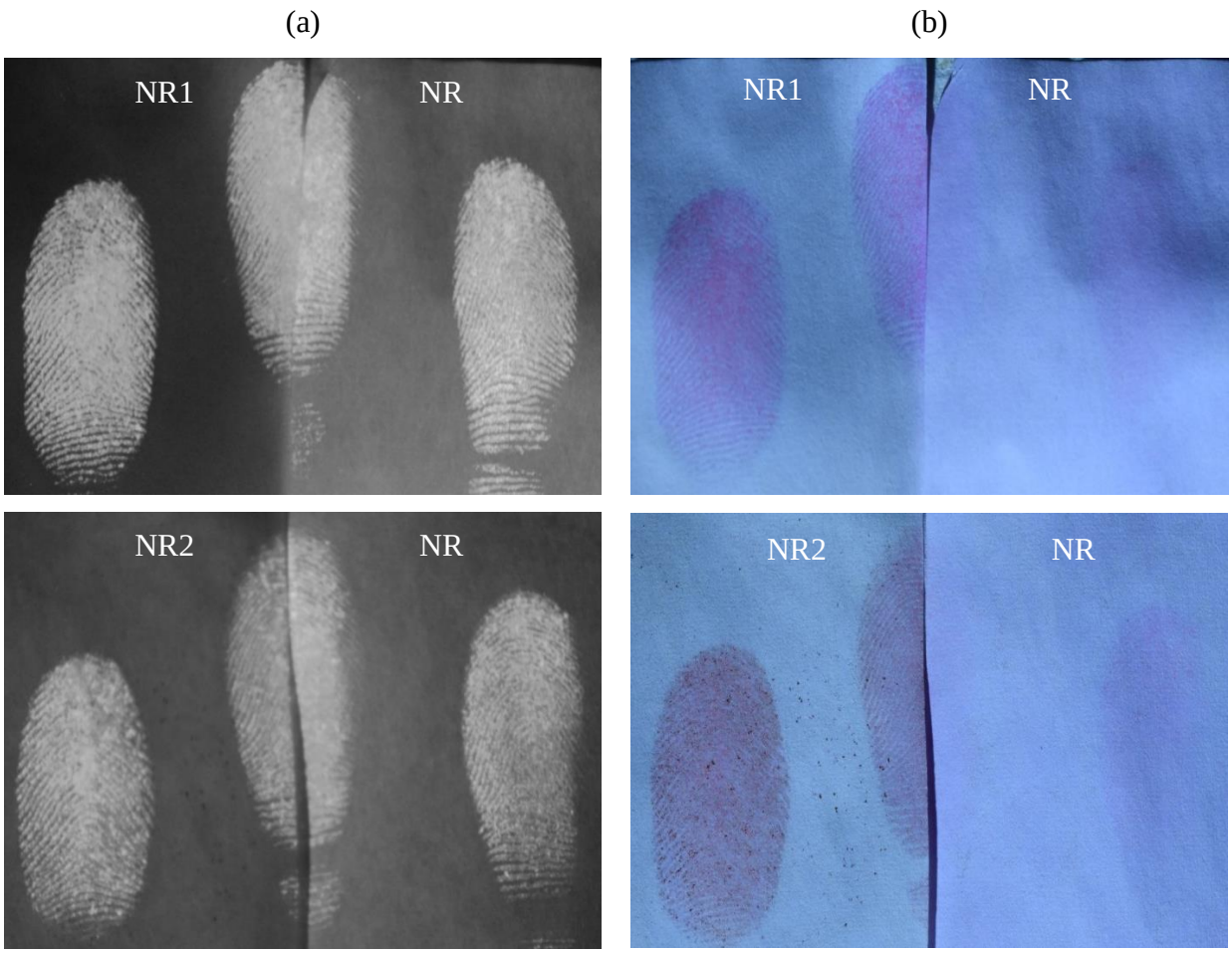


**Figure 5.5 Comparison of fingerprints developed by hydroxy-dialkylated derivatives of Nile red (left half) and NR (right half): (a) at 515 nm excitation wavelength of FLS and viewed with 550 nm long-pass barrier filter and (b) under white light**

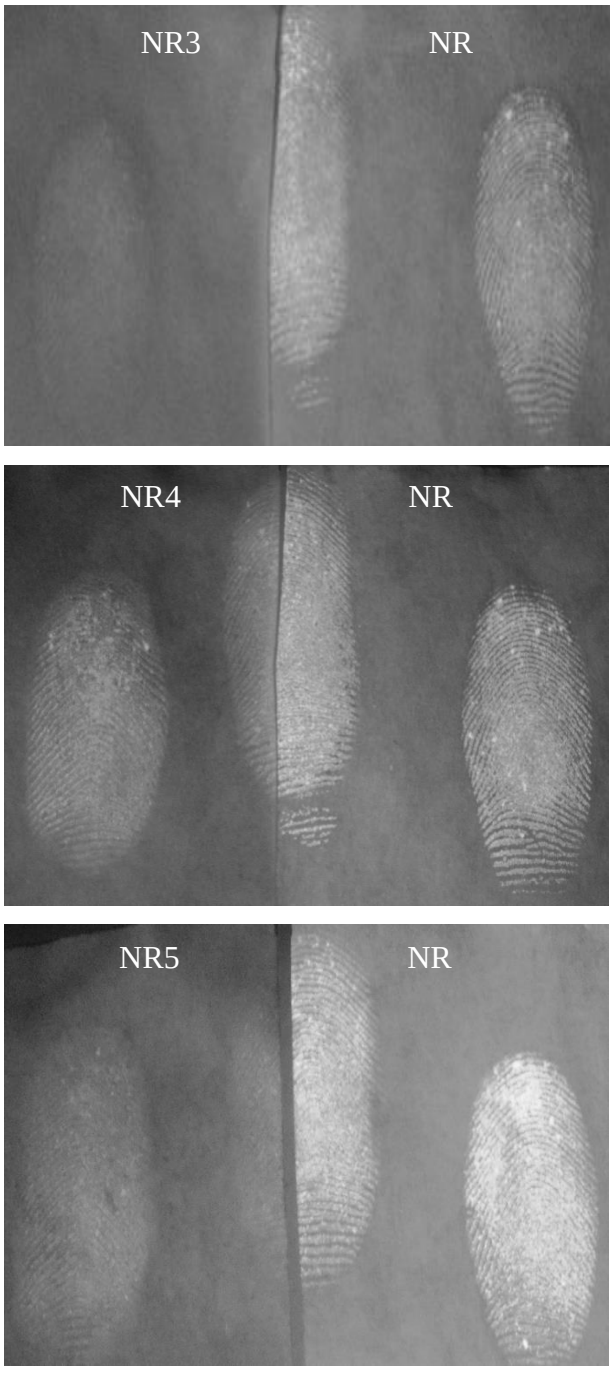


**Figure 5.6 Comparison of fingerprints developed by 2-hydroxy-dialkylated derivatives of Nile red (left half) and NR (right half) at 515 nm excitation wavelength of FLS and viewed with 550 nm long-pass barrier filter**

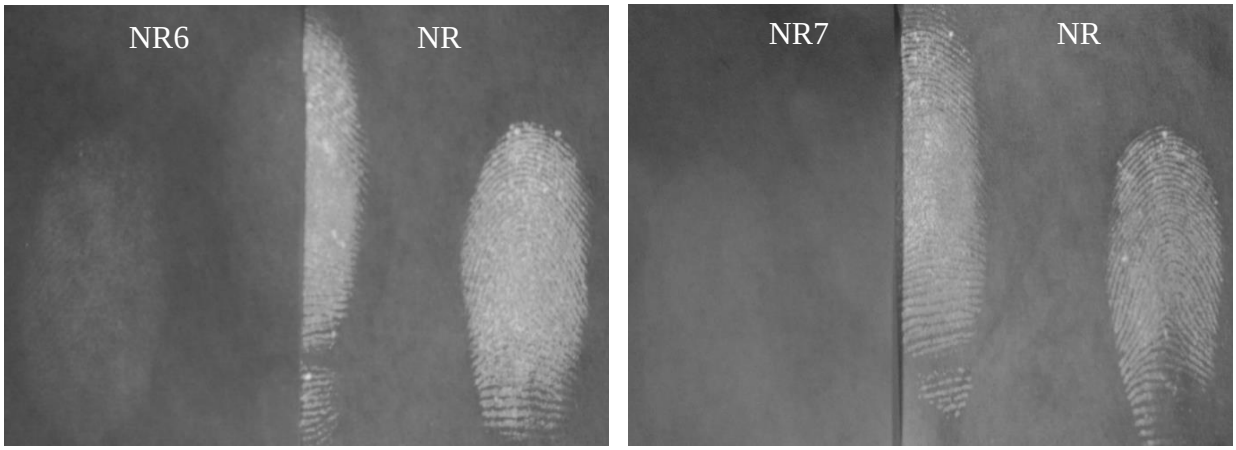


**Figure 5.7 Comparison of fingerprints developed by 2-hydroxy-monoalkylated derivatives of Nile red (left half) and NR (right half) at 515 nm excitation wavelength of FLS and viewed with 550 nm long-pass barrier filter**

### *5.3.4 Application of Nile blue derivatives to fingerprint devolvement*

Samples treated by the dialkylated derivatives were compared to those treated by Nile blue (all in the basic form of the dyes) as shown in Figure 5.8. The fingerprints developed by **NB1** and **NB2** appeared more luminescent with clear ridge pattern than those developed by Nile blue at CSS setting of the FLS. Furthermore, visible fingerprints were obtained as dark blue impressions with clear definition for dialkylated derivatives samples with the use of white light of FLS. However, no fingerprints were visible for Nile blue sample at the same setting of FLS. Thus, the two compounds are considered dual-fingerprint reagents because of the ability to reveal fingerprints that are visible by the naked eye (dark blue impressions) and luminescent when using FLS (yellow-orange impressions). The enhancement of fingerprint performance for **NB1** and **NB2** is due to the great hydrophobicity as characterized by logD (Table 5.2) resulting in stronger interaction with lipid components of fingerprint reside.

On the other hand, non-luminescent fingerprints were obtained for the monoalkylated derivatives samples relative to those for Nile blue sample (all in the basic form of the dyes) as shown in Figure 5.9. The inferior performance of **NB3** and **NB4** is attributed to the low hydrophobicity and type of groups attached to benzophenoxazine backbone as previously mentioned. **NB3** is less hydrophobic than Nile blue and thus unsuccessful fingerprint detection was obtained due to the weak interaction with fingerprint reside. Despite the similarity in hydrophobic properties of **NB4** and Nile blue, no development in fingerprint detection was observed. The chemical structure of **NB3** and **NB4** is analogous to Nile blue and **NB1** respectively with the exception that an extra alkyl group is attached to the amine at the 9-position in the latter dyes. **NB3** and **NB4** contain secondary amine at the 9-position which is considered a hydrogen donor that has the potential to form hydrogen bonds with hydroxide ions present in the working solution. The hydrogen bonds suppress the interaction of the dyes with fingerprint residue. Therefore, the use of these dyes to detect fingerprints is not suitable in forensic detection due to the hydrogen bonds and/or low hydrophobicity.

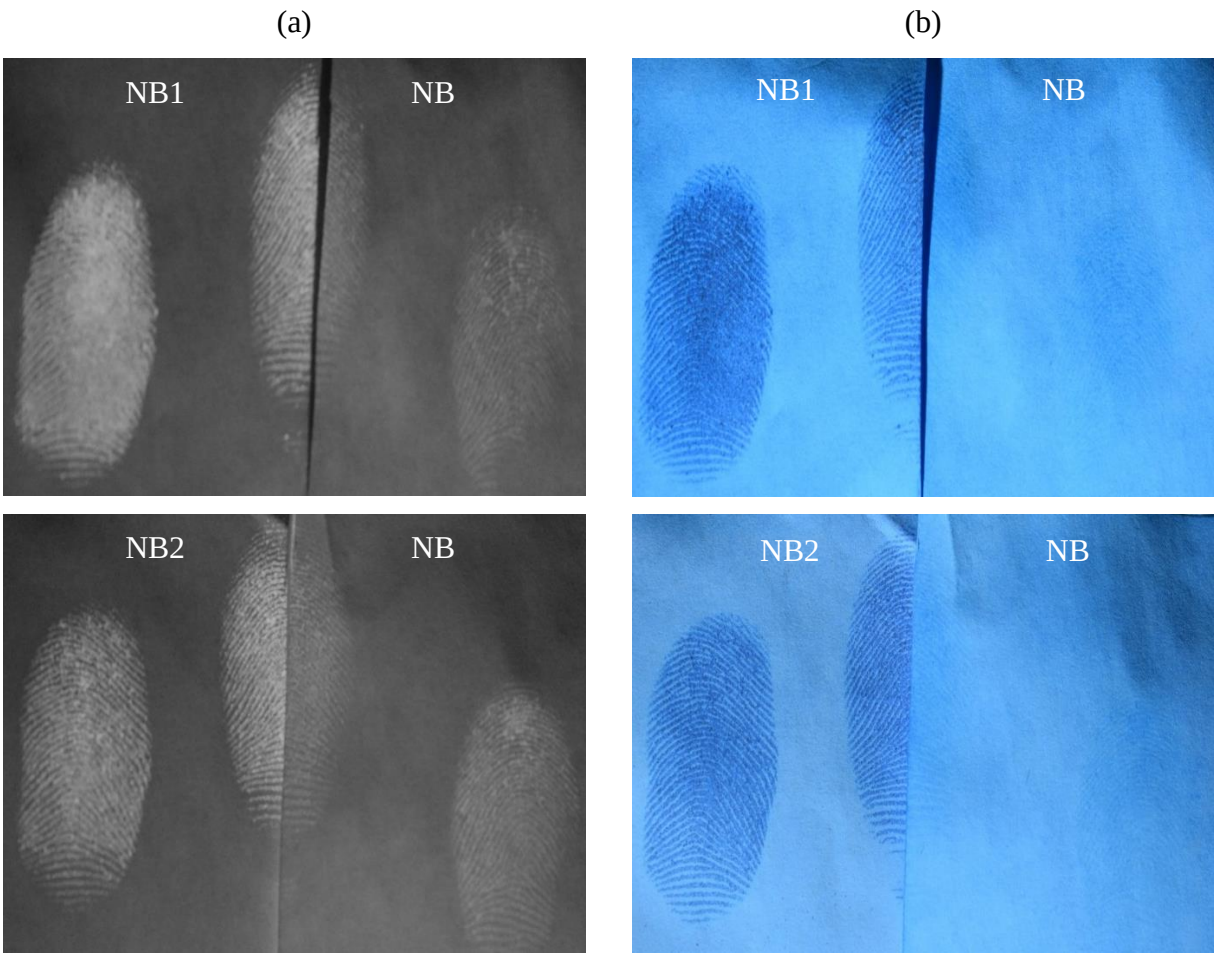


**Figure 5.8 Comparison of fingerprints developed by dialkylated derivatives of Nile blue (left half) and NB (right half): (a) at CSS of FLS and viewed with 550 nm long-pass barrier filter and (b) under white light**

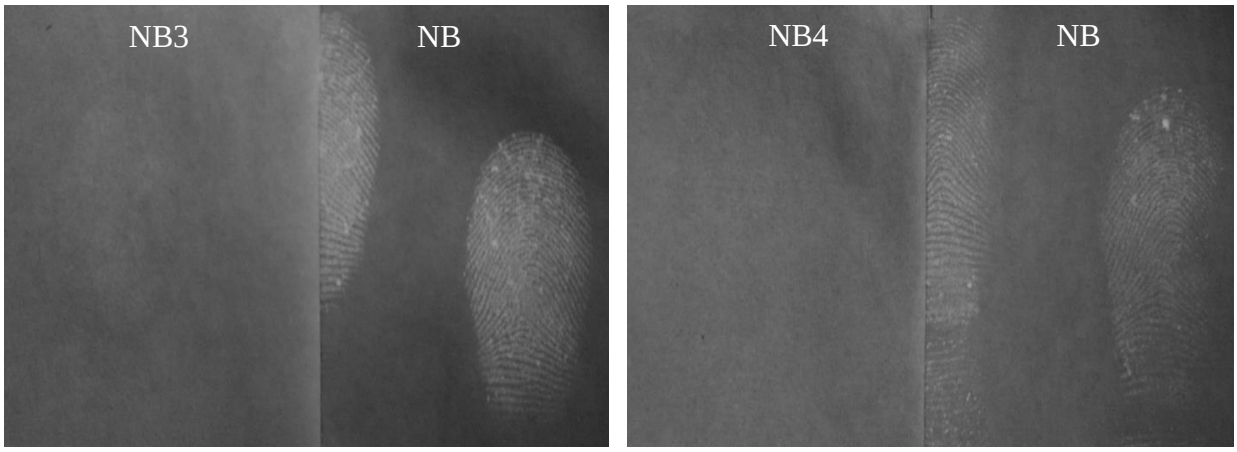


**Figure 5.9 Comparison of fingerprints developed by dialkylated derivatives of Nile blue (left half) and NB (right half) at CSS of FLS and viewed with 550 nm long-pass barrier filter**

**Table 5.2 LogD values of benzophenoxazine dyes at pH 12**

| Dye | LogD[a] |
|---|---|
| NR | 3.83 |
| **NR1** | 5.77 |
| **NR2** | 8.04 |
| **NR3** | 1.37 |
| **NR4** | 3.31 |
| **NR5** | 5.57 |
| **NR6** | 1.86 |
| **NR7** | 2.99 |
| NB | 3.79 |
| **NB1** | 5.72 |
| **NB2** | 7.99 |
| **NB3** | 2.80 |
| **NB4** | 3.76 |

[a] Calculated by ChemAxon

### *5.3.5 Performance evaluation of benzophenoxazine derivatives*

To assess the performance of benzophenoxazine dyes as potential fingerprint reagents, UC scale [38] was applied for comparison between the two methods A and B, in which method A is derivatives of Nile red or Nile blue and method B is corresponding parent dye, Nile red or Nile blue as shown in Table 5.3. For Nile red derivatives performance, dialkylated derivatives **NR1** and **NR2** showed improvement in fingerprint detection relative to Nile red in which they developed visible and luminescent prints with clear ridge patterns, and **NR1** displayed better background contrast. Consequently, the two dyes can be considered as dual-fingerprint reagents due to their great hydrophobicity compared to that of Nile red. However, no improvement in fingerprint detection was observed for the 2-hydroxy dialkylated derivatives and 2-hydroxy monoalkylated derivatives due to the interference effect and/or the low hydrophobicity. Faint or non-luminescent fingerprints and poor contrast were obtained by both types of Nile red derivatives.

For Nile blue derivatives detection performance, dialkylated derivatives **NB1** and **NB2** exhibited enhancement in developing fingerprints relative to Nile blue. Both dyes are considered dual-fingerprint reagents due to their ability to reveal visible and more luminescent prints with clear ridge details. However, weak fingerprints were developed by monoalkylated derivatives **NB3** and **NB4**. Therefore, these dyes are not useful reagents for fingerprint detection due to the low hydrophobicity and/or hydrogen bonds.

Besides the improved results for dialkylated derivatives of Nile red and Nile blue, these compounds exhibit high sensitivity to produce visible prints at dye concentration of 0.2 mM. This concentration is 5-fold less than the concentration needed for the dual-fingerprint reagent genipin, to develop visible prints at concentration of 10 mM.[33] In addition, the combination of color and luminescent properties of the developed prints by a single reagent offer visualization in the field

as well as in the laboratory. Moreover, the fluorescent prints are more practical as they can be recovered from dark-colored surfaces. Other than immersing the sample in water before and after the treatment, no pretreatment or post-treatment is needed to produce luminescent prints.

**Table 5.3 UC score of benzophenoxazine derivatives; (NR1-NR7) relative to Nile red and (NB1-NB4) relative to Nile blue**

| Dye | Score |
|---|---|
| **NR1** | +1 |
| **NR2** | +1 |
| **NR3** | -2 |
| **NR4** | -1 |
| **NR5** | -1 |
| **NR6** | -2 |
| **NR7** | -2 |
| **NB1** | +2 |
| **NB2** | +2 |
| **NB3** | -2 |
| **NB4** | -2 |

## 5.4 Conclusions

The use of two types of benzophenoxazine dyes as developing reagents to reveal latent fingerprints on porous surfaces was investigated. It was found the most significant property of the dye to develop fingerprints is hydrophobicity as indicated by logD value. In this work, hydrophobic dialkylated derivatives of Nile red and Nile blue (in the basic form) showed enhancement in developing fingerprints. **NR1**, **NR2**, **NB1**, and **NB2** detected fingerprints more effectively than their corresponding parent dyes producing more luminescent and visible prints.

Therefore, these dyes are considered as dual-fingerprint reagents. Furthermore, the application of the reagents is simple, sensitive, and effective suggesting their potential use in forensic detection. Besides the significant role of hydrophobicity for fingerprint development, other parameters such as the functional groups attached to the benzophenoxazine backbone and their ability to form hydrogen bonds or interact with solvent should be taken into consideration. Therefore, the use of low hydrophobic derivatives such as **NR3**, **NR6**, **NR7**, and **NB3** or hydrophobic derivatives containing interference substituents such as **NR4**, **NR5**, and **NB4** as fingerprint reagents was not sufficient for detection purposes. Further studies are needed to evaluate the implementation of the modified reagents to develop latent fingerprints on different substrates for a large number of donors and to reveal aged fingerprints.

**References**


1. D'Elia, V.; Materazzi, S.; Iuliano, G.; Niola, L., Evaluation and comparison of 1,2-indanedione and 1,8-diazafluoren-9-one solutions for the enhancement of latent fingerprints on porous surfaces. *Forensic Science International* **2015,** *254*, 205-214.
2. Jelly, R.; Patton, E. L. T.; Lennard, C.; Lewis, S. W.; Lim, K. F., Review: The detection of latent fingermarks on porous surfaces using amino acid sensitive reagents: A review. *Analytica Chimica Acta* **2009,** *652*, 128-142.
3. Chen, C. C.; Yu, Y. C.; Lee, H. C.; Giang, Y. S.; Wang, S. M., Latent Fingerprint Development on Thermal Paper Using Traditional Ninhydrin and 1,2-indanedione. *Journal of Forensic Sciences* **2016,** *61* (1), 219-225.
4. Marriott, C.; Lee, R.; Wilkes, Z.; Comber, B.; Spindler, X.; Roux, C.; Lennard, C., Evaluation of fingermark detection sequences on paper substrates. *Forensic Science International* **2014,** *236*, 30-37.
5. Barros, H. L.; Stefani, V., A new methodology for the visualization of latent fingermarks on the sticky side of adhesive tapes using novel fluorescent dyes. *Forensic Science International* **2016,** *263*, 83-91.
6. Yuan, C.; Li, M.; Wang, M.; Zhang, L., Cationic dye-diatomite composites: Novel dusting powders for developing latent fingerprints. *Dyes and Pigments* **2018,** *153*, 18-25.
7. Sharma, K. K.; Nagaraju, P.; Mohanty, M. E.; Baggi, T. R. R.; Rao, V. J., Latent fingermark development using a novel phenanthro imidazole derivative. *J. Photochem. Photobiol. A-Chem.* **2018,** *351*, 253-260.
8. Beaudoin, A., New Technique for Revealing Latent Fingerprints on Wet, Porous Surfaces: Oil Red O. *Journal of Forensic Identification* **2004,** *54* (4), 413.

9. Salama, J.; Aumeer-Donovan, S.; Lennard, C.; Roux, C., Evaluation of the Fingermark Reagent Oil Red O as a Possible Replacement for Physical Developer. *Journal of Forensic Identification* **2008,** *58* (2), 203.

10. Garrett, H. J.; Bleay, S. M., Evaluation of the solvent black 3 fingermark enhancement reagent: Part 1 — Investigation of fundamental interactions and comparisons with other lipid-specific reagents. *Science & Justice* **2013,** *53*, 121-130.

11. Sodhi, G. S.; Kaur, J., Fingermarks detection by eosin-blue dye. *Forensic Science International* **2001,** *115*, 69-71.

12. Brunelle, E.; Le, A. M.; Huynh, C.; Wingfield, K.; Halamkova, L.; Agudelo, J.; Halamek, J., Coomassie Brilliant Blue G-250 Dye: An Application for Forensic Fingerprint Analysis. *Analytical Chemistry* **2017,** *89* (7), 4314-4319.

13. Sodhi, G. S.; Kaur, J., Powder method for detecting latent fingerprints: a review. *Forensic Science International* **2001,** *120*, 172-176.

14. Barros, H. L.; Stefani, V., Micro-structured fluorescent powders for detecting latent fingerprints on different types of surfaces. *J. Photochem. Photobiol. A-Chem.* **2019,** *368*, 137-146.

15. Beaudoin, A., Fingerprint Staining Technique on Dark and Wetted Porous Surfaces: Oil Red O and Rhodamine 6G. *Journal of Forensic Identification* **2012,** *62* (4), 315-329.

16. Greenspan, P.; Fowler, S. D., Spectrofluorometric studies of the lipid probe, Nile red. *Journal of Lipid Research* **1985,** *26* (7), 781-789.

17. Bancroft, J. D.; Cook, H. C., *Manual of histological techniques and their diagnostic application*. Edinburgh ; New York : Churchill Livingstone, 1994.: 1994.

18. Ramotoeski, R. S., Composition of Latent Print Reside. In *Advances in Fingerprint Technology*, Lee, H. C.; Gaensslen, R. E., Eds. Boca Raton, Fla: CRC Press, 2nd ed.: 2001.

19. Martinez, V.; Henary, M., Nile Red and Nile Blue: applications and syntheses of structural analogues. *Chem.-Eur. J.* **2016,** *22* (39), 13764-13782.

20. Jose, J.; Burgess, K., Benzophenoxazine-based fluorescent dyes for labeling biomolecules. *Tetrahedron* **2006,** *62* (48), 11021-11037.

21. Tajalli, H.; Gilani, A. G.; Zakerhamidi, M. S.; Tajalli, P., The photophysical properties of Nile red and Nile blue in ordered anisotropic media. *Dyes and Pigments* **2008,** *78*, 15-24.

22. Day, K. J.; Bowker, W., Enhancement of Cyanoacrylate Developed Latent Prints Using Nile Red. *Journal of Forensic Identification* **1996,** *46* (2), 183-187.

23. Chesher, B. K.; Stone, J. M.; Rowe, W. F., Use of the Omniprint™ 1000 alternate light source to produce fluorescence in cyanoacrylate-developed latent fingerprints stained with biological stains and commercial fabric dyes. *Forensic Science International* **1992,** *57* (2), 163-168.

24. Castelló, A.; Alvarez-Seguí, M.; Verdú, F., Use of fluorescent dyes for developing latent lip prints. *Coloration Technology* **2004,** *120* (4), 184.

25. Braasch, K.; de la Hunty, M.; Deppe, J.; Spindler, X.; Cantu, A. A.; Maynard, P.; Lennard, C.; Roux, C., Nile red: Alternative to physical developer for the detection of latent fingermarks on wet porous surfaces? *Forensic Science International* **2013,** *230*, 74-80.

26. Frick, A. A.; Busetti, F.; Cross, A.; Lewis, S. W., Aqueous Nile blue: a simple, versatile and safe reagent for the detection of latent fingermarks. *Chemical Communications* **2014,** *50* (25), 3341-3343.

27. Ostle, A. G.; Holt, J. G., Nile blue A as a fluorescent stain for poly-beta-hydroxybutyrate. *Appl Environ Microbiol* **1982,** *44* (1), 238-41.

28. de la Hunty, M.; Spindler, X.; Chadwick, S.; Lennard, C.; Roux, C., Synthesis and application of an aqueous Nile red microemulsion for the development of fingermarks on porous surfaces. *Forensic Science International* **2014,** *244*, 48-55.

29. Wang, W.; Xing, J.; Ge, Z., Evaluation of Nile Red-Loaded Mesoporous Silica Nanoparticles for Developing Water-Soaked Fingerprints on Thermal Paper. *Journal of Forensic Sciences* **2018**.

30. Sangster, J., *Octanol-water partition coefficients : fundamentals and physical chemistry*. Chichester ; New York : Wiley, c1997.: 1997.

31. Kwon, Y., *Handbook of essential pharmacokinetics, pharmacodynamics and drug metabolism for industrial scientists.* New York : Kluwer Academic Publishers, c2002.: 2002.

32. Lee, S.-W.; Lim, J.-M.; Bhoo, S.-H.; Paik, Y.-S.; Hahn, T.-R., Colorimetric determination of amino acids using genipin from Gardenia jasminoides. *Analytica Chimica Acta* **2003,** *480*, 267-274.

33. Almog, J.; Cohen, Y.; Azoury, M.; Hahn, T. R., Genipin - A novel fingerprint reagent with colorimetric and fluorogenic activity. *Journal of Forensic Sciences* **2004,** *49* (2), 255-257.

34. Lennard, C. J.; Margot, P. A.; Stoilovic, M.; Warrener, R. N., Synthesis and evaluation of ninhydrin analogs as reagents for the development of latent fingerprints on paper surfaces. *J. Forensic Sci. Soc.* **1988,** *28* (1), 3-23.

35. Grigg, R.; Mongkolaussavaratana, T.; Anthony Pounds, C.; Sivagnanam, S., 1,8-diazafluorenone and related compounds. A new reagent for the detection of (α-amino acids and latent fingerprints. *Tetrahedron Letters* **1990,** *31* (49), 7215-7218.

36. Kobus, H. J.; Pigou, P. E.; Jahangiri, S.; Taylor, B., Evaluation of some oxygen, sulfur, and selenium substituted ninhydrin analogues, nitrophenylninhydrin and benzo[f]furoninhydrin. *J Forensic Sci* **2002,** *47* (2), 254-9.

37. Almog, J.; Klein, A.; Davidi, I.; Cohen, Y.; Azoury, M.; Levin-Elad, M., Dual fingerprint reagents with enhanced sensitivity: 5-methoxy- and 5-methylthioninhydrin. *J. Forensic Sci.* **2008,** *53* (2), 364-368.

38. Guidelines for the Assessment of Fingermark Detection Techniques. *Journal of Forensic Identification* **2014,** *64* (2), 174.

# 6 DYE-ENCAPSULATED SILICA NANOPARTICLES FOR FINGERPRINT DETECTION

## 6.1 Evaluation of Benzophenoxazine Derivatives-Encapsulated Silica Nanoparticles for Fingerprint Detection

### *6.1.1 Introduction*

Fingerprints have been considered one of the effective methods in forensic investigation for personal identification. Fingerprint analysis remains an extremely powerful tool to identify suspects as no two individuals ever had have and will have the same fingerprint characteristics.[1] There are a variety of methods for fingerprint development of including powder methods,[2] chemical reagents (ninhydrin, 1,2-indanedione, 1,8-diazafluoren-9-one),[3] spectroscopic techniques (Raman spectroscopy imaging, mass spectrometry, and infrared spectroscopy).[4-6] Recently, nanomaterials have received increasing attention in fingerprint recognition due to their advantages such as biocompatibility, good photostability, and cost-effective synthesis.[7] Moreover, the luminescent properties of nanoparticles can be enhanced by incorporating fluorescent molecules such as organic dyes covalently or non-covalently into the siloxane matrix. Some fluorescent dyes such as rhodamine 6G, rhodamine B, tris(2,20- bipyridyl)dichlororuthenium (II) hexahydrate (RuBpy) encapsulated into silica nanoparticles showed great development of fingerprints on non-porous surfaces.[8] Moreover, magnetic nanoparticles labeled with a fluorescent antibody allowed the detection of some illicit drugs such as benzoylecgonine, the major metabolite of cocaine, that present in fingerprints.[9]

Benzophenoxazine dyes such as Nile red and Nile blue have been used in fingerprint development. The initial use of the dyes was as a post-treatment of the fingerprints developed by

cyanoacrylate fuming.[10-11] Moreover, the dyes have contributed to fingerprint detection in such different ways: aqueous solution, methanolic-aqueous solution, and aqueous microemulsion formulation.[12-14] Recently, Nile red-encapsulated mesoporous silica nanoparticles have been proposed as a safe and sensitive method for fingerprint detection on thermal paper without the need of organic solvents.[15] Our previous work investigated several benzophenoxazine derivatives of different hydrophobicity for fingerprint detection. It was concluded that dialkylated derivatives of Nile red and Nile blue (**NR1**, **NR2**, **NB1**, and **NB2**) are considered dual-fingerprint reagents as they develop visible and luminescent prints with good background contrast due to the high hydrophobicity of the dyes. In this work, benzophenoxazine derivatives of improved results (**NR1**, **NR2**, **NB1**, and **NB2**) as well as the parent dyes (Nile red and Nile blue) were non-covalently encapsulated into silica nanoparticles by modified Stöber method and evaluated for developing fingerprints on several surfaces.

### *6.1.2 Experimental*

#### *6.1.2.1 Instrumentation and particle characterization*

Particle size determination analysis of 0.1 mg/mL F-SiNPs suspensions dispersed in ethanol was obtained using a Malvern Mastersizer (Malvern Instruments Ltd., Malvern, UK). Polydispersity index (PDI) and standard deviation were determined from three independent measurements of the dispersions of NPs. The zeta potential of NPs dispersions in ethanol was also recorded. Transmission electron microscopy micrographs were measured by the Zeiss LEO 912AB (Zeiss, Thornwood, NY). NPs separation required an Allegra 64R Centrifuge (Beckman Coulter Inc., Brea, CA). A SympHonly (SB20) pH-meter (Thermo Orion, MA, USA) was used for pH adjustment. Nano pure water was prepared using a Barnstead NANO pure DIamond Analytical

ultrapure water system (Fischer Scientific, NJ, USA). Fluorescence spectra were acquired using an ISS K2 multifrequency cross-correlation phase and modulation fluorimeter (ISS™ Focus and Discover, Champaign, IL, USA), equipped with a 300W xenon arc lamp. Fluorescence measurements were performed in 1.0 cm disposable plastic cuvettes. The fluorescence properties of the Benzo-SiNPs were studied by recording the emission spectra of the suspensions in a 4:1 (v/v) water/ethanol solvent.

#### *6.1.2.2 Chemicals and reagents*

Nile red (NR), Nile blue (NB), tetraethyl orthosilicate (TEOS) (99.99% trace metal basis), 1-hexanol (anhydrous, ≥99%), sodium hydroxide (pellets, 97+%, A.C.S. reagent), cyclohexane (anhydrous, 99.5%), ethanol (99.7%), and Triton™ X-100 (laboratory grade) were obtained from Sigma-Aldrich (MO, USA). Ammonium hydroxide solution (28%) and phenyltriethoxysilane (PTEOS) were obtained from Fisher Scientific (NJ, USA) and Chem-Impex International, Inc. (IL, USA), respectively. Nile red derivatives (**NR1** and **NR2**) were prepared by Walid Abdelwahab, the research group of Dr. Gabor Patonay whereas Nile blue derivatives (**NB1**, and **NB2**) were prepared by Vincent Martinez, the research group of Dr. Maged Henary. The chemical structures of the dyes are shown in Figure 6.1.

#### *6.1.2.3 Preparation of silica nanoparticles encapsulating benzophenoxazine derivatives*

Benzophenoxazine derivatives-encapsulated silica nanoparticles (Benzo-SiNPs) were prepared by modified Stöber method using a mixture of TEOS and PTEOS as alkoxysilane precursors. Six different dyes, three Nile red derivatives (NR, **NR1**, and **NR2**) and three Nile blue derivatives (NB, **NB1**, and **NB2**), were selected for silica nanoparticles encapsulating based on

their outstanding performance in fingerprint detection due to their high hydrophobicity as indicated by logD (Table 6.1) compared to the parent dyes, Nile red and Nile blue. Nile red derivatives-encapsulated silica nanoparticles (NR-SiNPs) and Nile blue derivatives-encapsulated silica nanoparticles (NB-SiNPs) were prepared by Walid Abdelwahab, the research group of Dr.Gabor Patonay.

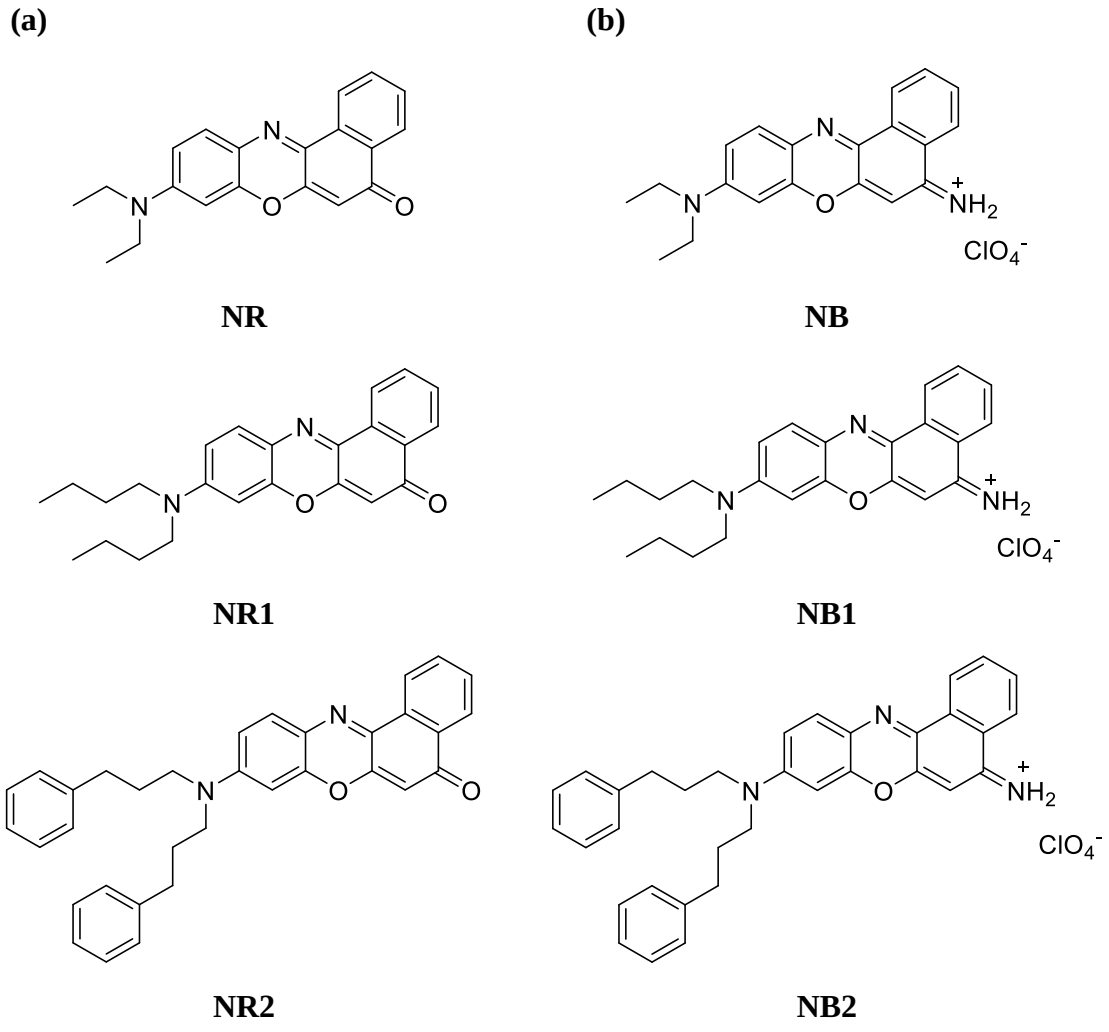


**Figure 6.1 Chemical structures of encapsulating dyes: (a) Nile red derivatives and (b) Nile blue derivatives**

**Table 6.1 LogD values of benzophenoxazine dyes at pH 7.4**

| Dye | LogD[a] |
|---|---|
| NR | 3.83 |
| **NR1** | 5.77 |
| **NR2** | 8.04 |
| NB | 0.60 |
| **NB1** | 2.53 |
| **NB2** | 4.80 |

[a] Calculated by MarvinSketch

#### *6.1.2.4 Fingerprint sampling*

Fingerprints were obtained from two donors: 26-year-old male and 42-year-old female and then developed after a day (24 hours) of deposition. Fingerprints were evaluated in three different substrates: glass microscope slides, aluminum foil, and petri dishes (polystyrene). Fingerprints were collected by instructing the donors to rub their fingers with their nose immediately prior to fingerprint collection. The donors were requested not to wash their hands during the two hours before collecting the samples.

#### *6.1.2.5 Fingerprint detection method*

For the detection of fingerprints, a suspension (5.0 mg/mL) in water: ethanol (4:1, *v/v*) of Benzo-SiNPs was prepared. The solution was sonicated for 10 min to allow for suitable particles dispersion. A small amount of the suspension (0.5-1.0 mL) was pipetted onto the sample using a transfer pipette. After 5 minutes, the excess solution was removed, and the sample was gently washed with a mixture of 4:1 (v/v) water: ethanol. After that the developed fingerprint was left to

dry at room temperature. The samples were visualized by forensic light source (FLS), Mini-CrimeScope 400 (MCS-400) (Spex Forensics, Edison, NJ) at an excitation wavelength of 555 nm. The fingerprint images were photographed using a digital camera (Nikon D3300) with a 580 nm long-pass filter. The fingerprint sample was placed on a black background to improve the contrast of the image during illumination and taking pictures.

### *6.1.3 Results and discussion*

#### *6.1.3.1 Spectroscopic studies of Benzo-SiNPs*

An examination of the emission spectra showed that spectroscopic characteristics of the working solutions of Benzo-SiNPs are influenced by the chemical structure of the dye and physical properties such as the hydrophobicity as shown in Figure 6.2. The emission maximum for NR-SiNPs was in the same range of about 610 nm. The fluorescence intensity increased as the hydrophobicity of the dye increased. The emission spectrum of the most hydrophobic derivative **NR2NPs** showed the highest intensity whereas that of the least hydrophobic derivative NRNPs displayed the lowest value. In the case of NB-SiNPs, a blue shift in the emission maximum was observed on going from the least hydrophobic dye NBNPs to the most hydrophobic dye **NB2NPs**. Similar to NR-SiNPs, there was an increase in the fluorescence intensity as the hydrophobicity of the dye increased in which **NB2NPs** showed the highest intensity whereas NBNPs displayed the lowest value.

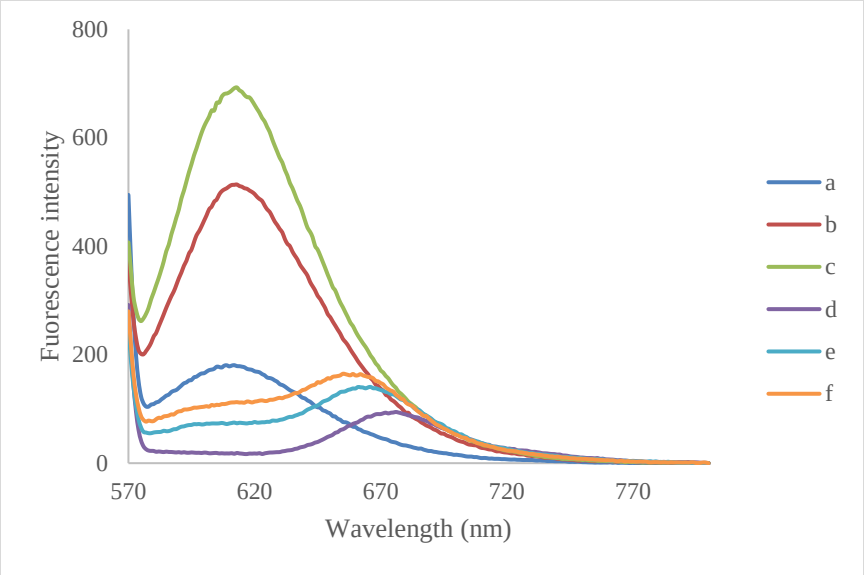


**Figure 6.2 Emission spectra of (a) NRNPs, (b) NR1NPs, (c) NR2NPs, (d) NBNPs, (e) NB1NPs, and (f) NB2NPs in water: ethanol (4:1, v/v) excited at 555 nm**

### *6.1.3.2 Fingerprint detection using benzophenoxazine silica nanoparticles*

To study the efficiency of Benzo-SiNPs for fingerprint detection, suspensions of these particles were used for three different non-porous surfaces: glass slides, aluminum foil, and petri dishes (polystyrene). Six benzophenoxazine derivatives of different hydrophobicity have been incapsulated into silica nanoparticles using one the binary mixture of TEOS and PTEOS and evaluated for fingerprint detection. It was observed that as the hydrophobicity of the encapsulated dye increases, the luminescence properties of developed fingerprints increase in all substrates. Sametband and his coworkers mentioned that gold nanoparticles with longer thiol chains provided superior fingerprint detection due to the hydrophobic interaction with fingerprint residue.[16] For the first substrate, glass slides, Benzo-SiNPs developed luminescent fingerprint ridges at 555 nm excitation wavelength of FLS, viewed with 580 nm long-pass barrier filter as shown in Figure 6.3. The surface of silica nanoparticles was modified with the hydrophobic precursor PTEOS as well

as TEOS which increased the hydrophobic interactions with sebaceous secretions of fingerprint residue providing luminescent fingerprints as confirmed in previous study. However, there was a background staining in the case of NB-SiNPs which could be due to unwanted interaction with the glass substrate. Nonetheless, the background staining did not obstruct fingerprint visualization. A comparable performance of Benzo-SiNPs was obtained on the other substrates, aluminum foil and petri dishes.

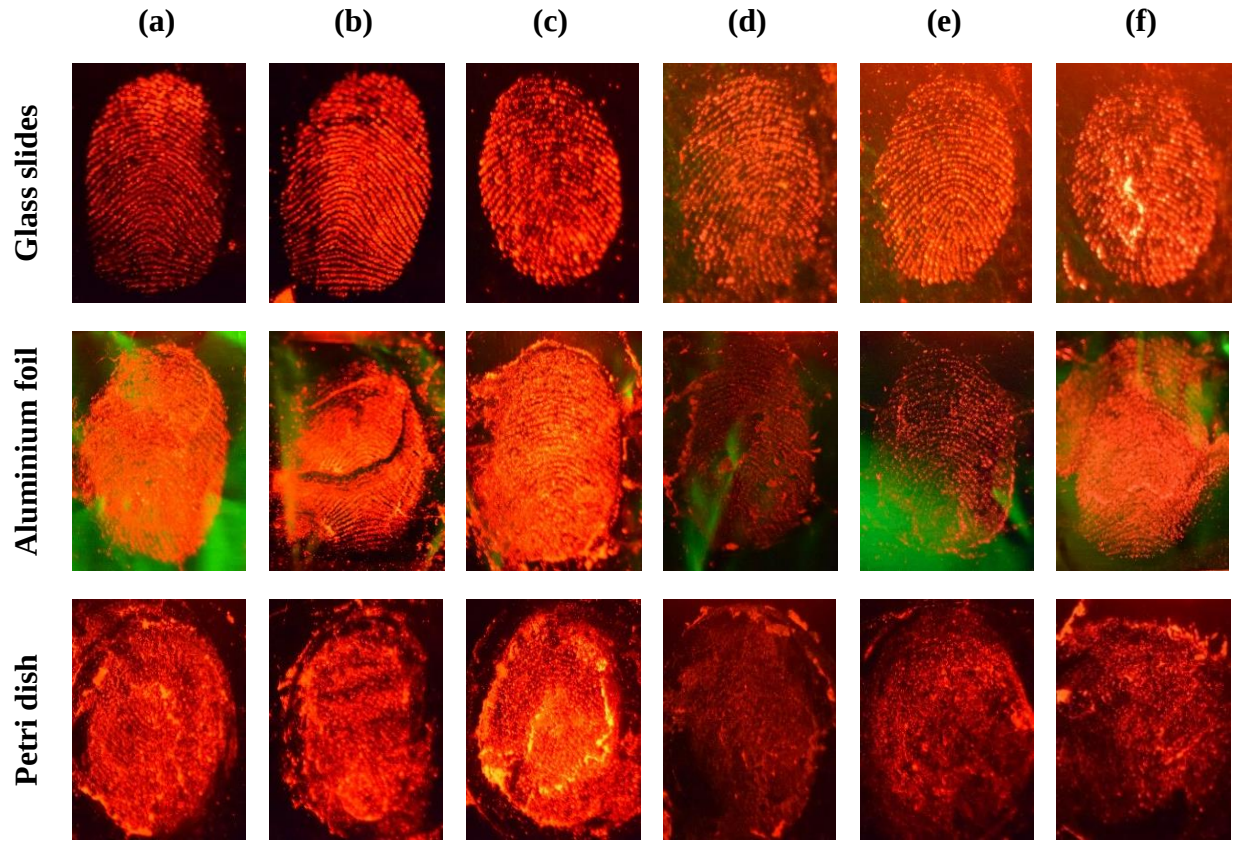


**Figure 6.3 Fluorescence images of fingerprints treated by 5.0 mg/mL suspensions Benzo-SiNPs in water: ethanol (4:1, v/v) of (a) NRNPs, (b) NR1NPs, (c) NR2NPs, (d) NBNPs (e) NB1NPs, and (f) NB2NPs, on different substrates at 555 nm excitation wavelength of FLS, viewed with 580 nm long-pass barrier filter**

### *6.1.4 Conclusions*

A series of Benzo-SiNPs was examined as developing agents for fingerprint detection on three non-porous surfaces. The surface of nanoparticles was modified by different precursors such as TEOS and PTEOS. It was found that the nature of the encapsulated dye plays an important role in fingerprint detection. Benzo-SiNPs developed luminescent fingerprints with good details due to the hydrophobic interaction with fingerprint components. However, silica nanoparticles with encapsulated dyes of high hydrophobicity such as NRNPs, **NR1NPs**, **NR2NPs**, and **NB2NPs** showed superior results compared to other nanoparticles encapsulating dyes of low hydrophobicity such as NBNPs and **NB1NPs**. Overall, Benzo-SiNPs fingerprint detection on glass slides was greater compared to the other two substrates.

## 6.2 A Comparative Study of Fluorescein Isothiocyanate-Encapsulated Silica Nanoparticles Prepared in Seven Different Routes for Developing Fingerprints on Non-Porous Surfaces



Journal of Fluorescence (2018) 28:1049-1058

DOI 10.1007/s10895-018-2268-6

Preparation of fluorescein isothiocyanate (FITC)-encapsulated silica nanoparticles (F-SiNPs) via seven different approaches to be used as developing agents for fingerprints detection is presented in this report. In this study, the suitability of each synthesis route toward incorporation of the selected fluorophore into silica matrix and its efficiency in fingerprints detection were systematically studied. The composition of the particles was designed to examine the hydrophobic and dipole-dipole interactions between the silicate backbone and both of the fluorescent reporter molecules and the fingerprint residues. F-SiNPs were prepared with two conventional sol-gel approaches; the Stöber method and the water in oil reverse microemulsion (WORM) method. The alkoxysilane precursor, tetraethoxyorthosilicate (TEOS) and its binary mixtures with phenyltriethoxysilane (PTEOS) or 3-aminopropyl triethoxysilane (APTES) have been used in preparing the F-SiNPs to study the effect of nanoparticles composition on fingerprints development. In addition, FITC was conjugated with APTES so it can be covalently bonded to the silica matrix and to be compared with non-covalently FITC-doped SiNPs. Moreover, the enhancement effect of introducing polyvinylpyrrolidone (PVP) onto the surface of the less hydrophobic F-SiNP on fingerprints detection on different non-porous surfaces was also investigated. The mean diameters of the F-SiNPs were between 4.1±0.6 and 110.4±31.1 nm as

obtained from the TEM size measurement for the nanoparticles prepared by the WORM and Stöber methods, respectively. The obtained results clearly highlight the advantages of using a mixture of TEOS and PTEOS alkoxysilane precursors in preparing F-SiNPs with remarkable encapsulation efficiency and clear detection of fingerprints due to efficient embedding of the fluorophore inside the silica network even without conjugation. It was also observed that both the Stöber and WORM methods can be used in preparing the F-SiNPs and that PVP coated particles did not show any significant enhancement in fingerprints visualization.

### *6.2.1 Introduction*

Detection of fingerprints at a crime scene is of great interest in forensic investigation mainly for collecting physical evidence. Fingerprints visualization requires a specific reaction of the developing agent with the fingerprint residue to obtain a clear contrast from the underlying substrate. This residue is a complex mixture of organic compounds such as proteins, amino acids, and lipids and some inorganic substances. Development of fingerprint can be achieved either through a chemical interaction between the reagent and the components found in the fingerprint deposit or via physical adhesion of a developing agent to the sticky fingerprint residue.[17-18]

Various methods such as powder dusting, cyanoacrylate fuming, and ninhydrin have been developed for fingerprint visualization. However, there is still a need for selective and sensitive optics-based reporters for fingerprint development. Recently, there have been increased interests in using nanoparticles (NPs) for fingerprints detection due to their adventurous properties. First, their small particle size enhances the detection of fingerprints due to increased resolution as small particles can adhere to the fingerprint residue with high affinity.[19] Second, the optical properties of fluorescent NPs allow detecting fingerprints with improved overall sensitivity.[8] Finally, surface

modification can be achieved by the incorporation of functional groups allowing sufficient interactions with certain components in the fingerprint residue, and thus increase the selectivity. Leggett et al. reported the use of antibody-functionalized gold NPs to specifically detect cotinine, a metabolite of nicotine, only present in fingerprints left by smokers.[20] Many types of NPs such as gold NPs,[21] quantum dots,[22-23] nanostructured powders,[24] and silica nanoparticles (SiNPs),[25-27] have been used as developing agents for fingerprints. Despite all advantages of NPs for fingerprint detection, there are still concerns regarding their toxicity, cost, and laborious procedures. SiNPs are a favorable candidate for fingerprints detection due to their great surface-to-volume ratio, biocompatibility and their photochemical stability.[25] Many studies suggest the use of dye doped SiNPs to overcome the downsides of fluorescent molecule labels. In fact, by embedding dyes into SiNPs a higher concentration of fluorescence emitters can be obtained within a single optical probe, which results in an enhanced signal to noise ratio. Furthermore, modification of SiNPs surface can be easily achieved by grafting the proper organosilane moieties to target various compounds in the fingerprint residue. For example, amphiphilic SiNPs were synthetized and used as a developing agent where the hydrophobic and hydrophilic nature of the used monomers made the surface of these particles sensitive to the amino acids present in the fingerprint residue.[26] Moreover, fluorophores such as organic dye molecules can be incorporated within the siloxane matrix during the synthesis process, providing superior optical properties and low background interference as presented in Theaker et al. and Abdelwahab et al. reports where they developed hydrophobic silica micro- and NPs encapsulating fluorescent dyes as developing agents for fingerprints detection.[27-28]

Many researches have been investigated the interaction between biomolecules by circular dichroism, electrochemical methods, and molecular modeling techniques.[29-31] Fluorescence

spectroscopy is one of the key techniques that used widely to study the binding interaction between biomolecules. However, this technique is subject to instrumental variation such as inner filter effect.[32] The main cause of this variation is attenuation of fluorescence intensity by absorption of the incident light or reabsorption of the emitted light by the molecule of interest which are called the primary and secondary inner filter effects, respectively.[33-34] The presence of inner filter effect could lead to erroneous results.[35] Nanosystems have also been utilized to study interaction between biological compounds using spectroscopic techniques. The interaction of ciprofloxacin with some biomolecules such as human serum albumin and lysozyme for example have been investigated using three different sizes of silver NPs.[36-37]

Synthesis of SiNPs is typically carried out through two commonly used sol-gel methods: the Stöber method[38] and the water in oil reverse microemulsion (WORM) method.[39] The modified Stöber process is used for the preparation of silica colloids by means of hydrolysis and condensation of the organosilicate monomers such as tetraethyl orthosilicate (TEOS), 3-aminopropyl triethoxysilane (APTES) and phenyltriethoxysilane (PTEOS) in alkaline alcoholic solutions (pH 11–12) and ammonia serves as a base catalyst. On the other hand, the NPs prepared by WORM show less polydispersity with better control of particle size allowed.[39-40] However, high amounts of surfactants and co-surfactants are needed in the synthesis process making tedious subsequent washing steps necessary.[41] Regardless of the synthesis route, several approaches have been proposed for coupling of organic fluorophores into the SiNPs platform.[42-43] The simplest approach is the non-covalent incorporation of dyes into the silica matrix. Nevertheless, the absence of a stable covalent attachment between the fluorophores and the silica matrix implies that the dye molecules can leak out of the NPs over time, resulting in a decrease in the brightness of the NPs, increase in the background signal and exposition of the fluorophores to the surrounding

environment making them less suitable for fingerprints detection.[44] On the contrary, the dye leakage can be effectively avoided by covalent dye encapsulation. The covalent incorporation of dyes into silica can be achieved by using an amine-containing organosilane as the crosslinker such as APTES which can form a covalent binding between its amine group and cyanate group of the dye leading to the formation of a thiourea linkage.[45] It is obvious that the covalent bonding approach is the best method for incorporation of a dye into SiNPs. However, the dye should have the necessary functional groups towards modification and conjugation with the silicate precursors. This concept might increase considerably the difficulty of dye selection and pre-modification.

To the best of our knowledge, most of the reports dealing with the application of fluorescently-labeled SiNPs in fingerprints development concentrated on the incorporation of fluorophores into the colloidal silica spheres and on the nature of these fluorophores.[46-48] Nevertheless, very few studies have been carried out that focus on the core and surface properties of the NPs used for fluorophore encapsulation and their effects on the efficiency of fingerprints detection in a systematic manner. It was suggested that for effective dye doping and fingerprints visualization, mixtures of TEOS and PTEOS have to be used in synthesizing the NPs, hence it was concluded that analogous hydrophobic and electrostatic interactions occur within these hydrophobic NPs between compatible groups within the fluorescein isothiocyanate (FITC) dye molecules or any other dye of a related structure and the silica matrix.[27] Moreover, it was found that the dye was not subjected to photo-bleaching under exposure to high intensity UV illumination. Hence, these NPs can be utilized as agents for developing fingerprints, including aged prints where the residues mainly consist of hydrophobic endogenous chemicals secreted by the donor, due to the hydrophobic nature of some of the proposed FITC-encapsulated silica

nanoparticles (F-SiNPs).[27] It should also be noted that as the proportion of PTEOS increases, the hydrophobicity of the resulting sol–gel also increases.[49]

In this study, a systematic investigation of several factors affecting the efficiency of developing fingerprints is presented. These factors include (i) method of SiNPs preparation, (ii) the method of fluorophore encapsulation into the NPs matrix, and (iii) nature of the used organosilicate precursors and (iv) surface modification of dye encapsulated SiNPs using adhesive agents such as polyvinylpyrrolidone (PVP) and its enhancing effect on the binding affinity to fingerprints. In order to study these factors, FITC-encapsulated silica nanoparticles (F-SiNPs), (Table 6.2) were prepared using seven approaches for the synthesis and systematic tuning of dye-doped SiNPs in the ultrasmall scale range, down to several nanometers, and tested as developing agents to visualize fingerprints on different non-porous surfaces including glass slides, Petri dishes (polystyrene), and aluminum foil.

This work provides a systematic guideline for synthesis parameters that permit production of stable, highly emitting, nanosized fluorescently-labeled optical reporters with optimal spectral properties, as well as cost-effective synthesis routes easy to scale up for commercial production to be utilized in forensic or bio-related applications.

### *6.2.2 Experimental*

#### *6.2.2.1 Materials and reagents*

All the chemicals used were of Analytical Reagent grade, and the solvents were of HPLC grade. All the following chemicals were produced by Sigma-Aldrich, MO, USA: fluorescein isothiocyanate (FITC) (isomer I, 90%), 1-hexanol (anhydrous, ≥99%), 3-aminopropyl triethoxysilane (APTES) (≥98%), tetraethyl orthosilicate (TEOS) (99.9% trace metal basis),

sodium hydroxide (pellets, 97+%, A.C.S. reagent), cyclohexane (anhydrous, 99.5%), ethanol (99.7%), and Triton™ X-100 (laboratory grade). Fisher Scientific, Fair Lawn, NJ, produced ammonium hydroxide solution (28%). Phenyltriethoxysilane (PTEOS) was supplied by Chem-Impex Int`l Inc., IL, USA whereas polyvinylpyrrolidone (PVP) was supplied by Alfa Aesar, MA, USA.

#### *6.2.2.2 Pre-modification of FITC*

In order to covalently incorporate FITC in the silica matrix, it was modified by inducing a reaction between the isothiocyanate group of FITC and the amine group of APTES to form a thiourea linkage. A known amount of FITC was added to 1-hexanol to make a 1.0 mM solution. 10 M equivalents of APTES were added and allowed to stir for 24 h in a round-bottom flask to get the FITC conjugated with APTES (FCA), Table 6.2. The reagents are air sensitive and the reaction needs to be completed in a closed container in the dark.

#### *6.2.2.3 Preparation of F-SiNPs*

To obtain F-SiNPs with narrow size distribution patterns, the amounts of all reagents for each preparation method were adjusted carefully in preliminary experiments. Seven synthesis routes are schematically illustrated in Table 6.2.

**Table 6.2 Composition of the F-SiNPs**

| FLSNPs | Fluorophore | Preparation method | NPs composition |
|---|---|---|---|
| FDTPS | FITC | Stöber | TEOS + PTEOS |
| FCTS | FCA | Stöber | TEOS |
| FCTAS | FCA | Stöber | TEOS + APTES |
| FCTPS | FCA | Stöber | TEOS + PTEOS |
| FCTPS-RM | FCA | WORM | TEOS + PTEOS |

6.2.2.3.1 Preparation of FITC doped (non-covalently) into the TEOS/PTEOS-based SiNPs (FDTPS)

FDTPS were prepared using a modified Stöber method where 0.30 mL 10 mM solution of FITC in ethanol was transferred into a 25-mL round flask containing 2.7 mL ethanol and mixed with 0.25 mL PTEOS. 0.20 mL ammonium hydroxide was added to the resulting solution to start the hydrolysis of the alkoxysilane precursor. The solution was stirred at low speed for 24 hours at room temperature. 0.5 mL TEOS and 0.25 mL PTEOS, dissolved in 5.0 mL ethanol were added to the hydrolyzed solution and further reacted with 0.10 mL ammonium hydroxide solution. The reaction was carried out for an hour at 0 °C with continuous sonication and frequent vortexing then stirred for another 24 hours at room temperature. The formed particles thus were centrifuged and washed three times with a solution composed of ethanol and DI water (1:1, *v/v*), then the residue was left to dry completely at 80 °C.

6.2.2.3.2 Preparation of three FITC covalently bonded-SiNPs (FCTS, FCTPS, and FCTAS)

FCTS, FCTPS, and FCTAS were also prepared by a modified Stöber method where 0.50 mL of the FCA conjugate solution were dissolved in 20.0 mL ethanol in a 50-mL round flask,

followed by the sequential addition of the proper volume of the alkoxysilane precursor(s), 1.60 mL DI $H_2O$, and 1.60 mL ammonium hydroxide solution. One mL TEOS was used in the case of FCTS preparation while 0.5 mL TEOS and 0.5 mL PTEOS were used in the case of FCTPS preparation. Similarly, 0.5 mL TEOS and 0.5 mL APTES were used in the case of FCTAS. The mixture was stirred at 400 rpm for 24 hours at room temperature. The formed particles thus were centrifuged and washed three times with ethanol and water, then the residue was left to dry completely at 80 °C, Table 6.2.

6.2.2.3.3 Preparation of FITC covalently encapsulated-SiNPs using WORM method (FCTPS-RM)

The micelles were prepared using 15.0 mL cyclohexane, 2.60 mL 1-hexanol, 3.55 mL Triton™ X-100, and 1.13 mL DI $H_2O$ which were stirred in a 50-mL round flask for 10 min to generate the microemulsion. After time elapsed, 0.50 mL of the FCA conjugate solution was slowly added to the microemulsion and stirred for 30 min at 120 rpm. Finally, 0.50 mL TEOS, 0.50 mL PTEOS, and 0.12 mL ammonium hydroxide were added and the solution was stirred for 24 h. Afterwards, 5.0 mL acetone were added and the NPs were collected by centrifugation and washed five times with absolute ethanol and two times with water to remove any unreacted chemicals and free dye conjugates, then the residue was left to dry completely at 80 °C, Table 6.2.

6.2.2.3.4 Surface modification of F-SiNPs with PVP

60 mg PVP were dissolved in a solution containing 30 mg of either FCTS or FCTAS in 5 mL ethanol, and the mixture was stirred for 24 hours at room temperature and then centrifuged for 20 min at 3800 rpm. The precipitate was re-dispersed in ethanol, and the dispersion was

centrifuged again then the residue was left to dry completely at 80 °C to obtain the corresponding PVP coated F-SiNPs, FCTS-PVP and FCTAS-PVP, respectively, Table 6.2.

#### *6.2.2.4 Instruments and particle characterization*

0.1 mg/mL F-SiNPs suspensions dispersed in ethanol were subjected to particle size determination analysis using a Malvern Mastersizer (Malvern Instruments Ltd., Malvern, UK). Polydispersity index (PDI), and standard deviation were obtained from three independent measurements of the dispersions of NPs. The zeta potential of NPs dispersions in ethanol was also measured. Transmission electron microscopy micrographs were conducted by the Zeiss LEO 912AB (Zeiss, Thornwood, NY). NPs separation required an Allegra 64R Centrifuge (Beckman Coulter Inc., Brea, CA). A SympHonly (SB20) pHmeter (Thermo Orion, MA, USA) was used for pH adjustment. Nano pure water was prepared using a Barnstead NANO pure DIamond Analytical ultrapure water system (Fischer Scientific, NJ, USA). All fluorescence spectra were performed on ISS K2 multifrequency crosscorrelation phase and modulation fluorimeter (ISS™ Focus and Discover, Champaign, IL, USA), equipped with a 300 W xenon arc lamp. 1.0 cm disposable plastic cuvettes were used for all fluorescence measurements. To investigate the fluorescence properties of the F-SiNPs, they were dispersed in a 1:1 (v/v) water/ethanol solvent and their emission spectra were recorded.

#### *6.2.2.5 Use of F-SiNPs as developing agents for fingerprints*

Fingerprints were collected from two donors: 26-year-old male and 42-year-old female and then developed after different time intervals of deposition. Fingerprints were obtained by requesting the donors to rub their finger with their nose immediately prior to fingerprints

deposition. The donors were instructed not to wash their hands within two hours prior to providing the samples. Fingerprints were deposited onto three different substrates: glass microscope slides, aluminum foil, and Petri dishes (polystyrene). Fingerprints were collected as half impressions on glass slides and aged for different time intervals. The left half was developed after one day and used as a reference for comparison with the right half which was developed after a week or a month. A concentration of 5.0 mg/mL suspensions for each of the F-SiNPs in a solvent composed of 1:1 (v/v) DI water: ethanol was prepared, then they were sonicated for 10 min to ensure sufficient particles dispersion. About 0.5–1.0 mL of the suspension was pipetted onto the sample using a transfer pipette. After 5 min, the excess solution was removed, and the sample was gently washed with a mixture of 1:1 (v/v) DI water: ethanol. After that the developed fingerprint was left to dry at room temperature. The photographs were recorded in a luminescence mode using the forensic light source (FLS), Mini-CrimeScope 400 MCS-400 (Spex Forensics, Edison, NJ) at an excitation wavelength of 445 nm or CSS setting. The fingerprint image was photographed using a digital camera (Nikon D3300) with a 520 nm long-pass filter. The sample was placed on a black surface to enhance the contrast of fingerprint image during illumination and taking pictures.

### *6.2.3 Results and discussion*

To achieve stable incorporation of small organic molecules such as dyes, either covalent copolymerization of the dye conjugate or strong non-covalent binding interactions between the added dye molecules and the backbone of the cross-linked silicate matrix are needed. These interactions are likely to arise from hydrophobic and hydrophilic groups in the dye molecules and the silicate backbone. To identify the factors leading to stable incorporation of the fluorogenic molecules into the SiNPs and efficient visualization of fingerprints aged for several time intervals

on three different non-porous surfaces, seven different routes for preparing F-SiNPs have been examined in this report. The produced SiNPs have been labeled with either FITC or its conjugate with APTES, FCA. Two of the most commonly used sol-gel methods for SiNPs preparation, the Stöber and WORM methods were used in this report. Moreover, encapsulation of the FCA dye conjugate through a stable covalent bond versus encapsulation of FITC itself non-covalently into the SiNPs matrix has been examined. In addition, three organosilicate monomers namely TEOS, PTEOS, APTES and their binary combinations were used to prepare the NPs, Table 6.2. Finally, the adhesive agent, PVP was introduced onto the surface of the less hydrophobic F-SiNP to investigate the enhancement effect on the binding affinity of PVP-coated F-SiNP to fingerprints.

#### *6.2.3.1 Particle characterization*

The physical nature and dimensions of the particles were derived from the DLS and TEM scans for FCTPS and FCTPS-RM, (Figure 6.4). The NPs were composed of discrete monodispersed spherical particles with an average diameter of 4.1 ± 0.6 and 110.4 ± 31.1 for the NPs prepared by the WORM and Stöber methods, respectively. The diameter obtained from TEM images, the mean hydrodynamic particle sizes by DLS, PDI, and zeta potential values were summarized in Table 6.3. TEM micrographs showed that the labeled F-SiNPs prepared by the WORM method had a spherical shape and a narrow size distribution of 4.1 ± 0.6 which was confirmed by the DLS measurements. Given that the size of FITC molecule is approximately 0.9Â × 1.2Â × 1.4 nm wide, it is reasonable to consider single molecule occupancy per particle avoiding any reabsorption or concentration quenching processes. On the other hand, NPs prepared by the Stöber method had a relatively larger diameter of about 110.4 ± 31.1 with a lower control on the

monodispersity of size and shape. The zeta potentials of FCTPS and FCTPS-RM in ethanol ranged from −12.8 to −26.7 mV, respectively, Table 6.3.

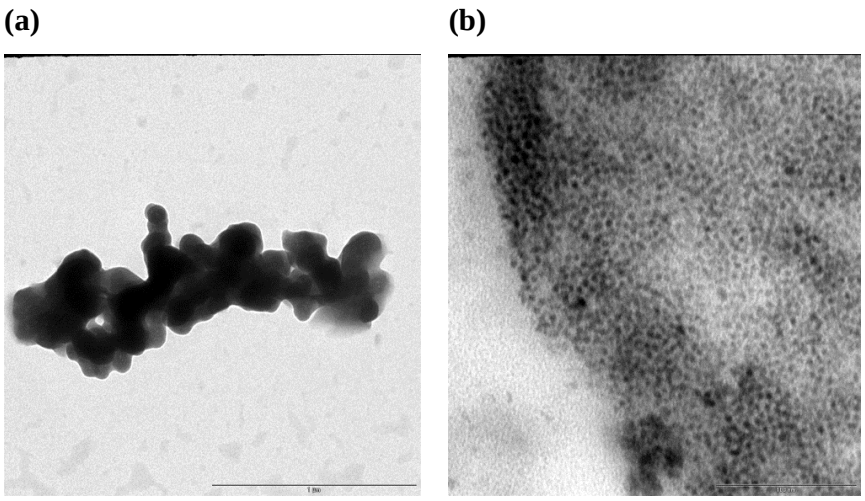


**Figure 6.4 TEM micrographs of (a) FCTPS and (b) FCTPS-RM**

**Table 6.3 Diameter determined by TEM and DLS, polydispersity index (PDI), zeta potential of 0.1 mg/ml labeled SiNPs in ethanol**

| F-SiNPs | Diameter (TEM) (nm) | Diameter (DLS) (nm) | PDI | Zeta potential (mV) |
|---|---|---|---|---|
| FCTPS | 110.4 ± 31.1 | 605.7 ± 131.5 | 0.48 | -26.7 ± 14.3 |
| FCTPS-RM | 4.1 ± 0.6 | 5.3 ± 0.4 | 1.00 | -12.8 ± 14.2 |

#### *6.2.3.2 Preparation method of the F-SiNPs*

Two different F-SiNPs, FCTPS and FCTPS-RM, were prepared to be used in this investigation. Both of them were prepared using a mixture of TEOS and PTEOS alkoxysilane

precursors.[27] FCTPS were prepared using the Stöber method[38] whereas FCTPS-RM were prepared using the WORM method.[39] The Stöber method has the advantages of simplicity besides avoiding using surfactants which requires extensive cleaning steps. However, controlling the particle size and shape is easily achieved using the WORM method, where the nanoreactors of water droplets in the oil phase define the particles dimension.[48] As expected, the WORM method resulted in NPs with a smaller size range of about 4.1 ± 0.6 nm and a better monodispersity in comparison with the Stöber method as can be revealed from the TEM and DLS measurements. However, the WORM method may imply several processing, technical and environmental limitations that make the production process more challenging to scale up for commercial applications. For example, suitable reaction vessels are needed, the organic solvents used for the water-in-oil emulsion are usually not environmentally friendly, the doping agent has to be hydrophilic or polar to be localized in the inner aqueous micellar core, and breaking of micelles and extensive washing steps to remove surfactant, solvents, and other by-products are necessary. Due to the simplicity and cost effectiveness of the Stöber method, it was chosen as the method of F-SiNPs preparation to investigate the other factors affecting fingerprints visualization.

#### *6.2.3.3 Covalent versus non-covalent fluorophore encapsulation into the SiNPs matrix*

Two different F-SiNPs, FDTPS and FCTPS, were prepared to be used in this investigation. Both of them were prepared using the Stöber method with equal volumes of TEOS and PTEOS alkoxysilane precursors.[27] FITC (logP 4.80) was non-covalently doped into a hydrophobic core composed of PTEOS (logP 3.25) then entrapped in a shell composed of TEOS (logP 1.68) and PTEOS in the case of FDTPS. The composition of the core and the shell of FDTPS allowed stable non-covalent encapsulation of the hydrophobic FITC dye molecules with minimal leakage under

the used experimental conditions. For FCTPS, APTES was used for crosslinking the FITC dye molecules with the silica matrix, where the binding between cyanate groups of the dye molecules and the amine groups of APTES causes the formation of a thiourea linkage.[50] The formed FITC conjugate with APTES, FCA, was covalently copolymerized into the SiNPs to form FCTPS. Investigation of the emission spectra of these NPs, confirmed the successful encapsulation of the relatively hydrophobic FITC dye, (Figure 6.5). The fluorescence maximum for all the F-SiNPs in this study was within the same range of the pure dye. However, minor red shifts and different spectral patterns were observed due to the differences in preparation method and encapsulation process. Thus, the surrounding environment and the confirmation attained by the fluorophore could be different for each F-SiNPs. To avoid the inner filter effect and/or other scattering problems due to the particulate nature of the samples, suspensions of five F-SiNPs have been analyzed and compared with the pure dye, FITC in water: ethanol (1:1, v/v) at excitation wavelength of 455 nm.

It is reported that the incorporation yield of non-covalently bound fluorophores is poor, as it is only based on physical adsorption forces.[51] Nevertheless, non-covalent embedding of FITC was made suitable using the hydrophobic alkoxysilane precursor, PTEOS, in the core and shell of the NPs, and this observation is consistent with other reports.[27, 52-54] It was also noted that the intensity of FDTPS fluorescence increased as the proportion of PTEOS in the initial monomer mixture increased.[27] A ratio of 1:1 (v/v) of the selected precursors was used thereafter in all incorporation experiments. However, it was found that the dye is prone to leaking from FDTPS under exposure to the used solvent for longer time so the more stable towards dye leakage, FCTPS, was found to be more suitable for developing fingerprints.

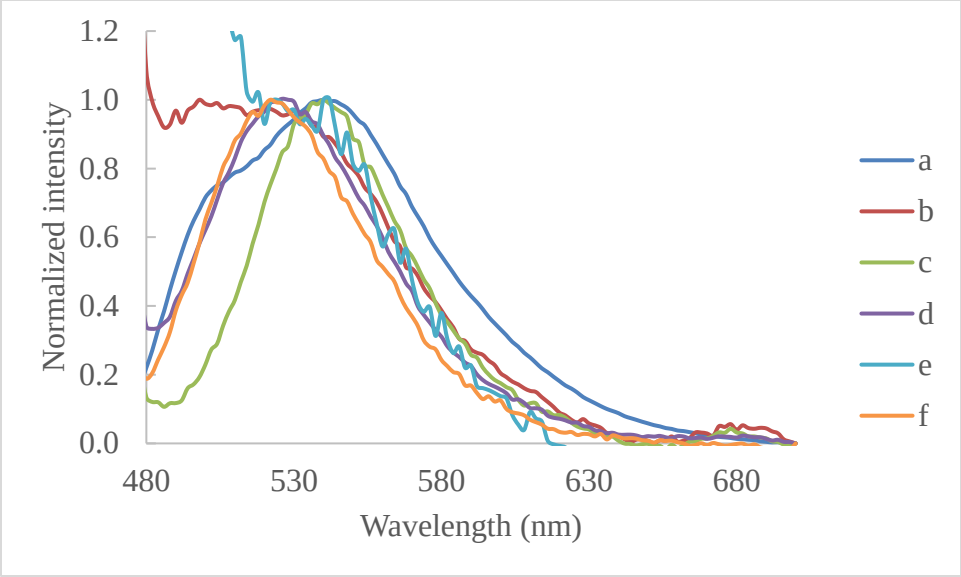


**Figure 6.5 Emission spectra of (a) FITC (b) FCTPS, (c) FCTPS-RM, (d) FDTPS, (e) FCTS, and (f) FCTAS in water: ethanol (1:1, v/v) at excitation wavelength of 455 nm**

#### *6.2.3.4 Type of the alkoxysilane precursor(s)*

Three different organosilicate monomers have been used in this investigation, namely TEOS (logP 1.68), PTEOS (logP 3.25), and APTES (logP -1.83) to incorporate FCA covalently into the silica platform. It is hypothesized that the planar aromatic phenyl groups of PTEOS would form hydrophobic interactions with the planar rings of FITC and that polar silanol groups present in the alkoxysilane precursors would form strong interaction with the polar functional groups of FITC, and thus a highly fluorescent and stable complex on encapsulation can be obtained.[22] Nonetheless, the nature of organosilicate monomers will not have a significant effect on the dye loading and its leaking from the NPs when the dye molecules are covalently bonded into the silica matrix to form highly stable F-SiNPs. In that case, the nature of the organosilicate monomers is expected to influence mainly the binding affinity to the fingerprints residue.

#### *6.2.3.5 Use of dye-encapsulated SiNPs suspensions as developing agents for fingerprints*

To investigate the binding affinity of F-SiNPs to the components of fingerprints, suspensions of these particles were applied on three different non-porous surfaces: glass slides, aluminum foil, and Petri dishes (polystyrene). For the first substrate, glass slides, when the binary mixture of TEOS and PTEOS used in forming the shell of FCTPS, FCTPS-RM, and FDTPS, clear luminescent fingerprint ridges were obtained for the three F-SiNPs suspensions at CSS setting of the FLS using a 520 nm long pass filter as depicted in Figure 6.6 (a, b, and c) (first row). The surface of NPs has been decorated with PTEOS in the case of FCTPS, FCTPS-RM, and FDTPS which increased the hydrophobic interaction between the phenyl group of PTEOS and the sebaceous secretion in the fingerprint residue resulting in an enhanced binding and reliable detection of fingerprints. Despite the differences in the preparation methods, the efficiency of these hydrophobic NPs as developing agents able to produce clear luminescent fingerprints with high contrast was observed and attributed to the PTEOS-modified hydrophobic surface. It was found that CSS setting could be the best choice for fingerprints visualization. However, a distinct definition in fingerprint detection can also be obtained using another setting of FLS at excitation wavelength of 445 nm viewed through the same filter as shown in Figure S1 where the fingerprints developed with FDTPS appeared luminescent with clear ridge pattern. When TEOS was used solely for the preparation of FCTS, weak luminescence fingerprints and poor contrast were obtained as depicted in Figure 6.6 (d) in both settings of FLS. Therefore, using these particles as developing agents for fingerprint detection is not practical. On the other hand, the binary mixture of TEOS and APTES used in preparing FCTAS resulted in luminescence ridges with an obvious background noise as shown in Figure 6.6 (e) using both CSS and 445 nm settings. The observed background noise could be due to undesirable interactions between the polar APTES with the glass

substrate which complies with the investigations presented by Moret et al. in understanding the mechanism of fingerprint development using SiNPs.[55] A comparable fingerprint detection behavior was noticed for the other two substrates: aluminum foil and Petri dishes as depicted in Figure 6.6 with a better performance on aluminum foil in comparison with Petri dishes. Luminescent fingerprint ridges were developed by three F-SiNPs, FCTPS, FCTPS-RM, and FDTPS at CSS setting of FLS, which again can be attributed to the hydrophobic interaction of fingerprint residue with these F-SiNPs whereas FCTP and FCTAS resulted in weak luminescent fingerprints with obvious noise, Figure 6.6 (d and e). Overall, the results obtained from developing fingerprints on glass slides were superior in comparison with the other two substrates. On the other hand, detection of aged fingerprints is important in forensic investigations because physical evidence are mostly collected hours or days after the crime. Therefore, in this investigation, the fingerprints were deposited on glass slides and aged for different time intervals as shown in Figure 6.6 and S2. Developing the 1-day-old half impression exhibited the same degree of luminescence and ridge details of the 1-week-old half impression using FDTPS. Moreover, the developed 1-month-old half impression, in the same way, resulted in acceptable fingerprint details, Figure 6.7 and S2. Thus, it is of interest to use F-SiNPs in forensic field to reveal old fingerprints because prints are found days after the crime.

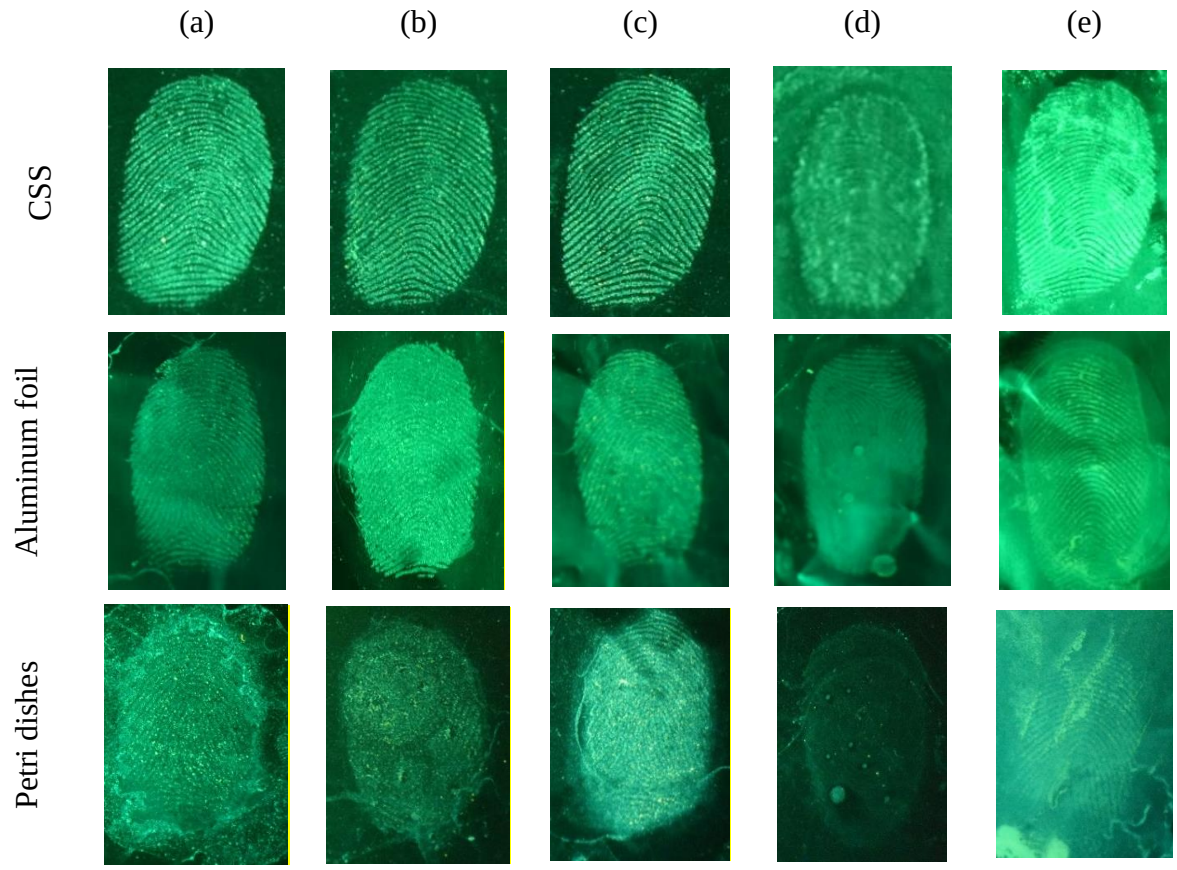


**Figure 6.6 Fluorescence images of fingerprints developed using 5.0 mg/mL F-SiNPs suspensions in water: ethanol (1:1, v/v) of (a) FCTPS, (b) FCTPS-RM, (c) FDTPS, (d) FCTS, (e) FCTAS, (f) FCTS-PVP, and (g) FCTAS-PVP at CSS settings of FLS on different non-porous surfaces**

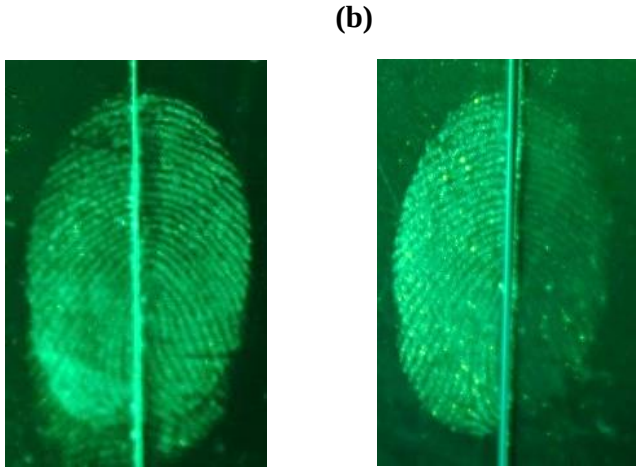


**Figure 6.7 Comparison of fingerprints developed using FDTPS on glass at different time intervals on glass slides: (a) after 1-day (left half) and after 1-week (right half) and (b) after 1-day (left half) and after 1-month (right half) at CSS setting of FLS**

Friction ridge features of a fingerprint have been classified into three levels of detail.[56] First- level detail describes the overall ridge pattern such as fingerprint orientation and ridge flow direction. The general information obtained from the first-level detail are not decisive. Thus, it cannot be used for personal identification. Second-level detail involves ridge formations and pattern minutiae such as ridge ending, bifurcation, and dots. Third-level detail includes the morphology of a ridge such as width, shape, and pores. Both second and third- level details enable identification and fingerprint matching due to the unique individual features. The typical features of second-level detail of fingerprint friction ridge of FCTPS, FCTPS-RM, and FDTPS are shown in Figure 6.8. Such features including bifurcations and ridge endings were slightly clear in fingerprints developed by FCTPS-RM, and FDTPS compared with FCTPS. Based on the obtained data, FCTPS could be a promising optical reporter nano-system candidate for forensic and bio-related applications due to its unique properties such as photochemical stability, minimum dye leakage, and cost-effective synthesis route easy to scale up for commercial production.

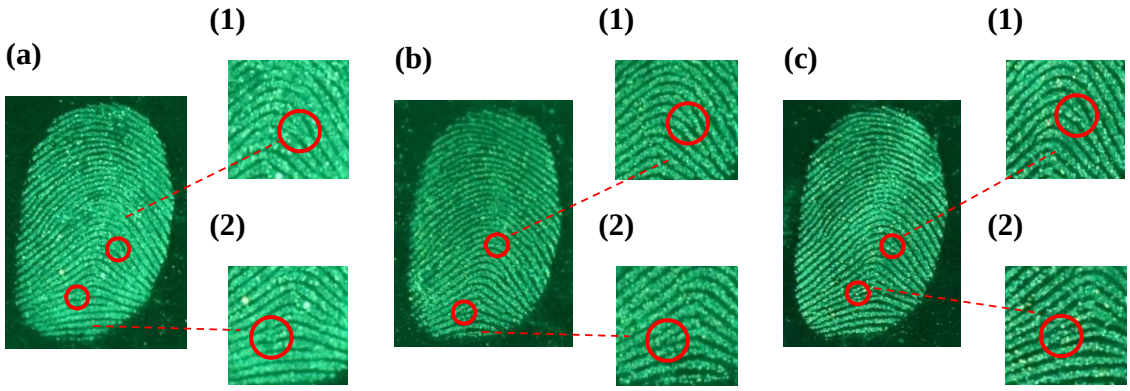


**Figure 6.8 Fluorescence images of fingerprints of (a) FCTPS, (b) FCTPS-RM, and (c) FDTPS, at CSS setting of FLS on glass slides, showing second-level detail of fingerprint friction ridge (1) bifurcation and (2) ridge ending**

#### *6.2.3.6 Surface Modification of Fluorescent SiNPs with PVP*

In order to enhance the fingerprints detection, the less hydrophobic FCTS and FCTAS were coated with the adhesive agent, PVP to improve their binding affinity to the hydrophobic components present in the fingerprint residue. PVP has been used as adhesive agent or binder in pharmaceutical industry because of its binding affinity to polar and nonpolar molecules contributed to intrinsic amphiphilic property of PVP.[57-58] Thus, compared to uncoated NPs, their PVP modified counterparts, FCTS-PVP and FCTAS-PVP should show much higher contrast fingerprints images on glass because of their high binding affinity.[19] Fingerprints detection using PVP-coated SiNPs as fluorescent labeling markers should be well-defined in terms of finger ridge details without background staining, resulting in a good definition of enhanced detection. However, it was observed that the PVP coated SiNPs did not result in any enhanced visualization as shown in Figure 6.9.

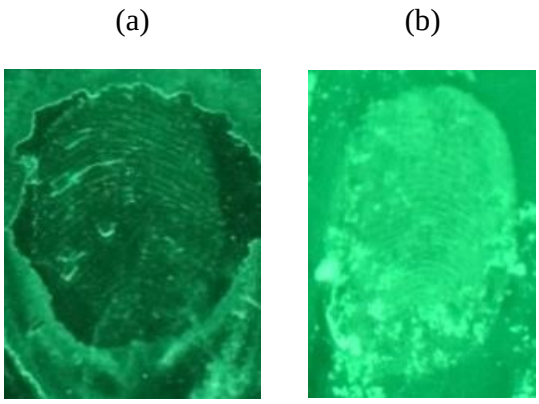


**Figure 6.9 Fluorescence images of fingerprints developed using 5.0 mg/mL F-SiNPs suspensions in water: ethanol (1:1, v/v) of (a) FCTS-PVP, and (b) FCTAS-PVP at CSS FLS settings on glass slides**

### *6.2.4 Conclusions*

Uniform F-SiNPs of small particle size with diameters in the range of 4.1–110.4 nm were fabricated in seven different routes, and characterized by DLS, TEM, and spectrofluorometric measurements. In this study, a systematic investigation of several factors affecting the efficiency of developing aged fingerprints on three different non-porous surfaces was carried out. FITC as a representative dye was loaded into the NPs matrix in order to increase the contrast of the developed fingerprints from the surrounding background while the nanometer-sized particles improve the resolution of the developed fingerprints. The obtained results indicated that the developed NPs are effective in fingerprint detection when the surface is modified with functional groups having the potential to react particularly with the most abundant components present in the fingerprint residue and not with the substrate. It was found that the most important factor affecting this application was the hydrophobic nature of the F-SiNPs surface. This can be obtained by using a mixture of TEOS and PTEOS alkoxyilane precursors during the formation of the core and shell of the NPs. That allowed proper loading of the used hydrophobic fluorophore and at the same time increased

the binding affinity to hydrophobic components of the fingerprints. Therefore, FCTPS, FCTPS-RM, and FDTPS are considered good developing agents where they developed clear luminescent fingerprints with a good contrast on glass slides, and can be used on other non-porous surfaces including aluminum foil and Petri dishes (polystyrene). Both the Stöber and WORM methods can be used. However, Stöber method is simpler, with a higher scalability potential of the production process. Moreover, FITC can be non-covalently or covalently encapsulated after being conjugated with APTES into the silica matrix for efficient fingerprints detection. However, the FCA covalently bonded-SiNPs are more stable and show minimized dye leakage. In addition, although the less hydrophobic F-SiNPs were coated on the surface with the adhesive agent, PVP to increase the binding affinity to fingerprints, they did not result in any enhancement effect on fingerprints development. Thus, these systematic investigations demonstrate the features that highly emitting dye-encapsulated NPs should hold in order to be utilized as reliable developing agents for fingerprints imaging applications in forensic science.

**References**


1. Su, B., Recent progress on fingerprint visualization and analysis by imaging ridge residue components. *Anal. Bioanal. Chem.* **2016,** *408* (11), 2781-2791.
2. Yuan, C.; Li, M.; Wang, M.; Zhang, L., Cationic dye-diatomite composites: Novel dusting powders for developing latent fingerprints. *Dyes and Pigments* **2018,** *153*, 18-25.
3. Chen, C. C.; Yu, Y. C.; Lee, H. C.; Giang, Y. S.; Wang, S. M., Latent Fingerprint Development on Thermal Paper Using Traditional Ninhydrin and 1,2-indanedione. *Journal of Forensic Sciences* **2016,** *61* (1), 219-225.
4. Song, W.; Mao, Z.; Liu, X. J.; Lu, Y.; Li, Z. S.; Zhao, B.; Lu, L. H., Detection of protein deposition within latent fingerprints by surface-enhanced Raman spectroscopy imaging. *Nanoscale* **2012,** *4* (7), 2333-2338.
5. Lauzon, N.; Dufresne, M.; Chauhan, V.; Chaurand, P., Development of Laser Desorption Imaging Mass Spectrometry Methods to Investigate the Molecular Composition of Latent Fingermarks. *Journal of the American Society for Mass Spectrometry* **2015,** *26* (6), 878-886.
6. Bhargava, R.; Perlman, R. S.; Fernandez, D. C.; Levin, I. W.; Bartick, E. G., Non-invasive detection of superimposed latent fingerprints and inter-ridge trace evidence by infrared spectroscopic imaging. *Anal. Bioanal. Chem.* **2009,** *394* (8), 2069-2075.
7. Yang, Y.; Liu, R.; Cui, Q.; Xu, W.; Peng, R.; Wang, J.; Li, L., Red-emissive conjugated oligomer/silica hybrid nanoparticles with high affinity and application for latent fingerprint detection. *Colloids and Surfaces A: Physicochemical and Engineering Aspects* **2019,** *565*, 118-130.

8. Moret, S.; Becue, A.; Champod, C., Functionalised silicon oxide nanoparticles for fingermark detection. *Forensic Science International* **2016,** *259*, 10-18.

9. Wolfbeis, O. S., Nanoparticle-enhanced fluorescence imaging of latent fingerprints reveals drug abuse. *Angew. Chem., Int. Ed.* **2009,** *48* (13), 2268-2269.

10. Day, K. J.; Bowker, W., Enhancement of Cyanoacrylate Developed Latent Prints Using Nile Red. *Journal of Forensic Identification* **1996,** *46* (2), 183-187.

11. Chesher, B. K.; Stone, J. M.; Rowe, W. F., Use of the Omniprint™ 1000 alternate light source to produce fluorescence in cyanoacrylate-developed latent fingerprints stained with biological stains and commercial fabric dyes. *Forensic Science International* **1992,** *57* (2), 163-168.

12. Braasch, K.; de la Hunty, M.; Deppe, J.; Spindler, X.; Cantu, A. A.; Maynard, P.; Lennard, C.; Roux, C., Nile red: Alternative to physical developer for the detection of latent fingermarks on wet porous surfaces? *Forensic Science International* **2013,** *230*, 74-80.

13. Frick, A. A.; Busetti, F.; Cross, A.; Lewis, S. W., Aqueous Nile blue: a simple, versatile and safe reagent for the detection of latent fingermarks. *Chemical Communications* **2014,** *50* (25), 3341-3343.

14. de la Hunty, M.; Spindler, X.; Chadwick, S.; Lennard, C.; Roux, C., Synthesis and application of an aqueous Nile red microemulsion for the development of fingermarks on porous surfaces. *Forensic Science International* **2014,** *244*, 48-55.

15. Wang, W.; Xing, J.; Ge, Z., Evaluation of Nile Red-Loaded Mesoporous Silica Nanoparticles for Developing Water-Soaked Fingerprints on Thermal Paper. *Journal Of Forensic Sciences* **2018**.

16. Sametband, M.; Shweky, I.; Banin, U.; Mandler, D.; Almog, J., Application of nanoparticles for the enhancement of latent fingerprints. *Chemical Communications* **2007,** (11), 1142-1144.

17. Champod, C.; Lennard, C.; Margot, P.; Stoilovic, M., *Fingerprints and Other Ridge Skin Impressions*. CRC Press: Boca Raton, 2004.

18. Becue, A.; Moret, S.; Champod, C.; Margot, P., Use of stains to detect fingermarks. *Biotechnic & Histochemistry* **2011,** *86* (3), 140-160.

19. Kim, Y. J.; Jung, H. S.; Lim, J.; Ryu, S. J.; Lee, J. K., Rapid Imaging of Latent Fingerprints Using Biocompatible Fluorescent Silica Nanoparticles. *Langmuir* **2016,** *32* (32), 8077-8083.

20. Leggett, R.; Lee-Smith, E. E.; Jickells, S. M.; Russell, D. A., "Intelligent" fingerprinting: Simultaneous identification of drug metabolites and individuals by using antibody-functionalized nanoparticles. *Angew. Chem.-Int. Edit.* **2007,** *46* (22), 4100-4103.

21. Gao, D.; Li, F.; Song, J.; Xu, X.; Zhang, Q.; Niu, L., One step to detect the latent fingermarks with gold nanoparticles. *Talanta* **2009,** *80* (2), 479-483.

22. Cai, K.; Yang, R.; Wang, Y.; Yu, X.; Liu, J., Super fast detection of latent fingerprints with water soluble CdTe quantum dots. *Forensic Science International* **2013,** *226* (1–3), 240-243.

23. Liu, J.; Shi, Z.; Yu, Y.; Yang, R.; Zuo, S., Water-soluble multicolored fluorescent CdTe quantum dots: Synthesis and application for fingerprint developing. *Journal of Colloid and Interface Science* **2010,** *342* (2), 278-282.

24. Mi, C.; McBean, K.; Ping, N.; McDonagh, A.; Maynard, P.; Lennard, C.; Roux, C., An evaluation of nanostructured zinc oxide as a fluorescent powder for fingerprint detection. *Journal of Materials Science* **2008,** *43* (2), 732.

25. Zhang, M.; Ou, Y.; Du, X.; Li, X.; Huang, H.; Wen, Y.; Zhang, X., Systematic study of dye loaded small mesoporous silica nanoparticles for detecting latent fingerprints on various substrates. *Journal of Porous Materials* **2017,** *24* (1), 13.

26. Huang, W.; Li, X. J.; Wang, H. F.; Xu, X. J.; Liu, H.; Wang, G. Q., Synthesis of Amphiphilic Silica Nanoparticles for Latent Fingerprint Detection. *Anal. Lett.* **2015,** *48* (9), 1524-1535.

27. Theaker, B. J.; Hudson, K. E.; Rowell, F. J., Doped hydrophobic silica nano- and micro-particles as novel agents for developing latent fingerprints. *Forensic Science International* **2008,** *174*, 26-34.

28. Abdelwahab, W. M.; Phillips, E.; Patonay, G., Preparation of fluorescently labeled silica nanoparticles using an amino acid-catalyzed seeds regrowth technique: Application to latent fingerprints detection and hemocompatibility studies. *Journal of Colloid and Interface Science* **2018,** *512* (Supplement C), 801-811.

29. Moosavi-Movahedi, A. A.; Chamani, J.; Ghourchian, H.; Shafiey, H.; Sorenson, C. M.; Sheibani, N., Electrochemical Evidence for the Molten Globule States of Cytochrome c Induced by N-Alkyl Sulfates at Low Concentrations. *Journal of Protein Chemistry* **2003,** *22* (1), 23-30.

30. Rashidipour, S.; Naeeminejad, S.; Chamani, J., Study of the interaction between DNP and DIDS with human hemoglobin as binary and ternary systems: spectroscopic and

molecular modeling investigation. *Journal Of Biomolecular Structure & Dynamics* **2016,** *34* (1), 57-77.

31. Marouzi, S.; Sharifi Rad, A.; Beigoli, S.; Teimoori Baghaee, P.; Assaran Darban, R.; Chamani, J., Study on effect of lomefloxacin on human holo-transferrin in the presence of essential and nonessential amino acids: Spectroscopic and molecular modeling approaches. *International Journal of Biological Macromolecules* **2017,** *97*, 688-699.
32. Martins Estevão, B.; Miletto, I.; Marchese, L.; Gianotti, E., Optimized Rhodamine B labeled mesoporous silica nanoparticles as fluorescent scaffolds for the immobilization of photosensitizers: a theranostic platform for optical imaging and photodynamic therapy. *Physical Chemistry Chemical Physics: PCCP* **2016,** *18* (13), 9042-9052.
33. Kubista, M.; Sjöback, R.; Eriksson, S.; Albinsson, B., Experimental correction for the inner-filter effect in fluorescence spectra. *Analyst* **1994,** *119* (3), 417.
34. Yappert, M. C.; Ingle, J. D., Jr., Correction of polychromatic luminescence signals for inner-filter effects. *Appl. Spectrosc.* **1989,** *43* (5), 759-67.
35. Wang, T.; Zeng, L.-H.; Li, D.-L., A review on the methods for correcting the fluorescence inner-filter effect of fluorescence spectrum. *Applied Spectroscopy Reviews* **2017,** *52* (10), 883.
36. Iranfar, H.; Rajabi, O.; Salari, R.; Chamani, J., Probing the Interaction of Human Serum Albumin with Ciprofloxacin in the Presence of Silver Nanoparticles of Three Sizes: Multispectroscopic and ζ Potential Investigation. *The Journal of Physical Chemistry B* **2012,** *116* (6), 1951-1964.
37. Pasban Ziyarat, F.; Asoodeh, A.; Sharif Barfeh, Z.; Pirouzi, M.; Chamani, J., Probing the interaction of lysozyme with ciprofloxacin in the presence of different-sized Ag nano-

particles by multispectroscopic techniques and isothermal titration calorimetry. *Journal Of Biomolecular Structure & Dynamics* **2014,** *32* (4), 613-629.

38. Stöber, W.; Fink, A.; Bohn, E., Controlled growth of monodisperse silica spheres in the micron size range. *Journal of Colloid and Interface Science* **1968,** *26* (1), 62-69.

39. Bagwe, R. P.; Yang, C.; Hilliard, L. R.; Tan, W., Optimization of Dye-Doped Silica Nanoparticles Prepared Using a Reverse Microemulsion Method. *Langmuir* **2004,** *20* (19), 8336-8342.

40. Gao, F.; Tang, L.; Dai, L.; Wang, L., A fluorescence ratiometric nano-pH sensor based on dual-fluorophore-doped silica nanoparticles. *Spectrochimica Acta Part A: Molecular and Biomolecular Spectroscopy* **2007,** *67* (2), 517-521.

41. Finnie, K. S.; Bartlett, J. R.; Barbé, C. J. A.; Kong, L., Formation of Silica Nanoparticles in Microemulsions. *Langmuir* **2007,** *23* (6), 3017-3024.

42. Liang, J.; Xue, Z.; Xu, J.; Li, J.; Zhang, H.; Yang, W., Highly efficient incorporation of amino-reactive dyes into silica particles by a multi-step approach. *Colloids and Surfaces A: Physicochemical and Engineering Aspects* **2013,** *426*, 33-38.

43. Rampazzo, E.; Bonacchi, S.; Juris, R.; Montalti, M.; Genovese, D.; Zaccheroni, N.; Prodi, L.; Rambaldi, D. C.; Zattoni, A.; Reschiglian, P., Energy transfer from silica core-surfactant shell nanoparticles to hosted molecular fluorophores. *The journal of physical chemistry. B* **2010,** *114* (45), 14605-13.

44. Santra, S.; Zhang, P.; Wang, K.; Tapec, R.; Tan, W., Conjugation of Biomolecules with Luminophore-Doped Silica Nanoparticles for Photostable Biomarkers. *Analytical Chemistry* **2001,** *73* (20), 4988-4993.

45. van Blaaderen, A.; Vrij, A., Synthesis and Characterization of Monodisperse Colloidal Organo-silica Spheres. *Journal of Colloid and Interface Science* **1993,** *156* (1), 1-18.

46. Lian, W.; Litherland, S. A.; Badrane, H.; Tan, W.; Wu, D.; Baker, H. V.; Gulig, P. A.; Lim, D. V.; Jin, S., Ultrasensitive detection of biomolecules with fluorescent dye-doped nanoparticles. *Analytical biochemistry* **2004,** *334* (1), 135-44.

47. Santra, S.; Wang, K.; Tapec, R.; Tan, W., Development of novel dye-doped silica nanoparticles for biomarker application. *Journal of biomedical optics* **2001,** *6* (2), 160-6.

48. Auger, A.; Samuel, J.; Poncelet, O.; Raccurt, O., A comparative study of non-covalent encapsulation methods for organic dyes into silica nanoparticles. *Nanoscale Res Lett* **2011,** *6* (1), 328.

49. Tapec, R.; Zhao, X. J.; Tan, W., Development of organic dye-doped silica nanoparticles for bioanalysis and biosensors. *Journal of nanoscience and nanotechnology* **2002,** *2* (3-4), 405-9.

50. Van Blaaderen, A.; Vrij, A., Synthesis and characterization of colloidal dispersions of fluorescent, monodisperse silica spheres. *Langmuir* **1992,** *8* (12), 2921-2931.

51. Ethiraj, A. S.; Hebalkar, N.; Kharrazi, S.; Urban, J.; Sainkar, S. R.; Kulkarni, S. K., Photoluminescent core-shell particles of organic dye in silica. *Journal of Luminescence* **2005,** *114* (1), 15-23.

52. Shahabi, S.; Treccani, L.; Rezwan, K., A comparative study of three different synthesis routes for hydrophilic fluorophore-doped silica nanoparticles. *Journal of Nanoparticle Research* **2016,** *18* (1), 28.

53. Canton, G.; Ricco, R.; Marinello, F.; Carmignato, S.; Enrichi, F., Modified Stober synthesis of highly luminescent dye-doped silica nanoparticles. *Journal of Nanoparticle Research* **2011,** *13* (9), 4349-4356.

54. Gao, X.; He, J.; Deng, L.; Cao, H., Synthesis and characterization of functionalized rhodamine B-doped silica nanoparticles. *Optical Materials* **2009,** *31* (11), 1715-1719.

55. Moret, S.; Becue, A.; Champod, C., Nanoparticles for fingermark detection: an insight into the reaction mechanism. *Nanotechnology* **2014,** *25* (42), 10.

56. Vanderkolk, J. R., Examination Process. In *The Fingerprint Sourcebook.*, Holder, E. H.; Robinson, L. O.; Laub, J. H., Eds. Washington, DC : U.S. Dept. of Justice, Office of Justice Programs, National Institute of Justice, [2011]: 2011.

57. Lee, J., Intrinsic adhesion properties of poly(vinyl pyrrolidone) to pharmaceutical materials: humidity effect. *Macromolecular bioscience* **2005,** *5* (11), 1085-93.

58. Benahmed, A.; Ranger, M.; Leroux, J. C., Novel polymeric micelles based on the amphiphilic diblock copolymer poly(N-vinyl-2-pyrrolidone)-block-poly(D,L-lactide). *Pharmaceutical Research* **2001,** *18* (3), 323-328.